Redistribution of moisture and ions in cement based materials

Magnus Åhs

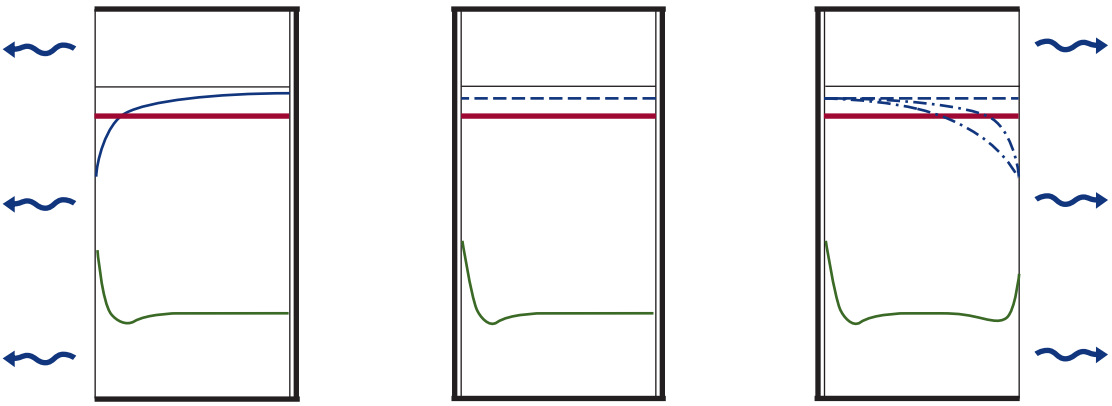

Division of Building Materials
Lund University

Redistribution of moisture and ions in cement based materials

Magnus Åhs

LUND UNIVERSITY

Doctoral Thesis, Report TVBM-1028, Division of Building Materials,
Lund Institute of Technology, Lund University, Lund 2011

ISRN LUTVDG/TVBM--11/1028--SE(1-86)
ISSN 0348-7911 TVBM
ISBN 978-91-7473-126-2

Lund University
Division of Building Materials
P.O. Box 118
SE-221 00 Lund, Sweden

Telephone:+46 46 222 74 15
Telefax:+46 46 222 44 27
www.byggnadsmaterial.lth.se

Preface

This doctoral thesis is the result of six years of research conducted at the division of Building Materials, Lund University. It was funded by SBUF, the Development Fund of the Swedish Construction Industry, FORMAS, the Swedish Research Council for Environment, Agricultural Sciences and Spatial Planning, NCC Construction Sweden, Skanska Sweden, maxit Group AB and Strängbetong AB. A part of this project was a partner project in NanoCem.

I would like to thank my supervisors, Professor Lars-Olof Nilsson and Professor Lars Wadsö at the division of Building Materials, for their encouragement and support throughout this research.

The practical work in this research was performed in cooperation with the technical staff at the division of Building Materials, Stefan Backe, Bo Johansson, Ingemar Larsson and last but definitely not least Bengt Nilsson. Their technical skills and experience simplified the laboratory work. Marita Persson and Britt Andersson, the administrative back bone of the division of Building Materials, have contributed to the completion of my thesis with their organizational skills.

Representatives from the construction industry are hereby acknowledged for their contributions to this work.

All my fellow Ph.D. students are hereby recognized for their contribution to this thesis.

Finally, I would like to express my gratitude to my wife Jessica for her support.

Abstract

There were two principal objectives for this thesis. The first was to develop a methodology and evaluation model of moisture redistribution in order to make the future relative humidity in a screeded concrete slab predictable. The second objective was to develop a method to determine the critical humidity for ion transport in concrete.

Residual moisture in screeded concrete slabs may be redistributed to the top screed surface under a semi-permeable flooring, thus elevating the relative humidity, RH, and possibly exceeding the critical humidity level. Passing the critical humidity level may result in material damage to the flooring and adhesive. In order to avoid such damage there is a need of a methodology to estimate the maximum humidity obtained underneath flooring.

The redistribution of residual moisture may increase the concentration of alkali at the contact area between the adhesive and concrete. This alkali increase may initiate and sustain adhesive deterioration, which is a common moisture related damage.

Several screeded concrete slabs with PVC flooring were prepared to reproduce and monitor moisture distribution and the subsequent redistribution. The moisture distribution before flooring and after a certain period of redistribution is presented. In addition, sorption isotherms including scanning curves were determined in a sorption balance for materials used in the floor constructions, viz, w/c 0.65 concrete, w/c 0.4 concrete, w/c 0.55 cement mortar, and Floor 4310 Fibre Flow, a self levelling flooring compound. Repeated absorption and desorption scanning curves starting from the desorption isotherm were also investigated.

The measurements performed made it possible to develop both a qualitative and quantitative model of moisture redistribution and to quantify the humidity achieved under the flooring. The hysteresis phenomenon of the sorption isotherm is considered in the model.

The model is well suited for estimations of the future RH underneath flooring in a screeded concrete slab and may also be used on homogeneous slabs.

Results from previous research suggested that early drying of the concrete slab can mitigate the increase in relative humidity that occurs when an impermeable floor covering is installed. A study was conducted to verify these results. The results of this new study of the effects of early drying could not demonstrate any significant difference between an early and late dehydration.

The redistribution of ions under different moisture conditions was investigated with a newly developed method. The method is divided into a precondi-

tioning of test specimens and also a method to determine the redistribution of potassium ions. This preconditioning provides a well defined moisture condition of the specimen, which is important for determining the critical humidity for the transport of ions. The redistribution is detected by examining the ion content distribution before and after the preconditioning of ion species already present in the concrete. Previous research in this area has been conducted through adding chloride ions to the specimens. However, redistribution of chloride ions is impeded in that they bind to the inner pore surfaces, which poses a risk that the critical moisture level may be affected/misjudged.

Key words

Moisture redistribution, ion redistribution, cement based materials, sorption isotherm, hysteresis, scanning

Sammanfattning

Nygjuten betong innehåller överskottsfukt som avges till omgivningen under uttorkningen. Om uttorkningen får fortsätta i en konstant luftfuktighet antar betongen så småningom samma fuktighet. Eftersom betong är ett tätt material tar det lång tid, ofta flera år, innan så har skett. Tills detta har inträffat sker en fukttransport från de inre delarna ut till ytan.

En del av överskottsfukten i betongplattor kan omfördelas till golvytan och därmed öka fuktigheten under en tät golvbeläggning. Eventuellt överskrids då den kritiska fuktnivån. I många sammanhang används en tunnare pågjutning för att jämna av ytan för att kunna lägga en golvbeläggning direkt på underlaget. Det här produktionssättet innebär att ny fukt tillkommer genom pågjutningen och omfördelningen av fukt kompliceras. Om den kritiska fuktnivån överskrids kan det leda till materiella skador på golv och lim. Det nya produktionssättet innebär ett behov av att kunna uppskatta den maximala fuktigheten under ett tätt golvmaterial även för pågjutna betongkonstruktioner.

Överskottsfukten innehåller joner från cementet, framför allt kalcium men också mindre mängder kalium och natrium, vilka alla höjer pH i fukten och gör den basisk. Den starkt basiska och fuktiga miljön har en negativ inverkan på många material. Golvlimmet under en PVC-matta är ett material som är känsligt för en sådan miljö. Genom att torka bort en del av överskottsfukten är det möjligt att limma golvmattan utan att riskera att limmet bryts ner.

Med dagens snabba byggtakt är det gynnsamt att torka bort så lite som möjligt av överskottsvattnet, med en viss säkerhetsmarginal, och ändå undvika att en fuktskada uppstår.

Målet med den här doktorsavhandlingen var dels att utveckla en modell och metod för att förutsäga den framtida relativa fuktigheten i en pågjuten betongplatta, och dels att utveckla en metod för att bestämma den kritiska fuktigheten för jontransport i betong.

Omfördelningen av kvarvarande fukt kan också föra med sig alkalijoner och öka koncentrationen i kontaktytan mellan lim och betong. Denna alkaliökning kan tillsammans med den omfördelade fukten initiera och upprätthålla nedbrytning av lim, vilket är en vanligt förekommande fuktrelaterad skada.

Flera pågjutna betongplattor med PVC-matta tillverkades för att skapa och följa fuktfördelningen och efterföljande omfördelning. Fuktfördelningen före golvläggning och efter en viss tid av omfördelning presenteras för de tillverkade betongplattorna. Dessutom bestämdes sorptionsisotermer inklusive scanningkurvor med en sorptionsvåg för materialen som användes, betong med vct 0.65 och vct 0.4 och ett cementbruk med vct 0.55, samt Floor 4310 Fibre Flow, en

självavjämnande golvmassa. Upprepade absorptions- och desorptionsscanningkurvor som startat från desorptionsisotermen bestämdes också.

De utförda mätningarna gjorde det möjligt att utveckla en kvalitativ och kvantitativ modell för fuktomfördelningen och att kvantifiera hur fuktigt det blir under en tät golvbeläggning. Båda modellerna tar hänsyn till inverkan av hysteres. Den kvantitativa modellen lämpar sig väl för bedömningar av den framtida fuktigheten, i % RF, under golv i en pågjuten betongplatta och kan också användas på homogena plattor.

Resultat från tidigare forskning antydde att en tidig uttorkning av betong plattan kan mildra höjningen av relativ fuktighet som sker vid omfördelning under en tät golvbeläggning. En studie genomfördes för att kontrollera dessa resultat. Resultaten från den nya studien av inverkan av tidig uttorkning kunde inte påvisa någon betydande skillnad mellan en tidig eller sen uttorkning.

Uttorkning av betong genererar en fukttransport mot den torkande ytan. Den fukttransporten kan leda till en anrikning av joner vid ytan. Omfördelning av joner vid olika fukttillstånd undersöktes därför med en nyutvecklad metod. Metoden är indelad i en förkonditionering av provkroppar och dels en metod för att mäta omfördelningen av kaliumjoner. Metoden innebär att fukttillståndet i provkroppen blir väldefinierat, vilket är viktigt för att bestämma den kritiska fuktigheten för transport av joner. Dessutom mäts omfördelningen av joner som redan finns i betong. Tidigare forskning på det här området har utförts med hjälp av tillsatta kloridjoner. Transporten av kloridjoner hindras i viss mån att omfördelas genom att de binds till de inre porytorna vilket innebär en risk när den kritiska fuktnivån ska bestämmas.

Papers

This thesis is based on the following papers, which will be referred to in the text by their Roman numerals. The papers are appended at the end of the thesis.

Paper I. Remote monitoring and logging of relative humidity in concrete, Åhs, M., (2005). Proceedings of the 7^{th} Symposium on Building Physics in the Nordic Countries, The Icelandic Building Research Institute, Reykjavik, Iceland, pp 181-187.

Paper II. A method for study sorption phenomena, Åhs, M., Sjöberg, A., Anderberg, A., (2005), Proceedings of the 10^{th} International Conference on Indoor Air Quality and Climate, Beijing, China, pp 1969-1973.

Paper III. Scanning sorption isotherms for hardened cementitious materials, Åhs, M., (2008), Construction and Building Materials, Volume 22, issue 11, pp 2228-2234.

Paper IV. Moisture distribution in screeded concrete slabs, Åhs, M., Sjöberg, A., (2008), Nordic concrete research No. 38, pp 179-192.

Paper V. A quantitative model of moisture redistribution in dual layer concrete slabs with regards to hysteresis, Åhs, M., (2008). Proceedings of the 8^{th} Symposium on Building Physics in the Nordic Countries, Report R-189, Dept. of Civil Engineering, Technical University of Denmark, Kgs. Lyngby, Denmark, pp 873-880.

Paper VI. Influence of early drying of concrete on humidity under impermeable flooring, Åhs, M., Nilsson, L.-O., *(Submitted to Cement and Concrete Research).*

Paper VII. A method to determine the critical moisture level for unsaturated transport of ions, Åhs, M., Nilsson, L.-O., Ben Haha, M., *(Submitted to Cement and Concrete Research).*

Contribution of co-authors

Paper II: Sjöberg contributed in planning the paper, and Anderberg gave detailed instructions on the functionality of the sorption balance.

Paper IV: Sjöberg contributed in planning the paper and assisted in the development of the qualitative model of moisture redistribution.

Paper VI: Nilsson contributed in planning the paper and assisted in the development of the qualitative model of redistribution of moisture after early drying.

Paper VII: Nilsson assisted in developing the moisture conditioning method, Ben Haha developed the method applied to obtain data from the conditioned specimens subjected to the SEM-EDS analysis and performed all SEM-EDS measurements.

Contents

Chapter 1

Introduction

Large quantities of moisture are found in cement based materials in the hardened state, especially in high water cement ratio, w/c, concrete. This moisture is a residue after curing and may cause damage to materials in contact with the concrete. Apart from the adverse impact of the material itself, the damage inflicted by the moisture may also considerably affect the residents' health and well-being. One example where a material may be damaged by this moisture is the adhesive underneath a PVC flooring. In order to avoid this, it is important to assess the moisture distribution in the floor structure, for example before the flooring is applied. By performing this assessment it is possible to estimate the future humidity exposure of the adhesive and the flooring material.

In order to prevent damage caused by the residual moisture the expected maximum humidity level should remain below the critical level. A typical example is concrete floors where this maximum humidity level is achieved just below the flooring when there has been time for the residual moisture inside the slab to be redistributed. A lot would be gained if this expected humidity could be better estimated, for instance on the basis of measurements performed prior to flooring. The critical humidity is often expressed as relative humidity, RH, which is convenient as the RH in a material is a good measure of the expected moisture condition in adjacent materials. In addition, RH measurements on cement based materials are reliable and less affected by uncertainties compared with moisture content measurements [1].

The maximum relative humidity achieved in a homogeneous concrete floor under the flooring may be estimated before the flooring is applied by using the RH method. The RH method includes detailed instructions on how to deter-

mine the RH in a concrete floor slab. Among others, the RH measurement is to be performed at a certain depth to estimate the RH obtained beneath the flooring on homogeneous concrete ground slabs after redistribution. In such slabs the maximum RH level achieved is said to correspond to an RH determined before application of the flooring, at a depth of 0.4h from the slab surface, where h is the thickness of the slab [1].

The Swedish RH method includes detailed instructions on how to report the determined RH together with an estimation of the achieved uncertainty [2]. One of the factors which adds to the uncertainty is temperature fluctuations. Former standards included such fluctuations with an estimated uncertainty. Logged in-situ measurements performed with certified equipment have shown unexpectedly large disturbances as a consequence of temperature fluctuations. This logging equipment, developed to monitor the drying process in concrete floors, is described in detail in Paper I. It has changed the Swedish standards to also include temperature logging.

This thesis presents a method to estimate moisture redistribution in a screeded concrete slab after the flooring is applied. The method considers not only the constituent materials and initial conditions, but also the desorption isotherms and scanning curves. The method is also applicable to homogeneous slabs with consideration taken to scanning.

Additionally, a method is proposed to determine the critical humidity for ion transport in concrete, which is an important factor in promoting adhesive deterioration. This was accomplished by designing an experimental conditioning procedure and by using SEM-EDS to detect alkali redistribution at low concentrations. The conditioning procedure was developed to generate a well-defined moisture state inside a concrete specimen, uniform both in terms of moisture content and relative humidity. This was achieved by utilizing thorough knowledge of moisture fixation and transport and their dependence on moisture history.

A brief theoretical background to cement based materials, moisture and ion transport related properties is presented in chapter 2. Furthermore, the developed qualitative and quantitative models concerning moisture redistribution are described in chapter 3. In addition, a qualitative model of ion redistribution in unsaturated concrete is proposed in that chapter. Input to the models is presented in chapter 4, where moisture properties such as sorption isotherms and examples of repeated scanning curves are shown. In chapter 5, the suggested quantitative model is verified by applying it to a number of screeded concrete slabs. There is a discussion of the presented models and some general conclusions in chapter 6. The last chapter provides suggestions for future research.

Chapter 2

Theoretical background

2.1 Structure of cement based materials

Concrete is made of water, cement and aggregate, and may be treated as a mixture of two separate phases, solid particles and a cement paste, see Figure 2.1. The main purpose of aggregate is to work as a filling material, hence reducing the cement content in the concrete mix. It also serves as a structure for the paste to fix during hardening.

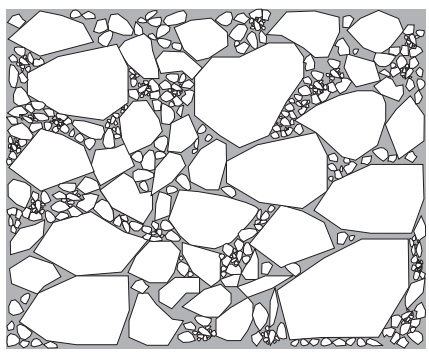

Figure 2.1: Illustration of concrete divided into two phases, white polygons and shaded area representing aggregate and cement paste respectively.

The cement paste is a mix of water and cement. Many different properties of cement paste and hardened concrete are affected by the mass ratio between water and cement, w/c. This ratio quantifies the density of cement grains in the ce-

ment paste, see Figure 2.2. The w/c affects pouring related properties important in fresh concrete, e.g. workability, stability and setting. In the hardened state other properties are affected, such as pore size distribution, porosity, permeability, diffusion coefficients, and moisture content in relation to relative humidity, the sorption isotherm.

Figure 2.2: Illustration of a high water cement ratio to the left and a low water cement ratio to the right. Water, reaction products (C-S-H gel and others), and cement grains are represented by the white area, lighter and darker shaded polygons respectively.

When cement and water are mixed, chemical reactions are initiated. The reaction that occurs when water becomes chemically bound to the crystal structure of cement is called hydration. At an early stage the hydration rate is high as there are a lot of available unhydrated cement grains surrounded by liquid water. The process slows down when the amount of available water and unhydrated cement decrease.

Reaction products start growing from the surfaces of the cement grains immediately after mixing, see Figure 2.3. As they multiply and grow the reaction products soon bridge the water filled gaps between cement grains and aggregate. The C-S-H gel connects the solid particles forming a complex fine lattice, the concrete hardens.

Figure 2.3: Polygons representing, from left to right, unhydrated, partly hydrated and almost completely hydrated cement grains. The hydration of a cement grain, the C-S-H gel and the unhydrated core are shown as a lighter and darker shaded area respectively.

All pores are believed to be irregular as they are made of building blocks of various shapes; their true shape has not yet been revealed. Many models have been presented throughout history in efforts to explain experimental data, one accepted model is the ink-bottle theory [3, 4]. This theory describes the pores as ink bottles with a narrow neck. Pictures taken with SEM show evidence that pores should be treated more like slit pores [5]. There are a number of more recent models, [6, 7], which were developed in efforts to find a better agreement with new experimental data. Furthermore, a number of models for the nanostructure of C-S-H are summarized by Richardson in [8].

Pores in concrete vary in size from nanometres found in the C-S-H gel, to centimetres, air voids remaining after pouring and compacting. Some of these pores are partly filled with water, some are emptied as the water chemically binds in the lattice and some still remain water filled. Among other things, the pore size distribution determines the concrete's ability to bind water from the surrounding atmosphere, it also influences the moisture transport and capillary suction.

2.2 Moisture fixation in cement based materials

Moisture becomes chemically fixed in the solid because of the cement/water reactions during hydration. Moisture from residual water, exterior liquid sources, and surrounding air becomes physically fixed on material surfaces and in capillary pores by forces originating from molecular attraction, such as cohesion, adhesion, and adsorption.

Moisture in air, which is a mixture of different gases, appears as vapour. The amount of water molecules in air is dependent on environmental conditions. Air above a plane water surface is for example completely saturated, see Figure 2.4, meaning that the maximum water vapour content is reached. The water vapour content is exerting a partial pressure on the air, expressed in Pascal. At atmospheric pressure and temperatures the saturation vapour content is mainly dependent on the temperature.

A practical way of defining the amount of water vapour in air is to relate it to the saturation vapour content, v_s. This relation is often called the relative humidity, RH, and is expressed as a ratio between actual, v, and saturation vapour content in percent RH (% RH).

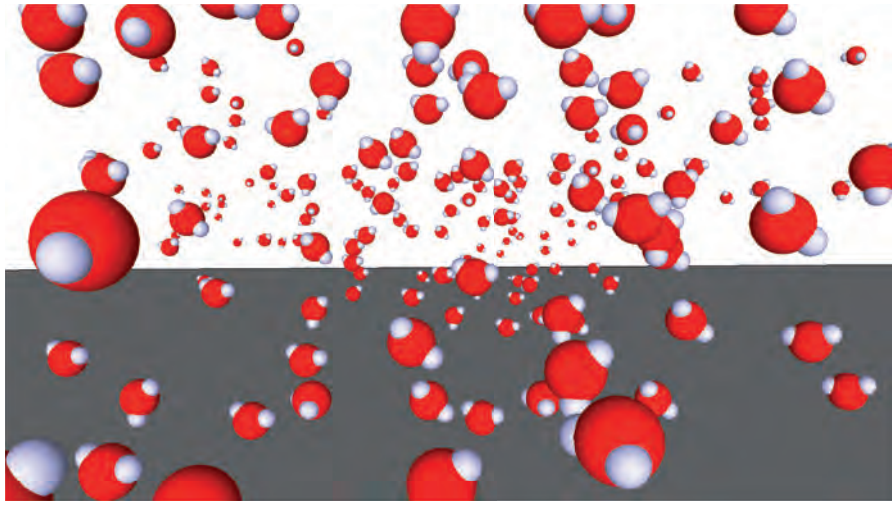

Figure 2.4: Illustration of water molecules in air moving randomly above a flat water surface, shaded area.

A proper definition of the moisture content in air includes both RH and temperature. For example air containing 0.0086 kg/m^3 at 20 °C is equal to a RH of 50 % RH at 20 °C. The RH is calculated using Eq. (2.1).

$$RH = \frac{v}{v_s} \tag{2.1}$$

The vapour content in indoor air is usually limited to about 0.004 - 0.020 kg/m^3. When the saturation vapour content is exceeded the vapour will condense on material surfaces and change to a liquid. The RH level in indoor air regularly fluctuates between some 30 - 70 % RH. Higher RH levels are frequently reached on a short time basis for instance in bathrooms when a resident takes a hot shower. RH below 30 % RH is also reached, for example, in hot indoor premises during winter time when the moisture content of the outdoor air is low.

Physical fixation of moisture vapour on a material surface is linked to the RH in adjacent air. The external and internal surfaces of a dry concrete prism exposed to a humid environment will bind moisture from the air. Water molecules will become attached to it and accumulate on exterior and interior surfaces, see Figure 2.5.

The energy surplus exhibited by the dry material surface will decrease as vapour molecules exhibiting energy deficit attach to the surface. This will hap-

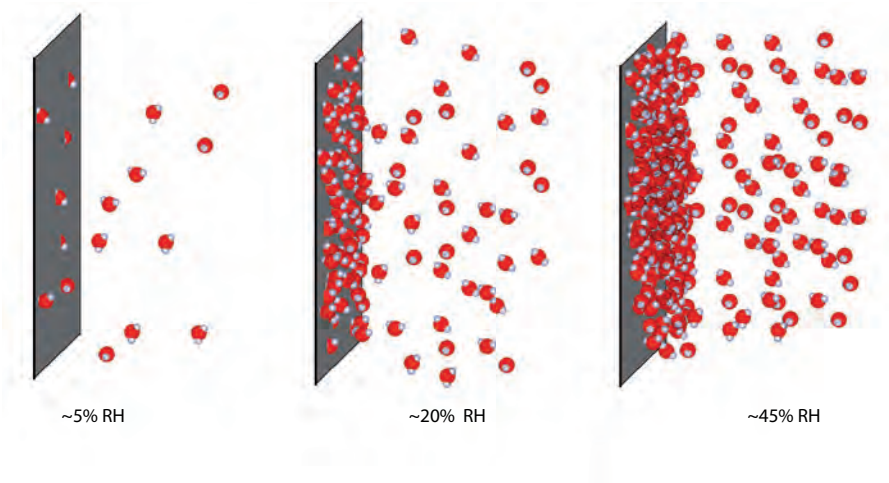

Figure 2.5: Adsorption of water molecules on a material surface, the adsorbate thickness grows from left to right with an increasing RH level.

pen as a result of the chemical potential difference of air borne water molecules and the water molecules attached to a material surface.

Water molecules are merely momentarily attached to the surface on locations called adsorption places. Bonds forming between molecules and surfaces are usually weak hydrogen or van der Waals forces. In contrast to ionic bindings these bindings are easily broken. Molecules continue accumulating on the surface until they reach the lowest possible energy level. This new energy level is called the equilibrium state. At this state an equal amount of molecules attaches to and leaves the surface. As the RH increases, further water molecules stay on the surface for a longer time, ultimately forming a thin water film on the surface.

The process when water molecules are accumulating on a surface is called adsorption and the thin film formed is called an adsorbate, see Figure 2.5. The opposite process is called desorption, when water molecules are released from the surface to the dry air.

Porous materials like concrete exhibit both exterior and interior surfaces available for adsorption, e.g. edges and pore wall surfaces. The pore surface area in ordinary concrete is in the range of 80 - 140 m^2/(g "dry" concrete) [9]. This comparatively large area partly explains the ability of porous materials to adsorb substantial amounts of moisture compared with solid nonporous materials such as metals. Pure adsorption only includes moisture attaching to the surface as a consequence of chemical potential differences.

As the RH increases, further water molecules attach to the adsorbate, ultimately generating a more liquid like film on the surface. There are many theories explaining the nature of adsorption and binding forces between adsorbed molecular layers. One example of monolayer adsorption is the Langmuir theory [10], multilayer adsorption theories include the BET [11] and Dent's gas adsorption theory [12], to mention two of the theories. Dent's equation shows similarities with adsorption isotherms determined for concrete at a relative humidity below some 45 % RH [13]. In Dent's theory water molecules change their properties as they are adsorbed on a surface. Adsorption on a dry material surface is believed to be stronger bound than that on surfaces covered with a film of water molecules. As more molecules become attached the thickness of water film increases, thus gradually decreasing the binding force.

Water surfaces in small pores will curve at the pore walls depending on surface tension forces [14] acting between the adsorbed moisture layers and the material. Suddenly at a certain RH a meniscus is created. This meniscus bridges the empty pore space separating the adsorbed moisture layers, see Figure 2.6.

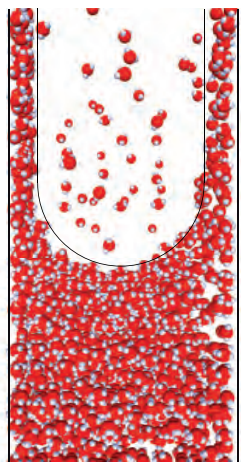

Figure 2.6: Illustration of water molecules moving above a curved water surface in a small pore in concrete.

A hydrophilic material such as concrete will exhibit concave water menisci. The concavity curvature at the pore wall becomes increasingly important as the pore size decreases, the capillary phenomenon exists at pore sizes between 1.4 nm - 0.1 μm. Below 1.4 nm the tensile strength of water is exceeded [13] therefore menisci are considered to be nonexistent below this pore radius.

Saturation pressure above a concave water surface is less than that over a flat surface, and also less over a flat surface than over a convex surface. The Laplace equation [15, 16], was used by Thomson in [17], to derive an expression for the relation between the saturation pressure above a curved surface, p, and the saturation pressure above a plane water surface, p_{sat}. This relation may be rewritten to the familiar expression known as the Kelvin equation Eq. (2.2),

$$\ln\left(\frac{p}{p_{sat}}\right) = -\frac{2 \cdot \gamma \cdot V_m}{T \cdot R \cdot r_m} \tag{2.2}$$

where,γ, is the surface tension, V_m, is the molar volume, T, is the absolute temperature, R, is the gas constant and, r_m, is the mean radius of curvature of the meniscus, also known as the Kelvin radius.

The number of water molecules that exceed the saturation pressure above a concave surface will condense on the meniscus formed by the water, until a new equilibrium is reached, thus enlarging the radius. This process, called capillary condensation, is believed to exist at RH levels exceeding some 45 % RH which corresponds to a Kelvin radius of 1.4 nm in a cylinder shaped pore. Above this level capillary condensation becomes the superior moisture binding mechanism.

The common term used for adsorbed and capillary condensed moisture put together is absorbed moisture. Concrete is able to physically bind substantial amounts of moisture, exceeding 100 kg/m^3.

The external and internal surfaces of a moist concrete exposed to a dry environment release moisture to the air. Completely filled pores at the surface will lose water molecules to the air and menisci will develop. These menisci will break when the saturation pressure above the concave pore radius is less than the actual vapour pressure. However, this breaking of the meniscus corresponds to a lower RH level than that for creating the menisci. All corresponding pores in connection to the surrounding atmosphere at an equal pore size will in due time release moisture to the air.

A sorption isotherm is a property that defines the mass of physically bound water held in a material with respect to RH at a specific temperature. It expresses the equilibrium moisture content in a material in relation to the corresponding RH. The equilibrium moisture content at a certain RH is higher for a saturated cement based material subjected to drying than for a completely dry material moistened to the same RH. The former process, drying of a saturated material sample, is called desorption and the latter absorption. If a process change occurs, for instance from drying to wetting, the RH increases corresponding to a scanning curve.

The desorption and absorption isotherm branches including a scanning curve of a w/c 0.65 concrete determined at 20 °C are shown in Figure 2.7.

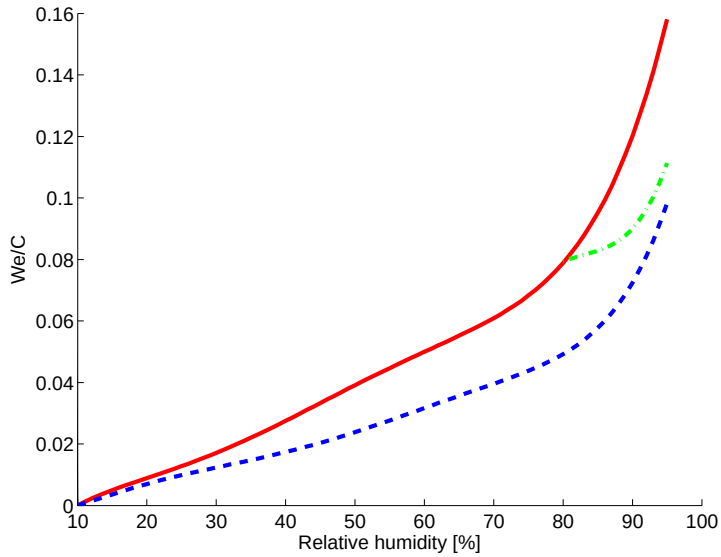

Figure 2.7: Sorption isotherm of a w/c 0.65 concrete between 10 - 95 % RH, including one absorption scanning curve determined from 80 - 95 % RH. The desorption isotherm is represented by the solid line, absorption scanning curve by the dash dotted line, and the absorption isotherm by the dashed line.

Inside this area spanned by the two sorption isotherms every combination of moisture content and RH is obtainable depending on the preceding moisture history. When a material like concrete is re-wetted at some humidity level, after an initial drying, the increase in RH will give rise to a new isotherm, a scanning curve, see dash dotted line in Figure 2.7.

A material showing a desorption isotherm separated from the absorption isotherm is said to exhibit hysteresis. A general definition of the hysteresis phenomenon by Everett [18] states that

> *A process is said to exhibit* hysteresis *if, when the direction of change of an independent variable x is reversed, a dependent variable Y fails to retrace the values through which it passed in the forward process; the dependent variable "lags behind" in its attempt to follow the changes in the independent variable…*

In other words a material is said to exhibit hysteresis if the moisture content in a material during desorption fails to retrace its values while it was absorbing moisture. Cement based materials like concrete exhibit hysteresis to a variable degree.

There are a number of theories of why adsorption hysteresis occurs in a porous material like concrete. The classical ink bottle theory developed from two articles by Kraemer [3] and McBain [4], is one example of a model which may explain the hysteresis phenomenon. The ink bottle theory is based on the assumption that the pores are interconnected with varying sizes of radii and have the shape of ink bottles.

One key requirement for adsorption hysteresis to occur is that there is at least one spontaneous irreversible step change when there is a change from a drying to a wetting mode. This irreversible step could be described to exist in an open ended cylinder where the building of a meniscus does not occur at the same humidity as its collapse, see Figure 2.8 left.

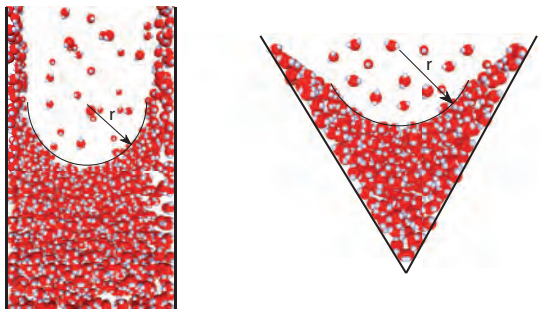

Figure 2.8: Illustration of a concave meniscus formed in a cylindrical (left) and a tapering (right) pore as a consequence of multiple layers of water molecules and capillary condensation, r is equal to the Kelvin radius.

This means that the capillary condensation phenomenon on its own is not enough to achieve hysteresis. In a tapering pore, see Figure 2.8 right, capillary condensation should occur reversibly, as capillary condensation during absorption occurs at the same RH level as it ceases during desorption.

2.3 Moisture transport in cement based materials

There are, traditionally, three basic mechanisms governing moisture flow through a material; capillary suction, diffusion and convection. Moisture flow through

a cement based material like concrete occurs in the cement gel and is governed by capillary suction. Transport of moisture through a gas, i.e. air, by convection originating from an external air pressure difference is insignificant in this study.

Diffusion is defined as transport of matter through a fluid, air or liquid, due to differences in chemical potential, both occurring in cement based materials. The chemical potential may be described as concentration differences occurring from unevenly distributed molecules in a confined fluid volume. The molecules will eventually become uniformly distributed because of diffusion. Such transport is spontaneous and comes from the random motion exhibited by all molecules immersed in a fluid.

The predominant diffusion in concrete takes place as water vapour transfer through air in the communicating pore system. Diffusion of entrained air through water also takes place in partly filled capillaries. Moisture diffusion also exists on a molecular level in the thin layer of adsorbed water molecules on the pore walls. A selection of findings shows that this surface diffusion exists in porous materials like amorphus silica [19], and porous glass [20]. In addition there are findings which have shown minute flow of condensate. In 1952, Carman showed such a flow [21].

The rate of diffusion in concrete is dependent on the porosity, moisture content and tortuosity of the concrete. The diffusion rate increases with porosity and decreases with moisture content and tortuosity.

The total flow is a sum of both vapour flow and capillary flow given by Eq. (2.3),

$$J_{tot} = J_v + J_l \Rightarrow J_{tot} = -\delta_v \frac{\partial v}{\partial x} - \frac{k_p \cdot \partial p_w}{\eta \cdot \partial x} \tag{2.3}$$

where, J_v, represents the vapour diffusion moisture flow and J_l, represents moisture flow due to pressure differences. δ_v, represents the vapour diffusion coefficient, v, represents the vapour content, x, represents the depth from surface, k_p, represents permeability, p_w, represents pore water pressure, η, represents viscosity, and x, represents tube length.

However, up to date it has not been possible to separate these two moisture flows. Diffusion and capillary suction are therefore usually treated as one, and represented by one resistance coefficient, called the diffusion coefficient, see Figure 2.9.

Irregularities of the pore system, see Figure 2.10, are described by the tortuosity factor. The tortuosity factor, τ, indicates the distance a water molecule has to travel to flow through the material, a tortuosity factor of 1 indicating a straight path.

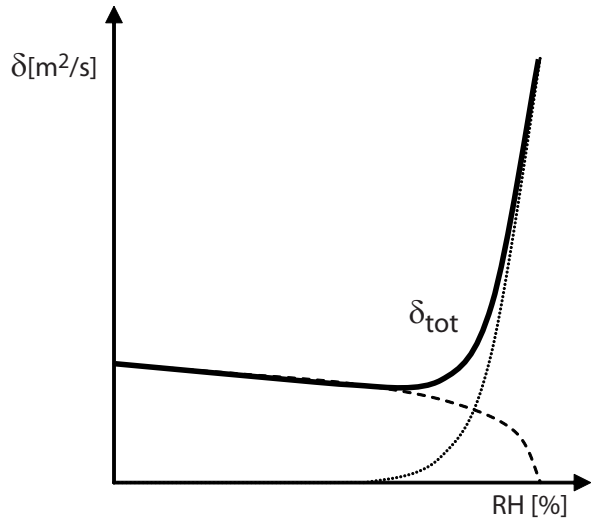

Figure 2.9: Illustration of the diffusion coefficient in relation to relative humidity. The dotted line represents the resistance to moisture flow as capillary suction, the dashed line the resistance to vapour diffusion, and the thick solid line the total diffusion coefficient.

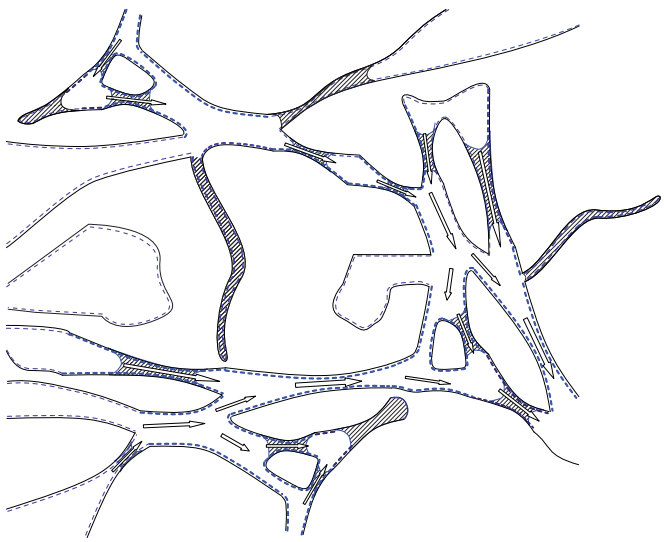

Figure 2.10: Illustration of the tortuosity, some pores are filled with water. Solid lines represent pore walls and dashed lines represent absorbed layers of water molecules. The arrows represent the direction of moisture flow.

2.4 Ion transport in cement based materials

Transport of ions in hardened cement based materials is dependent on moisture in a liquid state. Without water as a solvent, ions are crystallized and therefore unable to move. Ion transport in *saturated* concrete may occur because of concentration differences (diffusion in a liquid) and moisture flow (convection) because of a pressure difference, not necessarily coexisting and not necessarily unidirectional. In *unsaturated* concrete, transport of moisture is caused by moisture flow driven by the pressure difference due to concave menisci, capillary transport, adsorbed water flow and vapour diffusion in the air filled pores. Ions are not conveyed by the vapour diffusion mechanism. It is therefore presumed that the major part of ion transport is governed by the liquid flow, referred to as convective transport, and a minor part by ion diffusion in continuous paths of liquid pore water. The number of published studies describing ion transport in unsaturated concrete is fairly low [22–35].

Various quantities of liquid moisture in unsaturated concrete are found not only as capillary condensed water, but also as thin layers of adsorbed moisture. The quantity is mainly related, apart from temperature, to the RH in the pore system, pore size distribution and whether the present moisture state was obtained by drying or wetting, see section 2.2. This means that there is no fixed relation between the quantity of liquid moisture and RH. The maximum liquid moisture content occurs when the present moisture condition is obtained from a pure drying process. At high moisture content, most of the physically bound moisture is found as capillary condensed water, in contrast to low moisture content where all physically bound moisture exists as adsorbate on pore surfaces.

Ions are carried along with the convective transport in the direction of flow until an air filled pore is encountered. The air filled pore becomes an effective local obstacle to ion transport, as ions are unable to follow vapour diffusion. In such a case it is possible that the pore system offers a path in another direction. The thin liquid water film constituted by the adsorbed moisture may also add to the ion transport, however presumably to a limited extent compared to the convective ion transport by capillary suction. The diffusion mechanism of ions in the adsorbed moisture is disregarded in the following.

As mentioned above there are local obstructions to ion transport in unsaturated concrete. These obstructions occur because of a decrease in moisture content, i.e., the presence of continuous water paths is reduced, see Figure 2.11. This decrease in moisture content reduces the available liquid volume for ions to dissolve into.

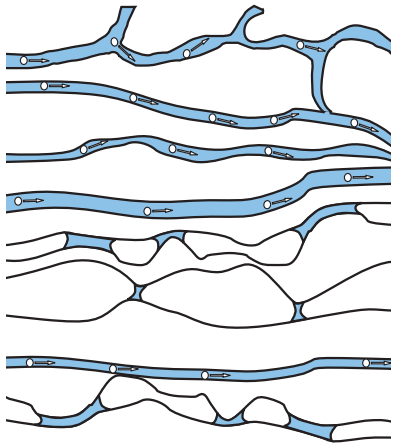

Figure 2.11: Illustration of ion movement in the pore network, some pores are filled with liquid moisture (shaded areas) some are not. Solid lines represent pore walls and pore menisci, and ions are represented by white circles. The arrows indicate the direction of ion movement as a consequence of moisture flow.

Pure desorption

During drying the breaking of the continuous liquid paths occurs first at the concrete surface since moisture interchange with the surroundings takes place there. Hence, it is reasonable to suppose that ion transport to the surface is the first to stop. When the concrete RH at the surface is below the critical RH, ion transport to it completely stops. As capillaries (also in the gel pores) are emptied below the critical RH there are no continuous paths of water reaching the surface. This conclusion is based on the postulate that capillary condensed moisture is removed from the pore system below the critical RH. When drying occurs at a RH level above the critical the quantity of capillary condensed moisture increases. This capillary condensed moisture provides an opportunity for ion movement to the surface.

Scanning

In addition to the breaking of continuous water paths, their growth at re-wetting is an important issue that must be taken into account. The growth does not occur at the RH level at which they are broken, but at a higher level. This means that the humidity increase after an earlier decrease must be considerably higher

than the former until the broken continuous paths are re-established. The opportunity for ion transport has therefore significantly decreased if the concrete has undergone drying before entering the current moisture state. This breaking and re-establishing is furthermore involved when the humidity decreases subsequent to an increase.

Ion accumulation

Ion accumulation may occur in proximity to the drying surface where the moisture content is too low to allow further transport. At a larger distance from the surface, ions are still conveyed towards the dry zone. This would mean that an ion content peak may form with a maximum at a certain distance from the surface [28, 34].

Transport of ions in the hygroscopic range has been reported previously in [23–26, 28–30, 36–38]. These authors suggest a number of different strategies to generate and determine ion transport. One technique is to put ground solid NaCl in contact with conditioned mortar specimens and thereafter determine the chloride ingress [23]. Another technique [24–26] has been to measure chloride ingress after exposure to Cl_2 at different degrees of saturation. Francy [28] used impedance spectrometry to quantify the chloride diffusion coefficient at various RH-levels. Nielsen and Geiker [29] immersed specimens conditioned to a series of RH-levels in a salt solution. Angst [30] mixed various amounts of NaCl into the concrete mixes. Wengholt-Johnsson [36] and Anderberg [37] studied alkali transport from a partly dried concrete to a screed. A completely different approach was applied by Nilsson et al. [38], they detected ion transport by determining the distribution of K_2O in concrete specimens subjected to a number of different drying conditions.

Chapter 3

Models

In this chapter a model of redistribution of residual moisture in homogeneous slabs is presented in the first section. In the second and third sections of this chapter two models are presented, a qualitative and a quantitative model, which may be utilized to comprehend and assess redistribution of residual moisture in screeded slabs. The fourth section presents a qualitative model of moisture redistribution after early drying and the fifth section presents a qualitative model of alkali redistribution.

3.1 Previous model of moisture redistribution

In 1978 a method was developed to determine the future maximum humidity obtained beneath flooring in a drying homogeneous concrete slab [1]. This model is based on the assumption that no moisture leaves the slab after flooring, that the slab base is also sealed, and that isothermal conditions are present. The residual moisture inside a sealed slab will be redistributed until the RH level settles on a uniform vertical level, see Figure 3.1. This method only gives a rough RH estimation as it is based on a computer simulation performed where a homogeneous w/c 0.65 concrete slab is subjected to single sided drying, and the effect of hysteresis is neglected. According to this model a standard depth of 0.4h was decided as an equivalent depth where the humidity level is equal to the maximum RH later achieved beneath the flooring. This relation between RH before and after flooring is based on a computer simulation performed in the late 1970s, where a homogeneous 100 mm concrete slab is drying from one side at 20 °C

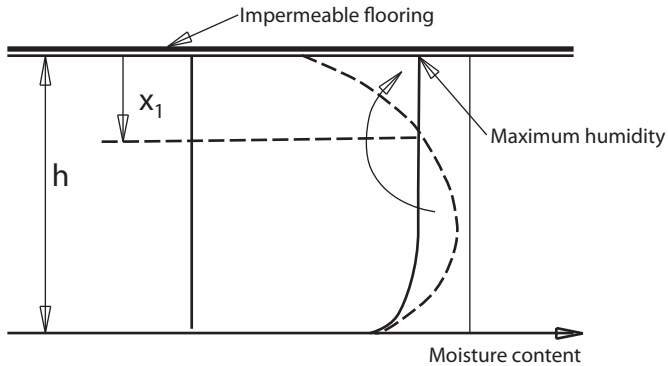

Figure 3.1: The depth x_1 at which the RH level prior to flooring corresponds to the maximum RH level that occurs after flooring installation [1].

and 40 % RH, [1]. Depending on the simulated drying time before flooring the depth from the surface varied between 0.35 and 0.42 of the slab thickness. The simulations are based on the simplification that the RH and moisture content may be described in one single equation. The relationship between RH and moisture content, sorption isotherm, is far more complex.

A sorption isotherm for a single concrete mixture was used in the simulation, without considering hysteresis. This omission of the hysteresis may have an impact on the estimated RH obtained from the simulation.

The method is not applicable to screeded floors. A new method is therefore needed in order to estimate the maximum humidity in such floors, a common construction today. This method is also applicable to homogeneous floor slab constructions and is an improvement to the current model. In the next section moisture redistribution is described qualitatively. In section 3.3 a proposed quantitative model is described.

3.2 Qualitative model of moisture redistribution

In this section a qualitative model is presented which describes the RH distribution for a two material combination, e.g. a screeded concrete slab. Three distinctive phases, drying of the slab, screed application and drying, and redistribution in the screeded slab after flooring, illustrate important stages from a moisture distribution perspective in the production of a screeded floor. These phases are presented together with a corresponding sorption isotherm and scanning curves in Figure 3.2.

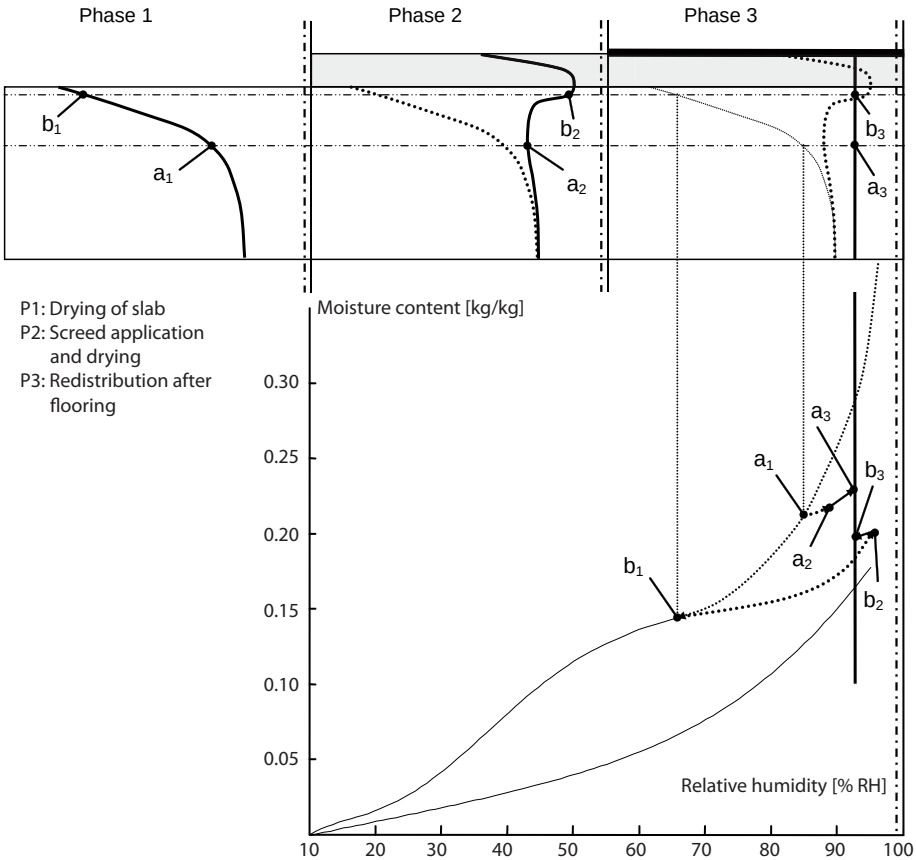

Figure 3.2: Phase 1 shows the distribution of residual moisture (as RH) in a concrete slab after some drying. A wet screed is applied in phase 2 and subjected to drying, and finally moisture is redistributed after flooring. Underneath a typical sorption isotherm is shown where a_i and b_i, indicate two material sections and the subscript indicates the corresponding phase number.

The slab represents a homogeneous slab sealed at the base which is drying upwards. Thick dotted lines show the initial moisture distribution in each phase and solid thick lines represent the moisture distribution just before the next phase is entered. The moisture distribution in phase 1 is included as a thin dotted line in phase 3 to facilitate comprehension of the overall moisture redistribution changes and corresponding changes in the sorption isotherm. These changes are indicated for two slab sections, a_{1-3} and b_{1-3}, which are particularly interesting from a moisture redistribution perspective.

In the first phase a concrete slab drying from one side only is shown. The moisture distribution clearly demonstrates a high humidity at the slab base and a lower humidity at the surface. A wet screed is applied on the semi-dry concrete slab in the second phase. This wet screed dries from the top surface and simultaneously moisture penetrates downwards into top surface of the slab. Later, some of the moisture is redistributed towards the slab base. In addition the screed top dries as shown before the second phase is finished. Finally, the third phase shows the moisture distribution when phase 2 is left and after flooring when internal moisture redistribution is completed.

In Figure 3.2 letters (a) and (b) represent material sections where the moisture content follows a particular path in the typical sorption isotherm diagram displayed in the same figure. Letter (a) corresponds to a section somewhat above the slab centre. In the first phase the moisture content decreases, following the desorption isotherm down to point a_1. Subsequently, after screed application, this section's moisture content increases, following an absorption scanning curve up to point a_2 and finishes at point a_3. Letter (b) illustrates a material section somewhat below the top surface of the slab where the moisture content decreases to point b_1, following the desorption isotherm. In phase 2 the moisture content increases by following an absorption scanning curve up to point b_2 and finally decreases finishing at point b_3 by following a desorption scanning curve.

3.3 Quantitative model of moisture redistribution

A theoretical model is proposed that suggests how the future moisture distribution in a screeded slab, which occurs after flooring is applied, can be estimated. The following simplifications are made:

- no further drying of the slab will occur; residual moisture will be redistributed
- isothermal conditions
- moisture transport is not quantified
- homogeneous materials

When a screeded slab is sealed the residual moisture will be redistributed, ultimately attaining a uniform vertical RH distribution, see the red line in Figure 3.3.

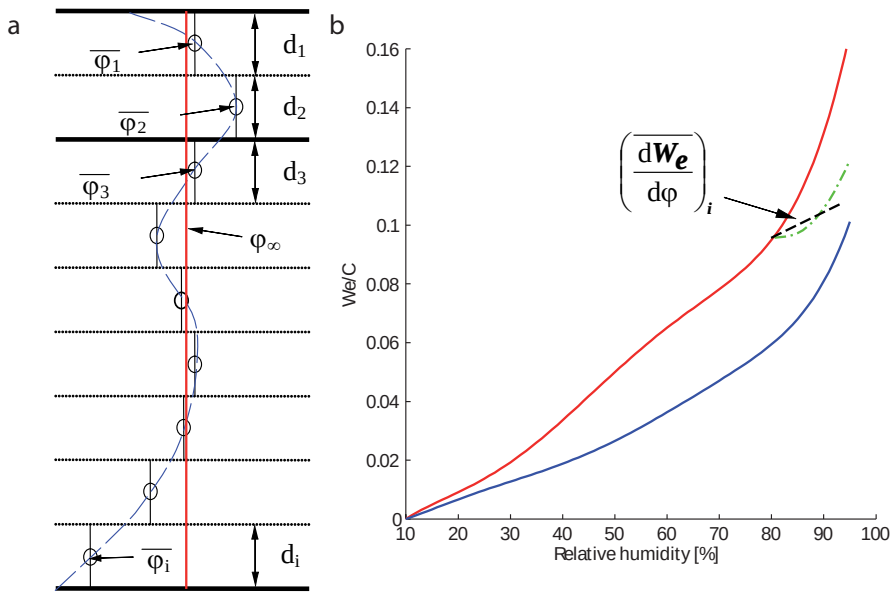

Figure 3.3: Illustration (a) shows the RH distribution in a screeded slab before flooring is applied (dashed line). The solid red line illustrates a possible uniform RH distribution after sealing. Illustration (b) shows a typical sorption isotherm including one scanning curve (dash dotted line) and the average moisture capacity (dashed black line) for this scanning curve.

The change in moisture content in each section is given, provided that each section's moisture history, RH change, and "moisture capacity" are known. The moisture capacity, ξ, for a certain RH is defined by Eq. (3.1),

$$\xi = \frac{dW_e}{d\varphi} \tag{3.1}$$

where, dW_e, represents the difference in evaporable water in kg/m^3, $d\varphi$ represents the difference in relative humidity in % RH, see the dashed line in Figure 3.3.

This property shows how much a moisture content change is affected by a change in RH. Figure 3.4 shows that a change in RH from 80 - 85 % RH does not change the moisture capacity as much as a change from 85 - 90 % RH does. In other words a steep sloping isotherm gives rise to a high moisture capacity and a gentle sloping isotherm gives rise to a low moisture capacity. This means that

small moisture transfers from wet to dry regions in a concrete change the RH level according to the previous history of the moisture receiving region.

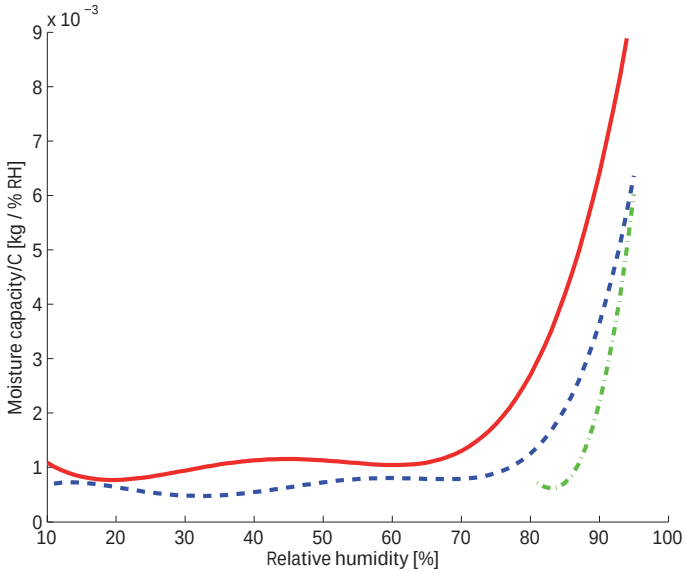

Figure 3.4: Illustration of the moisture capacity of a w/c 0.65 concrete including the moisture capacity of a scanning curve determined in the 80 - 95 % RH range. The moisture capacity of the desorption isotherm is represented by the solid line, the absorption scanning curve by the dash dotted line, and the absorption isotherm by the dashed line.

As the total moisture content will be maintained in the sealed slab it is possible to calculate the uniform RH level. This is done by adding the change in moisture content in all sections. As no moisture is lost this sum must be zero. The solution to this problem is obtained by iteration.

Based on the assumption that no moisture will escape from the screeded slab, the uniform RH level will settle somewhere in between the extremes of the RH distribution prior to sealing. A reasonable initial guess may be the mean RH. The next step will be to determine the moisture history of each section in order to assign a realistic moisture capacity.

Judging from Figure 3.3 both the slab base and screed sections have only experienced drying prior to flooring. Therefore they must be assumed to have reached their moisture content and corresponding RH level by following the desorption isotherm. Top slab sections, on the other hand, have experienced both drying and wetting prior to flooring, thus obtaining their moisture content

and RH level by following a scanning curve. The above qualitative analysis is of great importance when the future redistribution of moisture is determined.

The future moisture content in each section is determined from the preceding drying-wetting history as well as the expected moisture gains or losses to adjacent sections in the future. If a section following a desorption isotherm will lose moisture to attain the guessed RH level, its moisture capacity will be determined from the desorption isotherm. If, on the other hand, a section follows the desorption isotherm and suddenly starts to gain moisture, the moisture capacity is obtained from a scanning curve. And finally, sections already following an absorption scanning curve will either continue to follow the absorption scanning curve or, if losing moisture, follow a scanning desorption isotherm.

The assumption of no further drying implies that the moisture content per square metre of the screeded slab is constant before and after the flooring.

The above reasoning and simplifications could represented by an arithmetic expression Eq. (3.2),

$$\sum_{\Delta x_i} (\overline{\varphi_i} - \varphi_\infty) \cdot d_i \cdot \left(\overline{\frac{dW_e}{d\varphi}} \right)_i = 0 \tag{3.2}$$

where $\overline{\varphi_i}$, expressed in [% RH], represents the RH determined in section d_i, φ_∞, expressed in [% RH], represents the uniform moisture distribution obtained after a redistribution is finished, d_i represents the thickness of the section expressed in [m], $\left(\overline{\frac{dW_e}{d\varphi}} \right)_i$ expressed in [kg/m^3]represents the average moisture capacity of section d_i obtained from the sorption (scanning) isotherm at the current RH.

By rearranging Eq. (3.2), Eq. (3.3) is obtained.

$$\sum_{\Delta x_i} \overline{\varphi_i} \cdot d_i \cdot \left(\overline{\frac{dW_e}{d\varphi}} \right)_i - \sum_{\Delta x_i} \varphi_\infty \cdot d_i \cdot \left(\overline{\frac{dW_e}{d\varphi}} \right)_i = 0 \tag{3.3}$$

Equation (3.3) shows the change in moisture content with respect to each section's change from $\overline{\varphi_i}$ to φ_∞. As the slab is assumed sealed no moisture is lost, thus the sum the moisture content changes in all sections is 0 (zero). Equation (3.3) may be rewritten as

$$\sum_{\Delta x_i} \overline{\varphi_i} \cdot d_i \cdot \left(\overline{\frac{dW_e}{d\varphi}} \right)_i = \sum_{\Delta x_i} \varphi_\infty \cdot d_i \cdot \left(\overline{\frac{dW_e}{d\varphi}} \right)_i \tag{3.4}$$

As the final uniform RH, φ_∞, is constant throughout the slab it may be moved outside the summation mark.

$$\sum_{\Delta x_i} \overline{\varphi_i} \cdot d_i \cdot \left(\overline{\frac{dW_e}{d\varphi}} \right)_i = \varphi_\infty \sum_{\Delta x_i} d_i \cdot \left(\overline{\frac{dW_e}{d\varphi}} \right)_i \tag{3.5}$$

Finally the sum on the left side of Eq. (3.5) is divided by the sum of the section thickness multiplied by moisture capacity leaving the uniform RH, φ_∞, on the right side resulting in Eq. (3.6).

$$\varphi_\infty = \frac{\sum_{\Delta x_i} \overline{\varphi_i} \cdot d_i \cdot \left(\overline{\frac{dW_e}{d\varphi}} \right)_i}{\sum_{\Delta x_i} d_i \cdot \left(\overline{\frac{dW_e}{d\varphi}} \right)_i} \tag{3.6}$$

The resulting φ_∞ is thereafter compared with the initial guess. If the difference is large then a new calculation needs to be performed by replacing the initially guessed φ_∞ with the resulting φ_∞. The moisture capacity for each section changes accordingly. This model is verified in chapter 5.

3.4 Qualitative model of redistribution of moisture after early drying

The purpose of this section is to suggest a qualitative model that considers aspects of hydration in a homogeneous floor structure with respect to redistributed moisture during drying. It is assumed that some of the redistributed moisture becomes a part of the solid matter and thereby reduces the increase in humidity below a semi-permeable flooring.

The model assumes a drying environment below 80 % RH before a non-permeable flooring is applied on the floor structure. This is to achieve a substantial humidity decrease at the concrete surface facing the dry environment. Exposure to a dry environment reduces the rate of cement hydration [39, 40], and these dry conditions are mainly achieved in shallow parts of a floor structure. The reduction in degree of hydration may have an impact on the humidity below the adhesive in a floor structure after flooring. The less hydrated cement grains may react with the redistributed moisture and therefore bind some of it chemically. This additional hydration may lower the anticipated RH at the surface, by a delayed self-desiccation, hence reducing or even preventing a moisture damage, i.e. adhesive deterioration.

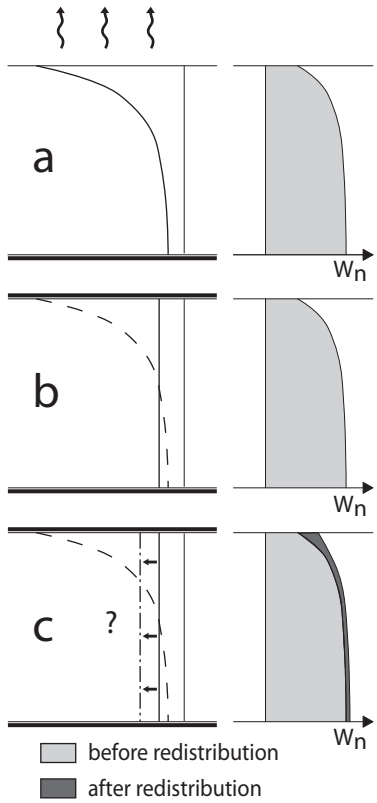

Figure 3.5: a) Single sided drying of a concrete floor slab b) Redistribution of moisture under an impermeable flooring without considering additional chemical binding c) Redistribution of moisture and chemical binding of redistributed moisture.

The suggested mechanism behind the decrease in humidity caused by a continuing hydration is illustrated in Figure 3.5.

The left figures (a-c) show the moisture distribution, MD, and the right figures show the distribution of degree of hydration, represented by w_n. The solid line in (a) represents the MD before redistribution, and in (b) and (c) they represent the MD after redistribution. The dashed lines in (b) and (c) represent the MD before redistribution and the dash dotted line in (c) represents the expected humidity after redistribution. The figures represent from top to bottom

a) The original moisture distribution before redistribution in a floor slab dried from one side only.

b) The floor slab after moisture redistribution where no additional hydration has occurred.

c) The floor slab after moisture redistribution where additional hydration has occurred, especially in the top part with most drying, and the level of humidity has decreased compared with Figure 3.5b.

3.5 Qualitative model of ion redistribution during drying

The aim of this section is to propose a simple qualitative model of ion redistribution in a homogeneous concrete slab subjected to drying. The following assumptions are made:

- Ion transport occurs only at a RH above a certain critical level.
- Ion transport will be larger at a higher RH-level.

Redistribution of ions, in this case, is initiated by a dry environment surrounding the moist concrete structure. This surrounding environment generates a moisture flow, which may convey ions to the drying surface. As mentioned in section 2.4, ions are only able to migrate in liquid moisture in the capillaries. Therefore, ion transport decreases with the emptying of the capillaries.

When drying occurs at a RH below a critical RH level, capillaries in the concrete structure become air filled when equilibrium is attained. Until the surface material reaches a humidity below the critical RH level, some capillaries are still able to convey ions to it. The ions are consequently gradually prevented, because of the air filled capillaries, from reaching the surface. Because of these obstacles, ion accumulation occurs at a small distance from the surface, where enough capillaries are still filled with liquid moisture. This accumulation process continues until the humidity drops below the critical RH level further into the material. This kind of drying process may create a peak of ions located next to the surface, see Figure 3.6 left.

Drying may also occur at a higher humidity level, at which moisture filled capillaries reach the surface during drying and still do at equilibrium until moisture transport ends. The ions are therefore conveyed to and accumulated at the surface, see Figure 3.6 right. The accumulation at the surface in this case does not stop until equilibrium with the surrounding humidity is attained. The peak at the surface gives rise to an uneven distribution which generates a potential for

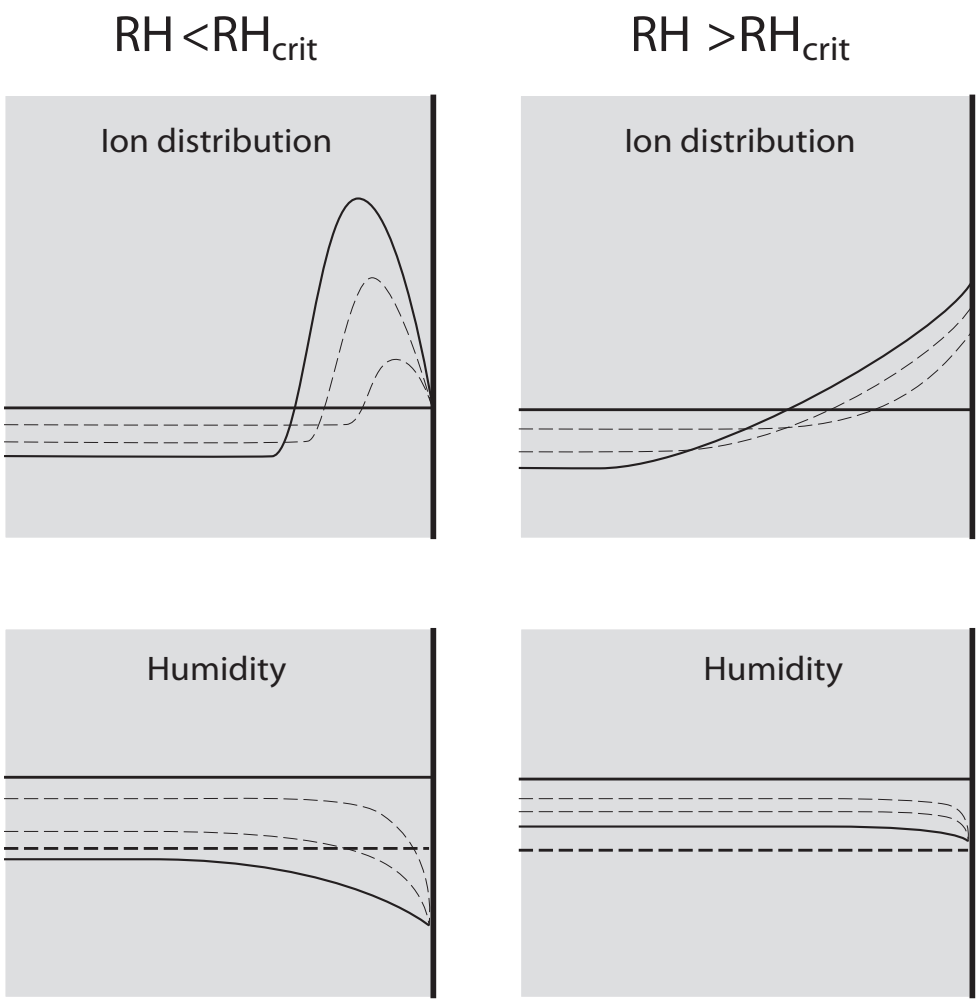

Figure 3.6: Redistribution of ions during drying at a surrounding humidity below (left) and above (right) the critical humidity (thick dashed line).

a diffusion process transporting ions in the opposite direction to moisture flow. This diffusion transport is not hindered as effectively as if the drying climate were lower than the critical humidity.

Both of these drying actions may be combined into one qualitative model of ion redistribution during drying, see Figure 3.7. This model is based on the material's pore system and an assumption that the system to some extent consists of inter-connected pores in which continuous liquid paths are present above a certain humidity, see Figure 3.7a. The humidity at which these paths occur and

are able to convey ions is defined as the critical humidity, RH_{crit}. Furthermore, the pore system in cement based materials is characterized by a wide range of pore sizes. The pore size distribution is decisive for the quantity of liquid moisture at a certain moisture level, and an increase in the moisture level corresponds to an increase in liquid moisture. It is therefore reasonable to assume that there is an increase in ion movement when the humidity increases, see Figure 3.7b.

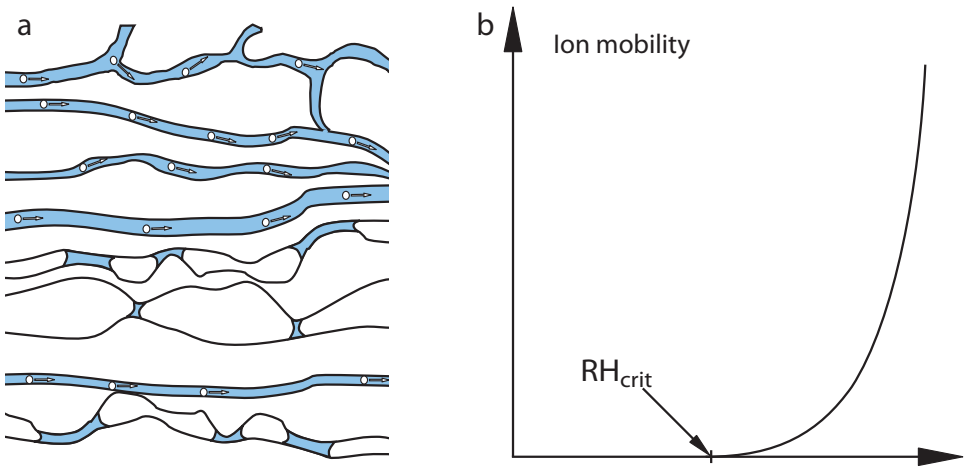

Figure 3.7: Qualitative model of ion redistribution during drying.

Chapter 4

Experimental work

The experimental work in this thesis is presented in this chapter. The manufacture of a number of screeded floor slabs and different materials used in this work is presented in section 4.1. The sorption measurement, applied to determine sorption isotherms of the materials used in the screeded floor slabs, is described in section 4.2 including results. Two methods to determine both absorption and consecutive desorption scanning curves, a comparison between the two and the results obtained are presented in section 4.3. The determined moisture transport properties for some of the materials used are presented in section 4.4, besides the evaluation method. A description of experimental work to investigate the possible beneficial effects of applying drying at an early stage is presented in section 4.5. Finally, the work performed to determine redistribution of alkali in partially saturated concrete is introduced in section 4.6.

4.1 Moisture redistribution

The conducted experimental work followed two basic courses. First of all, test specimens in three batches were manufactured with the aim to replicate the essential characteristics of three common screeded concrete floor constructions. Secondly the material properties were investigated on samples continuously extracted from the floor constructions in order to detect possible property transformations.

Batch 1 was intended to replicate a homogeneous ground slab, Batch 2, an intermediate floor structure, and finally Batch 3, a hollow core slab, HCS. These

batches were produced in full scale regarding thickness, covering an area of 0.5 - 1 m^2, see Figure 4.1.

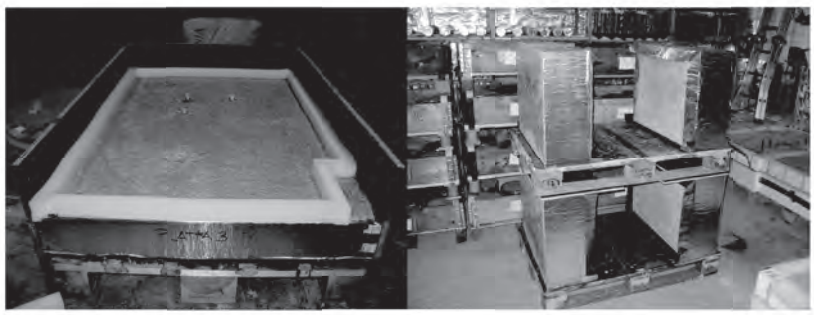

Figure 4.1: Left picture shows one floor construction in Batch 1 prepared for screed application, one corner was spared for sample extraction from the slab. Right picture shows four floor constructions from Batch 2, vertically tilted in a climate conditioned room and not yet covered with screed.

In total, nine concrete floor slabs were produced in this research. Eight homogeneous slabs were manufactured at the laboratory and one HCS was delivered from a factory. The homogeneous slabs were prepared to reproduce two different screed application scenarios, application on a slab subjected to a short period of drying and application on a slab subjected to a longer period of drying. The HCS was prepared to reproduce a situation where a centre hollow core was filled with concrete at the slab end prior to screed and flooring application.

Four cement based materials were used to manufacture the screeded slabs, see Table 4.1. The homogeneous structural slabs were manufactured by using a w/c 0.65 concrete, C. The cement mortar has a w/c 0.55, M, and Floor 4310 Fibre Flow, SFC were used for screed application. Both the concrete and mortar were mixed and poured at the laboratory. The self-levelling flooring compound was delivered as a dry powder mix from the factory. Water was added to the dry powder and mixed in the laboratory according to instructions from the manufacturer. Finally, the HCS was manufactured in a factory by using a w/c 0.4 concrete, C_{HCS}.

Table 4.1: Mixture for each used material. Quantities are presented in kg/m^3.

Material	C	M	C_{HCS}	SFC[1]
Portland Cement CEM II/A-LL 42.5 R	250	400		
Portland Cement CEM I 52.5 R			390	
Portland Cement				1-5
Aluminous Cement				5-20
Gypsum				2-10
Water	162	220	147	20
Dolomite 0.002-0.1 mm				31
Sand 0.1-1 mm				47
Sand 0-8 mm	967	1672	973	
Sand 6-13 mm			851	
Sand 8-12 mm	489			
Gravel 8-16 mm	489			
Polymer				1-5
P30			1.2	
Glenium 51	1.5	2.9		

[1]Mixture according to manufacturer mass-% of dry powder, density 1900kg/m^3

All slabs were subjected to certain drying times in suitable climate rooms before and after screed application. Then a PVC flooring, 2 mm Tarkett Eminent, was installed on all nine slabs by using a water based floor adhesive, CascoProff Solid. Material combinations and application sequences are described in detail in Table 4.2.

Table 4.2: Slab material combination, application sequence, and drying plan.

Batch No.	1				2				3
Slab	1	2	3	4	5	6	7	8	9
Material	C	C	C	C	C	C	C	C	C
1st Drying [days]	105	105	110	110	9	11	408	408	28[2]
Screed	SFC	SFC	M	M	M	SFC	M	SFC	SFC
2nd Drying [days]	48	96	98	90	261	259	40	40	138
Adhesive [m^2/l]	3.6	3.6	3.5	4.3	3.1	3.0	3.3	3.0	3.0
Flooring	PVC	PVC	PVC	PVC	PVC	PVC	PVC	PVC	PVC
Redistr.1[days]	206	158	149	157	269	269	91	91	273
Redistr.2[days]					702	702	729	729	

[2]Initial drying time of the C filling of the mid core, the HCS is cast approx. 60 days earlier.

The humidity distribution was determined in each slab prior to floor application on samples obtained by using a core drill, see Figure 4.2. Subsequent to

floor installation the slabs were put back into the climate room. The moisture distribution was determined once more after a certain time of moisture redistribution, see Table 4.2, and in slabs 5-8 the moisture distribution was determined once again after more than two years after flooring. These moisture distributions are shown in chapter 5. A detailed description of slab preparation, material application and climate conditions is found in Paper IV.

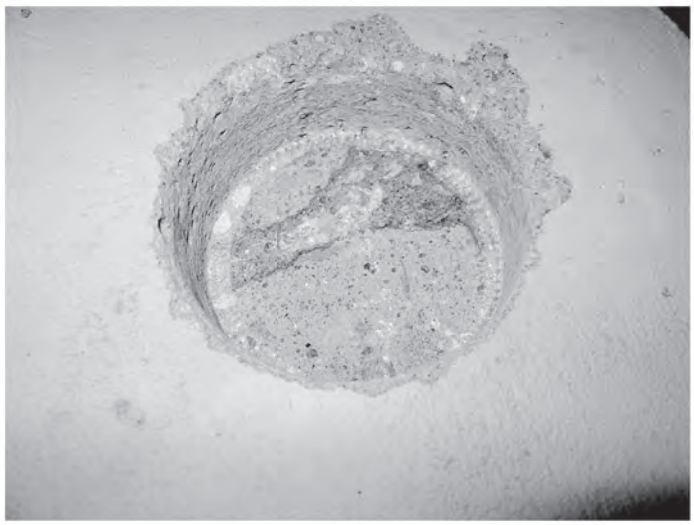

Figure 4.2: The remaining hole from a core drill, 90 mm in diameter, after extracting samples for moisture distribution determination before flooring. Drilling was performed from the top in a homogeneous slab from Batch 1. Note the clear breaking zone separating the mortar screed from the concrete material.

4.2 Sorption measurements

Several sorption measurements were performed on a number of small material samples, 20 - 100 mg, which were obtained from the floor constructions. All but two material samples were chiselled out from the top surface of the material at a depth of about 20 - 25 mm. The two other samples were taken from a depth of 200 mm, in one of the concrete slabs. To avoid carbonated material 10 - 15 mm of the surface material was discarded before sampling. The samples were mainly removed from material subjected to a certain drying time in a 60 % RH at a temperature of 20 °C. Details of the sorption isotherm evaluation are presented in Paper III together with results.

A gravimetric vapour sorption balance, DVS, was used for all sorption isotherm determinations. Its key component is a balance, Cahn D-200, that continuously determines the mass of a sample subjected to a sequence of well-defined constant or variable RH levels. These RH levels are generated from a mixture of dry and saturated nitrogen gas. The generated humid gas stream is split in two before one half passes the reference and the other passes the sample pan. In order to achieve stable conditions the balance is installed inside a climate controlled cabinet. For a detailed description of the sorption balance see Paper II.

Desorption, absorption and scanning curves were determined by changing the RH in the sorption balance stepwise in a certain sequence. The measurements always started with a saturated specimen, which had earlier been subjected to drying. Therefore, the desorption isotherms represent the 2^{nd} desorption. Typical RH sequences are shown in Figures 4.3 and 4.4. The difference between the two sequences is the way RH changes during scanning, with drying followed by wetting or wetting followed by drying. In Figure 4.3 RH changes gradually with time. In Figure 4.4 the change is stepwise.

Each sample was put on a saturated piece of cloth inside a sealed glass container for a minimum period of 24 hours prior to the test, in order to become capillary saturated. Subsequently it was loaded into the sorption balance and subjected to the test sequence.

In order to obtain the asymptotic mass corresponding to each RH level each step change was evaluated by curve fitting according to Eq. (4.1) [41],

$$m(t) = m_f - (m_f - m_0)e^{-k(t-t_0)} \tag{4.1}$$

where $m(t)$ represents the sample mass at the time t, m_0 is the initial mass for each curve fitting, m_f represents the asymptotic final mass, k is a curve fitting constant and t_0 is the initial time for each curve fitting. An illustration of the result from using Eq. (4.1) is shown in Figure 4.5. The best fitting curve was

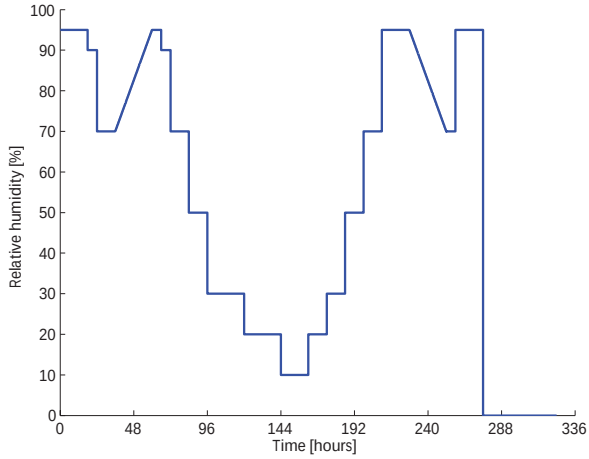

Figure 4.3: Illustration of a typical RH test sequence used in Paper III, where an absorption and desorption scanning curve is determined by using a linearly increasing and decreasing RH.

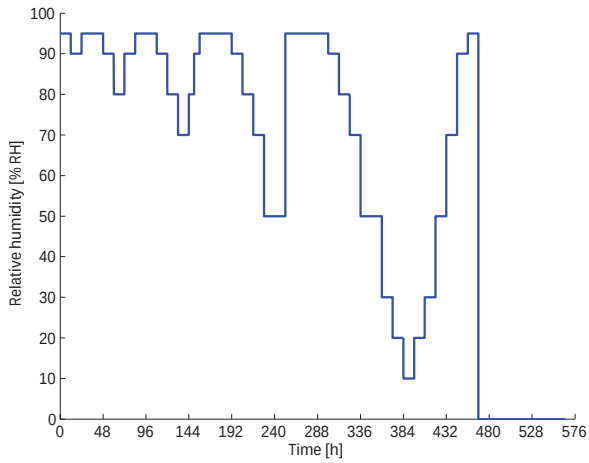

Figure 4.4: Illustration showing a typical test sequence for determining the boundary sorption isotherm loop including inner scanning curve loops by using the most recent method, where RH step changes are used, instead of linearly increasing/decreasing RH.

obtained by the least squares method. This curve fitting is further explained in Paper III. Note that the sample was subjected to 0 % RH at the final step of each test sequence, see Figures 4.3 and 4.4. This arrangement of the 0 % RH exposure was decided on the basis of the hypothesis that chemically bound moisture may be released at RH levels below 10 % RH, thus possibly destroying the material structure [42]. The dry mass was therefore obtained from the curve fitted asymptotic mass at 10 % RH.

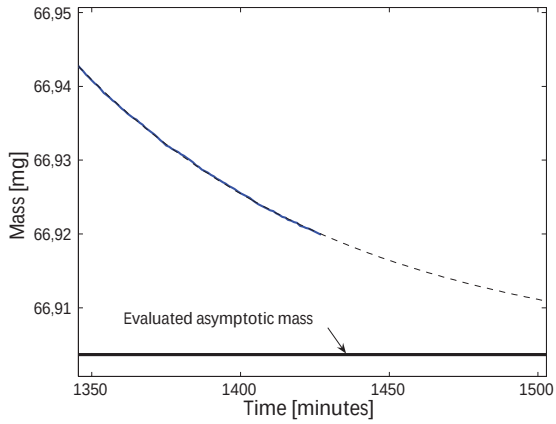

Figure 4.5: Curve fitting of the recorded mass in an RH step to determine the asymptotic final mass for each RH step.

Sorption isotherms were determined for four different materials, two concretes, C and C_{HCS}, cement mortar M, and one flooring compound, SFC. The moisture content is quantified as the evaporable moisture content, W_e, divided by cement content, C, for materials C, C_{HCS}, and M. The cement content was estimated by first quantifying the Ca content in each C, M, and C_{HCS} sample. This was accomplished by using inductively coupled plasma atom emission spectroscopy, ICP-AES. A detailed description of the applied method and the results obtained is found in Paper III. For material SFC the moisture content per mass of material is represented as a fraction of mass at 10 % RH.

Desorption and absorption isotherms for the four materials are shown in Figures 4.6 - 4.9. Additional isotherms determined for C, M, and SFC are found in Paper III. The isotherms determined for material C on samples removed 20 mm from the slab top deviated significantly from isotherms determined on samples removed 20 mm above the slab base. The other materials showed a smaller deviation.

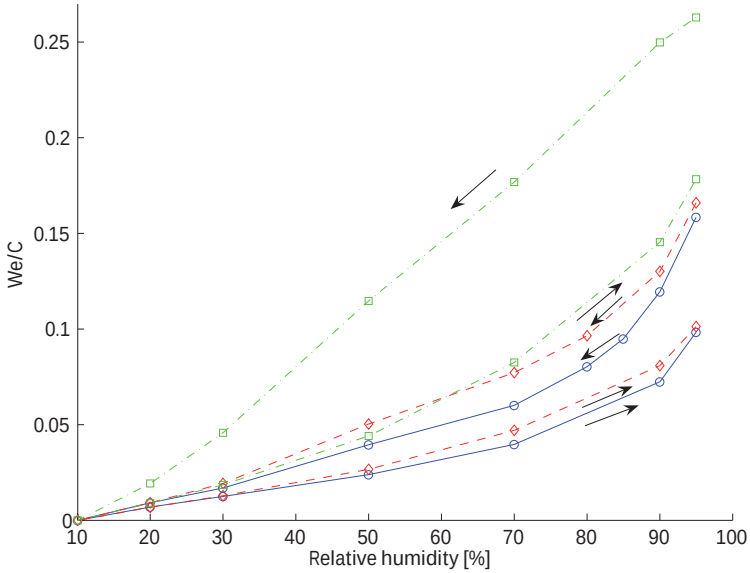

Figure 4.6: Sorption isotherms determined for three samples of material C. One sample, 16 months old (dash dotted line), extracted about 20 mm from the surface facing air, and two samples 9 (dashed) and 12 (solid) months old, extracted about 20 mm from the base surface.

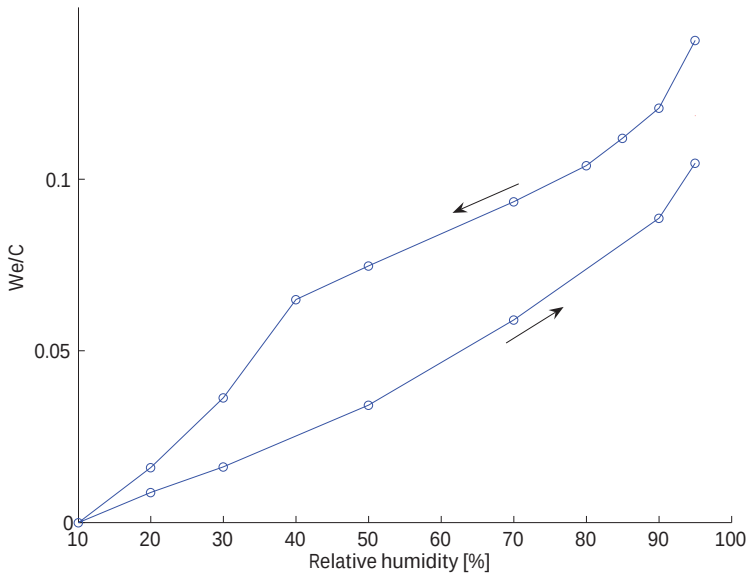

Figure 4.7: Sorption isotherm determined for one sample of material C_{HCS}.

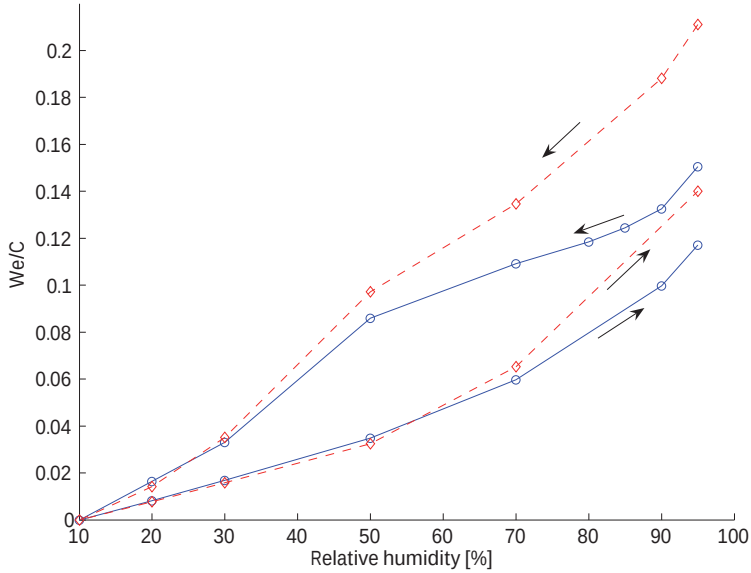

Figure 4.8: Sorption isotherms determined for two samples of material M, w/c 0.55 cement mortar. The dashed line represents a sample subjected to drying for 1 month and the solid line 12 months of drying.

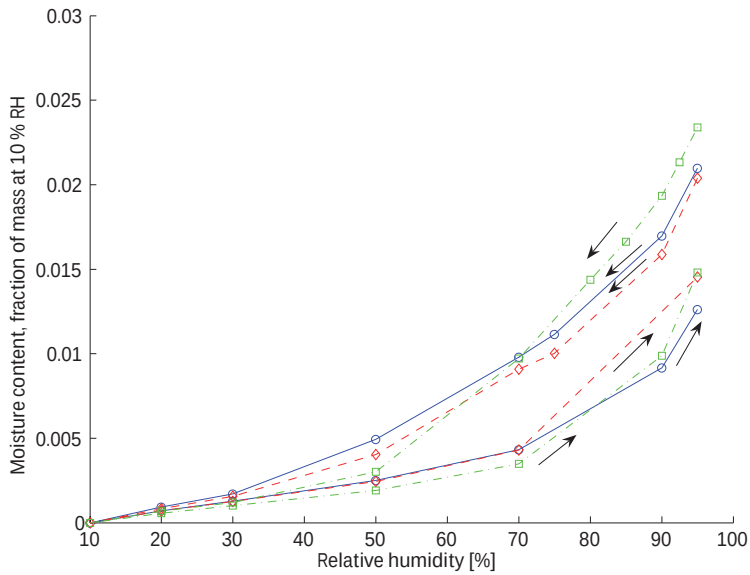

Figure 4.9: Sorption isotherms determined for three samples of material SFC, Floor 4310 Fibre Flow.

4.3 Scanning curves

In each of the first test series, two scanning curves were obtained by two sections of linearly increasing/decreasing RH, ramp, one starting from the desorption isotherm and the other from the absorption isotherm. This method was previously used for determining scanning curves for self-levelling flooring compounds [43]. The RH level was kept constant for a certain time before and after the scanning determination sequence, in order to achieve sample mass equilibrium.

However, as equilibrium, in a strict sense, was not obtained no matter how long RH was kept constant, the scanning ramp initially became disturbed by a mass loss/gain, see Figure 4.10. In Figure 4.10 the x-axis represents time in

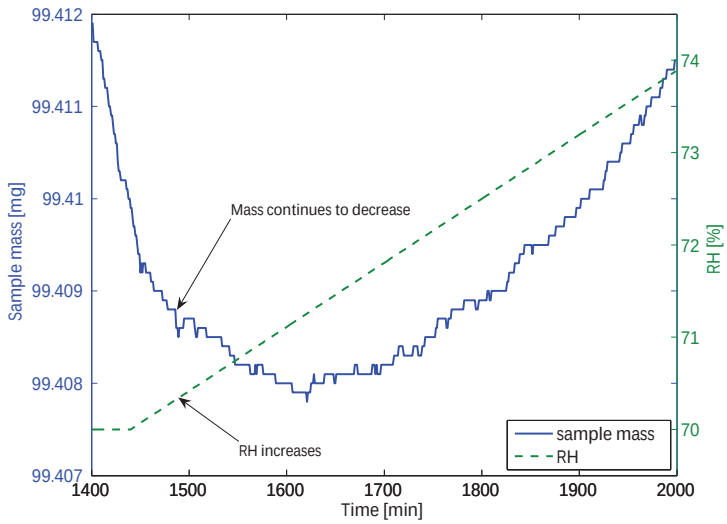

Figure 4.10: Equilibrium is not obtained before the RH ramp starts at 1440 min and 70 % RH.

minutes, the left hand y-axis represents sample mass in mg and the right hand y-axis represents RH in % RH. As can be seen in Figure 4.10 the sample mass, solid line, still decreases beyond 1440 minutes, even though the generated RH increases, dashed line. Therefore a time lag effect was obtained. In addition, the error increased even more as the curve fitted asymptotic mass was used.

This effect was compensated for by linearly superimposing the difference between the recorded and asymptotic mass, thereby reducing the error. Unfortunately, it was not feasible to apply curve fitting according to Eq. (4.1) on

scanning sections determined from a linearly increasing/decreasing RH. Instead a calculation was performed to compensate for the time lag effect obtained, by linearly superimposing the difference between recorded and asymptotic mass. The curve fitting method, time lag compensation, and the sorption isotherms obtained are presented in detail in Paper III.

The test sequence for scanning curve determination was modified by inserting a step wise RH change before the gradual RH change see Figure 4.11. In this way it was possible to compare a scanning curve evaluated by using Eq. (4.1) with a scanning curve obtained by using the time lag compensation evaluation. The results from this investigation clearly show that the scanning curve slope in-

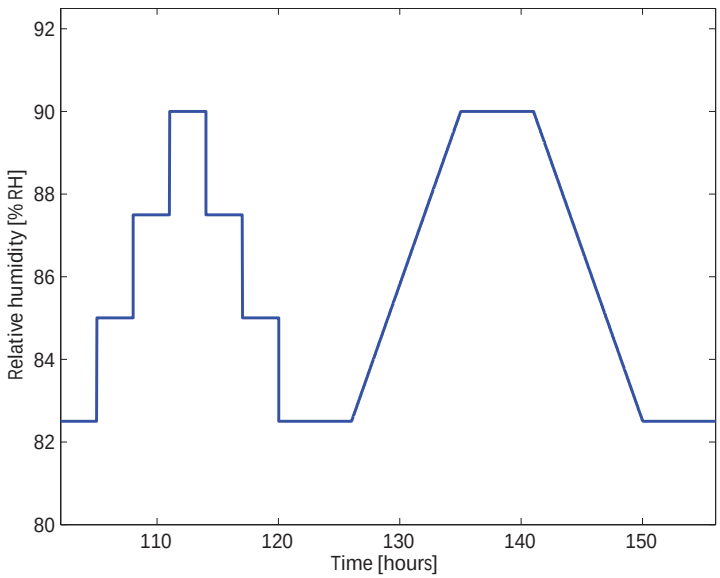

Figure 4.11: Detail of test sequence for comparing one scanning curve obtained by stepwise RH-changes with a scanning curve obtained by gradual RH-changes.

creases faster by using the stepwise RH changing method, see Figure 4.12. The scanning curve obtained by using the recorded sample mass, dashed line, contain less moisture compared with the scanning curve obtained by using the time lag compensation, solid line. In turn, the scanning curve obtained from stepwise changes to the ramp, dash dotted line, contains more moisture compared with the time compensated scanning curve obtained from the ramp.

In order to decrease possible remaining time lag effects, the previous method was further developed in the later test series. By replacing the RH ramps in

the test sequence with a sequence of small discrete RH steps, potential time lag effects were minimized. Thus the attained scanning curves were less affected by the non-existing equilibrium caused by earlier RH steps.

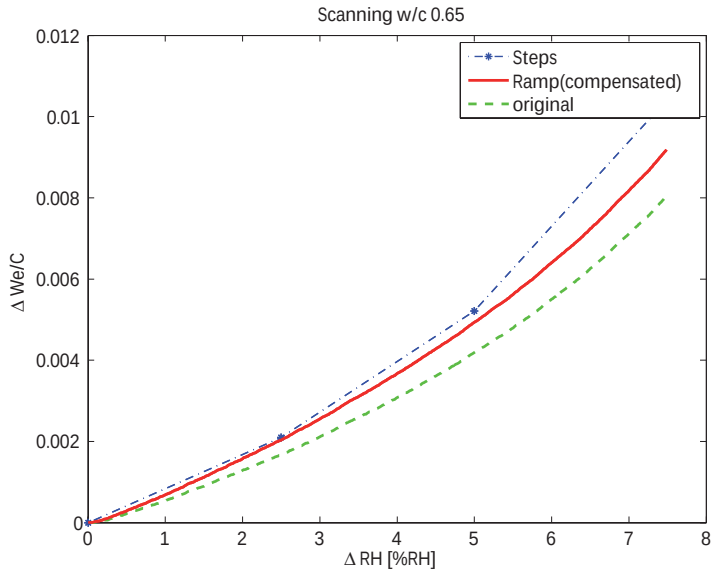

Figure 4.12: A comparison of the absorption scanning curves determined by using untreated data, a gradual RH change (time lag compensated), and a stepwise RH change, dashed, solid, and dash dotted line respectively. The point of origin represents the starting points at the desorption isotherm where scanning starts.

These new sets of scanning curves all started only from the desorption isotherm. In addition, the scanning absorption curves were directly followed by a desorption scanning curve, thus forming a small loop inside the main boundary loop. This approach was chosen, as such a sequence of moisture changes may occur at the top surface of a concrete slab when a screed is applied.

Figure 4.13 gives an example that illustrates where the different scanning curves are located with reference to the sorption isotherm.

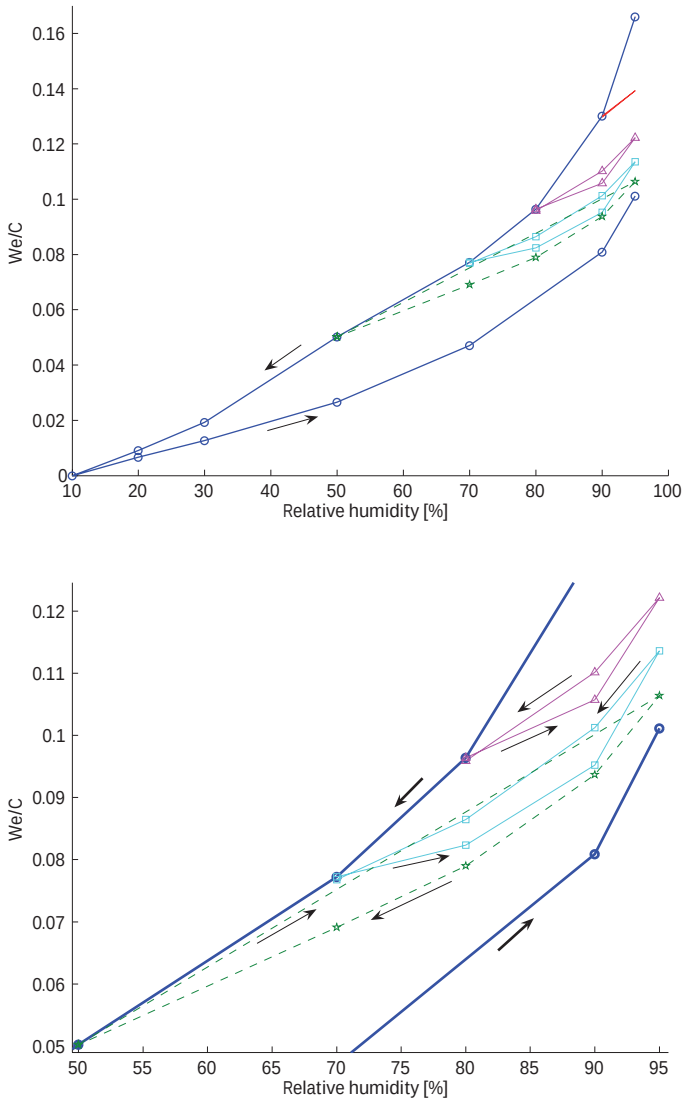

Figure 4.13: The top diagram shows the absorption and desorption isotherm of a w/c 0.65 concrete including a number of sequential scanning curves starting at different RH, 90, 80, 70 and 50 % RH. This sample is taken 20 mm from the slab base. The bottom diagram shows a detail of the achieved scanning curves where arrows indicate whether absorption or desorption scanning are determined.

Absorption scanning curves

To be able to show the scanning curves in detail, curves for different starting points on the desorption isotherm have been combined into one diagram from the starting point at the desorption isotherm.

Figures 4.14 - 4.17, display absorption scanning curves starting from RH_0 on the desorption isotherm for each separate material. Curves marked RH_0=82.5 are not "pure" absorption scanning curves. Originally they started scanning at 80 % RH, but experienced a number of inner absorption/desorption scanning cycles before starting at 82.5 % RH, inner scanning.

The x-axis in Figures 4.14 - 4.17, represents the change in RH. The y-axis in Figures 4.14 - 4.16, represents the change in We/C. In Figure 4.17, the y-axis represents the change in moisture content. The starting point of each scanning curve is indicated as RH_0 at the end of each displayed absorption scanning curve. Line markers indicate the determined We/C with reference to the starting point. The dashed line in Figure 4.14 suggests an estimated absorption scanning curve beginning from 50 % RH, since the moisture content was not determined at intermediate RH steps.

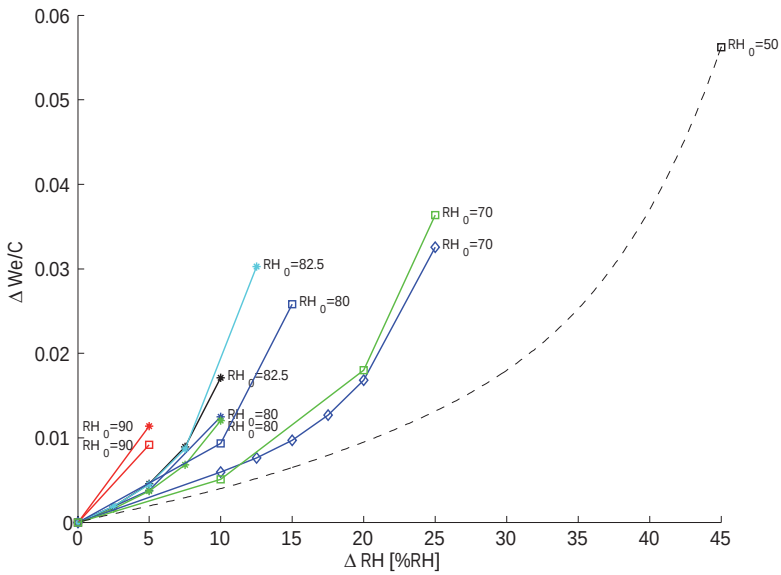

Figure 4.14: Absorption scanning curves for three samples of w/c 0.65 concrete, material C, expressed as changes in We/C and RH from the starting point RH_0 of the desorption isotherm. The three line markers stars, squares, and diamonds represent three separate samples.

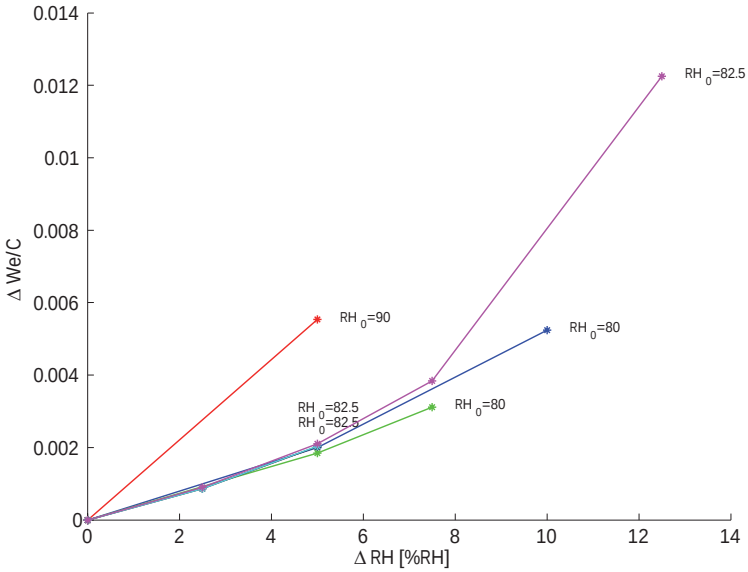

Figure 4.15: Absorption scanning curves determined for one sample of w/c 0.40 concrete, material C_{HCS}.

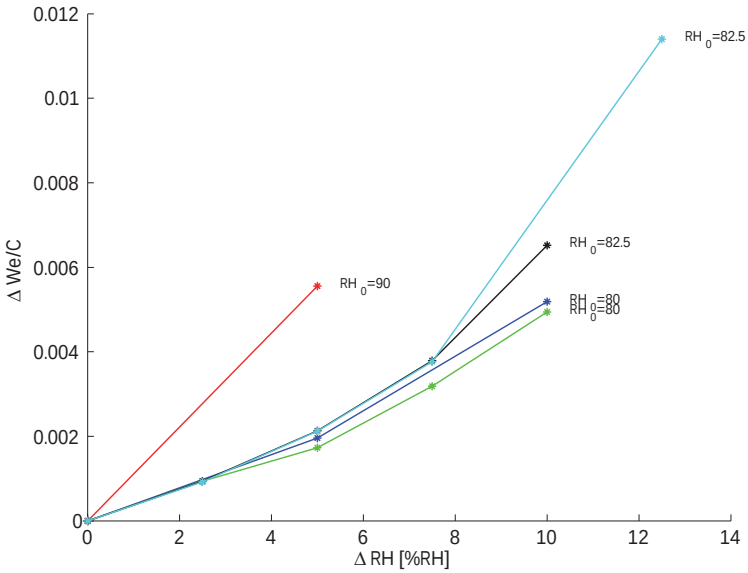

Figure 4.16: Absorption scanning curves determined for one sample of w/c 0.55 cement mortar, material M.

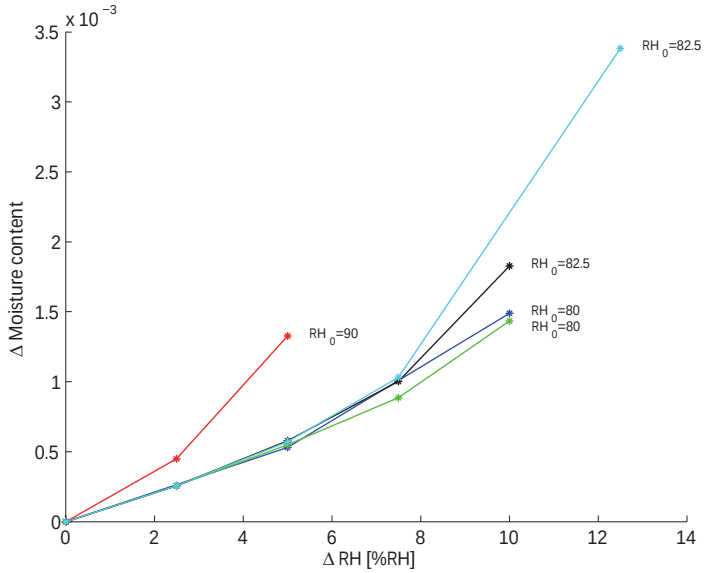

Figure 4.17: Absorption scanning curves determined for one sample of Floor 4310 Fibre Flow, material SFC.

There is a clear relationship between the absorption scanning curves obtained and the starting point on the desorption isotherm. The slope of an absorption scanning curve starting at a lower RH is shallower than a slope starting from a higher RH level. In addition the scatter of the absorption scanning curves is low.

The absorption scanning curves obtained at a starting point of 90 % RH appear to be linear, in Figures 4.14 - 4.16. Such results were obtained since the moisture content was not determined for intermediate RH levels.

Desorption scanning curves

Desorption scanning curves are shown in a similar manner as the absorption isotherm, with the starting point of the absorption scanning curve as a common reference.

Figures 4.18 - 4.21, display desorption scanning curves starting from the end point of a prior absorption scanning curve. The x-axis in Figures 4.18 - 4.21, represents the change in RH from that starting point. The y-axis in Figures 4.18 - 4.20, represents the change in We/C. In Figure 4.21, the y-axis represents the change in moisture content. RH_0 defines the starting point on the preceding absorption scanning curve, line markers indicate the We/C obtained.

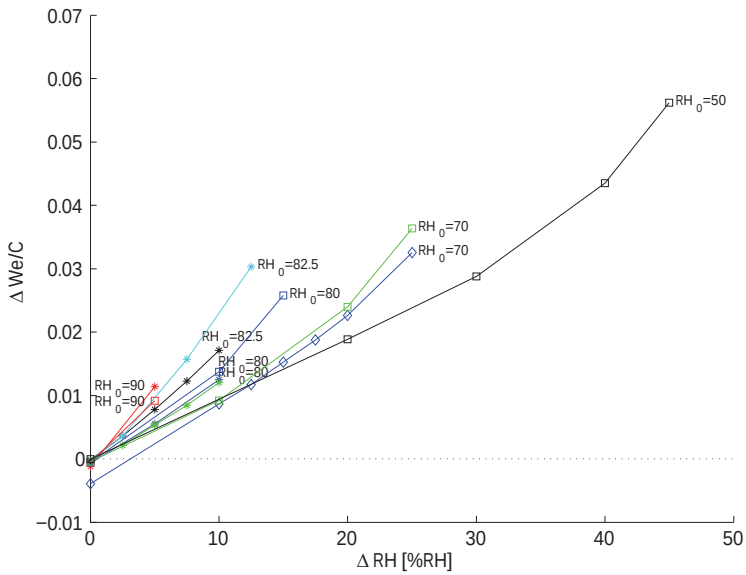

Figure 4.18: Desorption scanning curves starting from the absorption scanning curve for w/c 0.65 concrete, material C, expressed as changes in We/C and RH from the starting point RH_0 of the absorption scanning curve.

The determined desorption scanning curves clearly show that they are dependent on the starting point RH, RH_0. In addition most of the desorption scanning curves approximately end on the starting point. This suggests that an absorption scanning curve taking off from the desorption isotherm at a particular moisture content returns to the starting point, thus closing the loop. The path back is dependent on where the absorption ends and desorption starts. The above may imply that if a complete saturation occurred when absorbing moisture, then the desorption scanning curve would follow the desorption isotherm

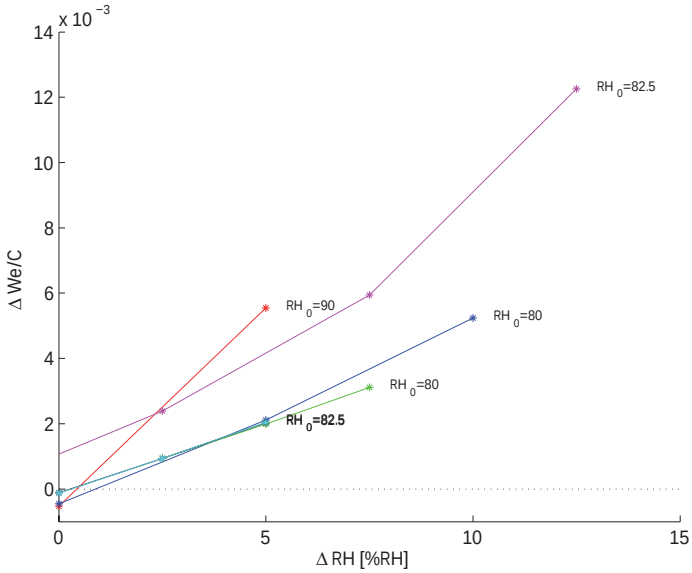

Figure 4.19: Desorption scanning curves starting from the absorption scanning curve for w/c 0.40 concrete, material C_{HCS}.

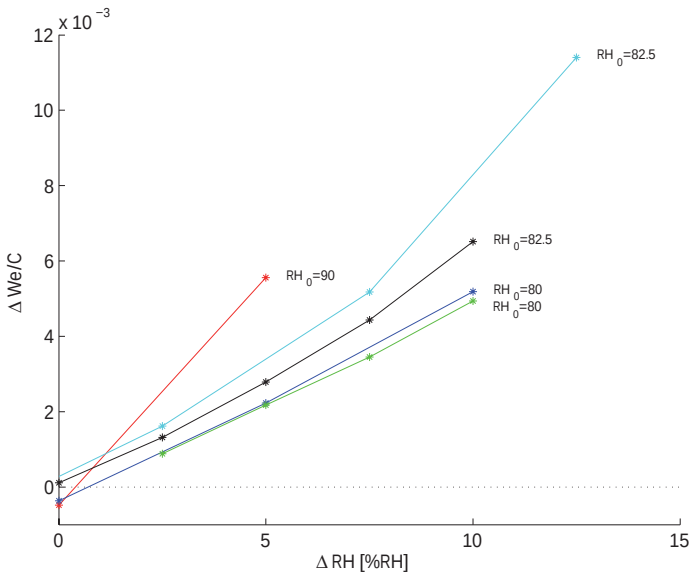

Figure 4.20: Desorption scanning curve starting from the absorption scanning curve for w/c 0.55 cement mortar, material M.

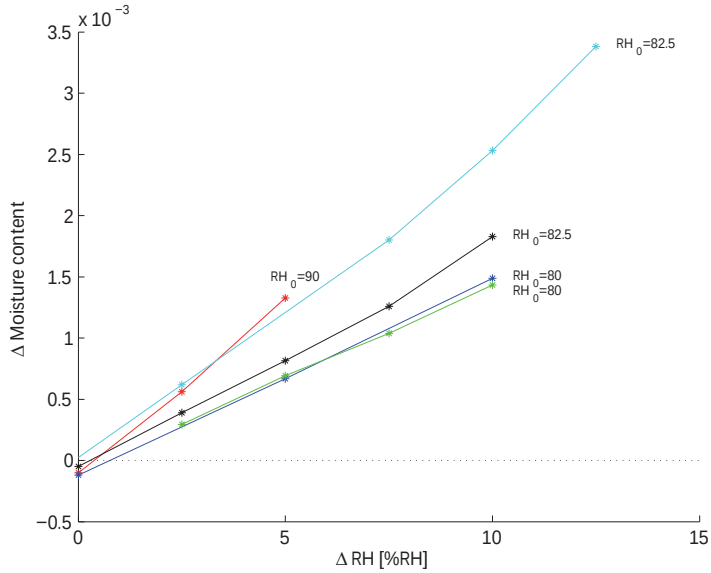

Figure 4.21: Desorption scanning curve starting from the absorption scanning curve for Floor 4310 Fibre Flow, material SFC.

when returning to the starting point provided there was no change in material characteristics, i.e., hydration would occur throughout the saturation procedure. This may not be true for the 1^{st} desorption isotherm, however.

4.4 Moisture transport properties

Moisture redistribution through a screeded concrete slab is slow. Therefore it may take a long time to reach a complete redistribution. When flooring is applied early on a moist screed, thus achieving an uneven moisture distribution, the model may underestimate the actual humidity obtained beneath the flooring, because the ”local” redistribution in the screed is much faster than the overall redistribution in the whole slab. To be able to quantify these effects, moisture transport properties must be known. However, moisture transport properties were not included in the quantitative model described in section 3.3. Moisture transport coefficients were determined in order to illustrate possible differences in the materials used, to be used if such considerations were to be included in future model development.

Moisture transport coefficients were determined for C, M, SFC, and coated plywood by using the cup method. This method is based on moisture loss determinations performed on closed impermeable vessels, where the top is ”sealed” with the investigated semi-permeable material. The cup is stored in a climate room where the surrounding climate is kept constant at 55 % RH and 20 °C.

A small container of saturated salt solution is put inside the vessel, see Figure 4.22. The mass of each vessel is determined on a calibrated balance, hence monitoring the expected mass loss. Several humidity levels may be achieved inside the vessel by using a number of different salt solutions.

In this study five different salt solutions were used to generate a specific RH at 20 °C [44], see Table 4.3.

Table 4.3: Salt solutions with deionized water and the generated RH.

Salt solution	NaBr	NaCl	KCl	KNO_3	K_2SO_4	H_2O
RH [% RH at 20 °C]	59.1	75.1	85.1	94.6	97.6	100

Cylindrical samples of w/c 0.65 concrete, w/c 0.55 cement mortar, and Floor 4310 Fibre Flow, were extracted from Batch 1 by using a water lubricated core drill. These cores were subdivided into 13 - 20 mm thick discs by using a wet saw, in order to separate screed from concrete material and to obtain smooth specimen surfaces. The mean diffusion coefficients for w/c 0.65 concrete were determined by using four to nine discs per each salt solution. Furthermore, the mean diffusion coefficients for the two screeds were determined by using one to two discs per each salt solution.

The mean diffusion coefficients for plywood were determined on three discs per each salt solution. The mean flows were calculated and used to calculate

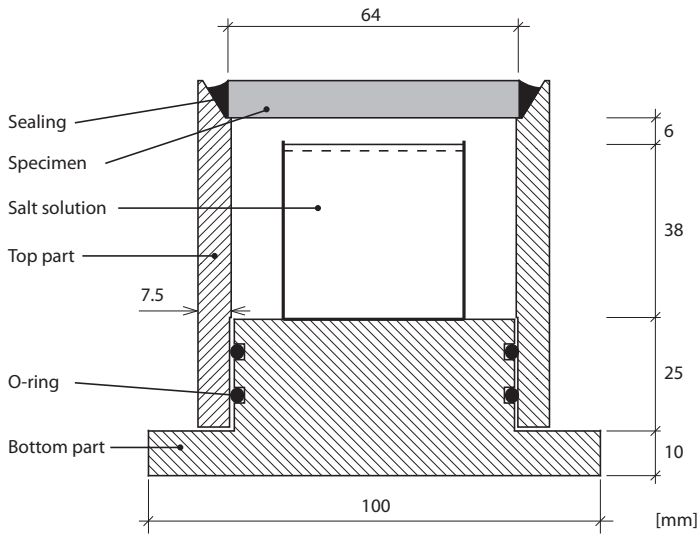

Figure 4.22: Illustration showing the cup used to determine diffusion coefficients of materials C, M, SFC and coated plywood.

the resistance of the air layer between the salt solution surface and the base of the specimen, thus obtaining the actual boundary RH. The final evaluation of average diffusion coefficients was performed by using a method described in [45].

Diffusion coefficients for the flooring material, Tarkett Eminent, were determined on one sample per each RH level, by using glass cups with a larger diameter, 183 mm, to reduce possible edge effects and increase the resolution.

The results of the evaluated mean diffusion coefficient for the w/c 0.65 concrete, the w/c 0.55 cement mortar and Floor 4310 Fibre Flow are shown in Figure 4.23. The mean diffusion coefficient between 55 % RH and 60 % RH seems too low in comparison with the higher levels. This is possibly either a consequence of the low difference between the outside and the inside climate or an error in the generated 55 % RH climate.

The mean diffusion coefficient of the PVC flooring material shown in Figure 4.24 is two orders of magnitude lower than that for the cement based materials, thus it is much less permeable than those materials. The mean diffusion coefficient at 55 to 75 % RH also seems too low compared with the coefficients obtained at a higher humidity. The flooring cups were stored in the same room as the concrete sample cups, it is therefore possible that the relative humidity was other than 55 % RH.

The mean diffusion coefficients for coated 13 mm plywood, determined on

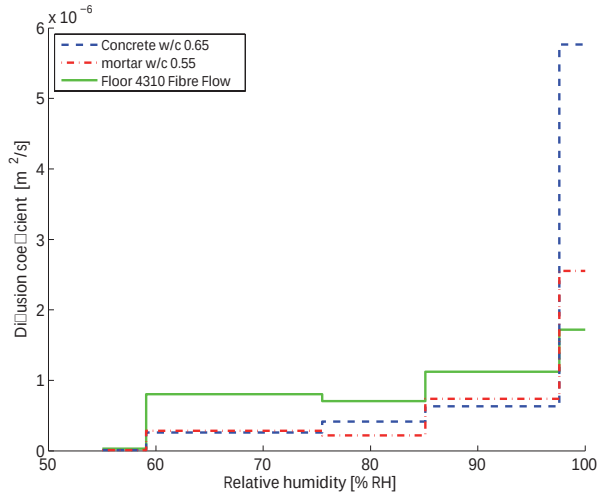

Figure 4.23: Mean diffusion coefficient of material, C, w/c 0.65 concrete, M, w/c 0.55 cement mortar, and SFC, Floor 4310 Fibre Flow. The diffusion coefficient was determined in the interval 55 - 100 % RH.

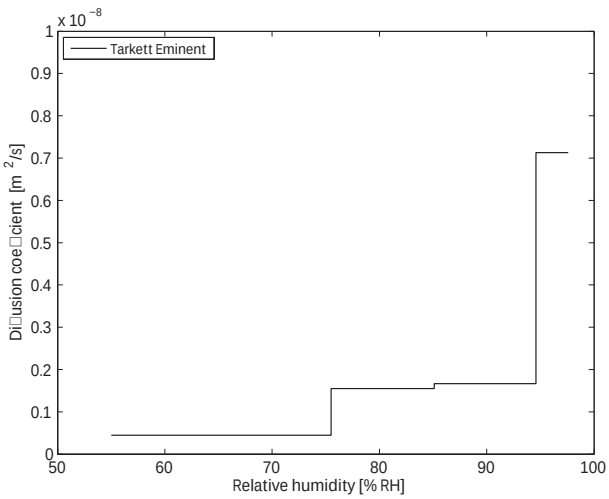

Figure 4.24: Mean diffusion coefficient of a Tarkett Eminent, 2 mm, homogeneous PVC flooring. The diffusion coefficient was determined in the interval 55 - 97.6 % RH.

three discs per salt solution shown in Figure 4.25, are of the same magnitude as for the cement based materials. The mean diffusion coefficient in the 55 - 60 % RH range, in this case also, is unexpectedly low. The plywood sample cups

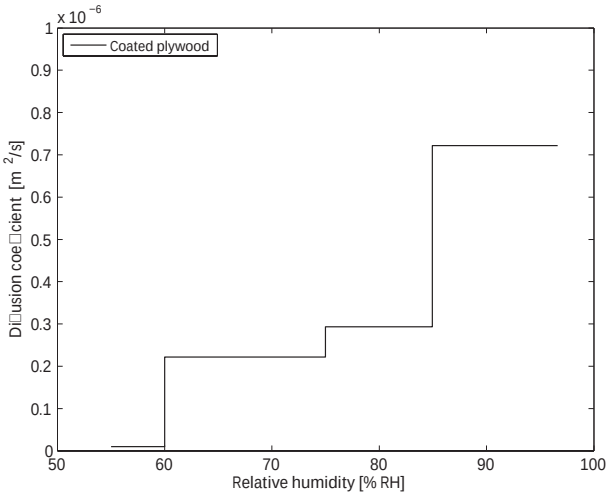

Figure 4.25: Mean diffusion coefficient for coated plywood 13 mm, used as formwork. The diffusion coefficient was determined in the interval 55 - 97.6 % RH.

were stored in the same climate room as the concrete sample cups, thus the low mean diffusion coefficients may be explained correspondingly.

4.5 Redistribution of moisture after early drying

Redistribution of moisture in a newly cast and somewhat dried concrete floor structure causes an increase in humidity at the concrete - adhesive interface. This humidity increase may adversely affect materials in contact with the concrete floor and contribute to deterioration, e.g. adhesive degradation [46, 47]. It is therefore important to limit the moisture content of the concrete by drying, or limit its exposure to external moisture sources. If it is not properly dried there is a risk of material deterioration. All measures that may prevent such an increase are therefore of interest.

Results from two independent studies showed unexpectedly low humidities below the sealed surface after redistribution [48, 49]. Additional, long-term self desiccation was one mechanism that was suggested to explain the large decrease in humidity below the flooring. If drying starts immediately after casting, the humidity in the concrete surface region decreases. This will limit the time for hydration under optimum humidity conditions, i.e. when enough moisture is present. The less hydrated cement in the surface region may react further with the later redistributed moisture from the slab base and increase its degree of hydration, thereby decreasing the humidity. However, the authors were not able to validate the suggested explanation for these interesting findings with available data.

An experiment was designed to repeat the findings shown in the two previous studies and test the model in section 3.4. Special attention was given to match the moisture distribution before the surface was sealed, to attain sufficient accuracy in RH measurements, and to monitor possible leakage. In addition it was important to rapidly reduce the humidity to less than 80 % RH in the upper part of the concrete, in order to hinder further hydration. This was accomplished by using a concrete with a w/c ratio of 0.65. The mix specification is shown in Table 4.4.

Table 4.4: Mix specification for the concrete used in the study of effects of early drying of humidity. Quantities are presented in kg/m^3.

Material	C
SH cement, CEM I 52.5 R	250
Water	162.5
Dry sand 0-8 mm	976.4
Dry gravel 8-12 mm	976.4

The theory of the impact of early drying was tested by comparing two drying treatments applied to w/c 0.65 concrete prior to sealing the surface, i.e. flooring. One population was dried directly, one day after curing, and the other was sealed 30 days before drying at 55 % RH and 20 °C. Each sample consisted of a 100 mm thick and 310 mm wide concrete cylinder, which was poured in a 20 mm thick polypropylene form. The moisture distribution was determined on all specimens by using calibrated Vaisala RH sensors. These were installed through drilled holes equipped with inserted 80 mm long plastic tubes. The centre of the sensor was located at a distance of 20-55 mm from the drying surface, with a distance of 5 mm between each sensor, see Fig 4.26.

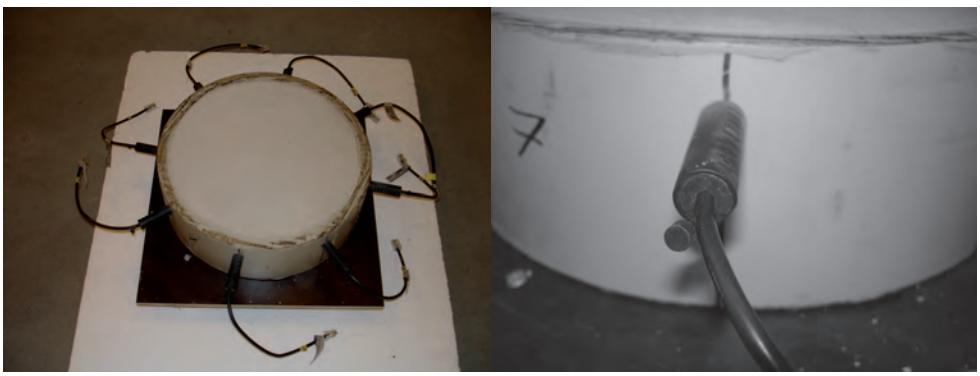

Figure 4.26: A concrete specimen with attached moisture sensors is shown to the left. A close-up of the rubber plug seal at the sensor cable is shown to the right.

Batch 1 was allowed to dry for 59 days prior to sealing. At this time the sensor with the centre 20 mm from the surface showed a reading of 80 % RH or less. This reading demonstrated that the upper 20 % of the concrete cylinder, at least once during drying, was exposed to a humidity that limits hydration. Batch 2 was sealed once the mean moisture distribution (at all depths) was found to match the mean moisture distribution determined just before sealing Batch 1, within an accuracy of $\pm$ 1 % RH.

After drying, the moisture in the specimens was allowed to redistribute for nearly 3 months. Subsequently the internal moisture distribution was determined including the humidity directly under the seal. This was done to establish that redistribution was completed, indicated by a uniform RH distribution through the specimen, see Figure 4.27. The humidity under the seal in Batch 1 was compared with the humidity in Batch 2 using a two sample student t-test.

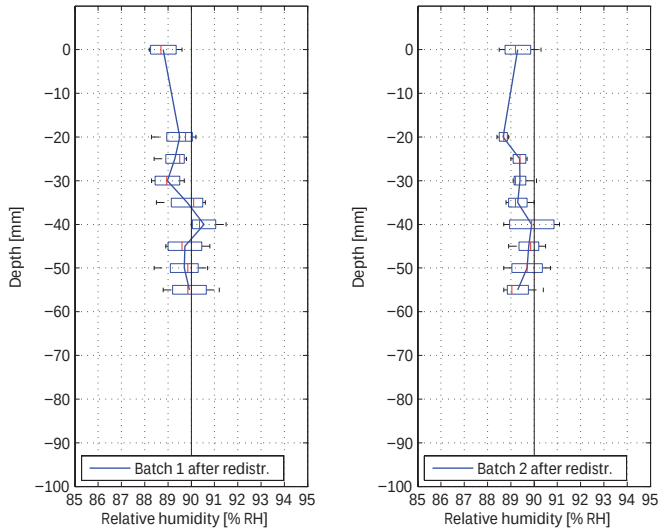

Figure 4.27: The moisture distribution after redistribution in Batch 1 is shown to the left and that in Batch 2 is shown to the right. On each box, the central mark is the median and the edges of the box are the 25^{th} and 75^{th} percentiles. The lines from the ends of the box (whiskers) extend to the most extreme data points considered not to be outliers.

The test showed that there was no significant difference in mean humidity between the two batches tested on a significance level of 5 %. A more detailed description of the method and results is found in Paper VI.

4.6 Critical limit for ion transport

Ion transport is an important factor for the durability in several applications. Here, alkaline deterioration of adhesives under a PVC flooring is in focus. Therefore, alkali is used when studying ion transport. Redistribution of potassium was determined on mortar specimens exposed to a certain drying treatment. The mix specification for the two mortars is described in Table 4.5.

Several sets of five specimens were first dried at 55 % RH and 20 °C for various periods, see Figures 4.28A and 4.29A. This 1^{st} drying lowered the average moisture state to a variable degree, represented by the solid curved line, see Figures 4.28A and 4.29A. A longer drying period obviously generated a lower average humidity. Then the specimens were sealed to allow redistribution to occur, until a uniform moisture distribution in terms of RH was reached, represented

Table 4.5: Mix specification for the materials used in the ion transport investigation. Quantities are presented in kg/m^3.

Material (w/c)	L (0.4)	H (0.65)
CEM I 52.5 R	702	333
Water	281	217
CEN-Standard sand EN 196-1 0-2 mm	1199	1602

by the dashed line, see Figures 4.28B and 4.29B. Redistribution was judged to be finalized when the RH (RH_{0-1} and RH_{0-2}) at both sides were equal, within an accuracy of $\pm$ 0.5 % RH.

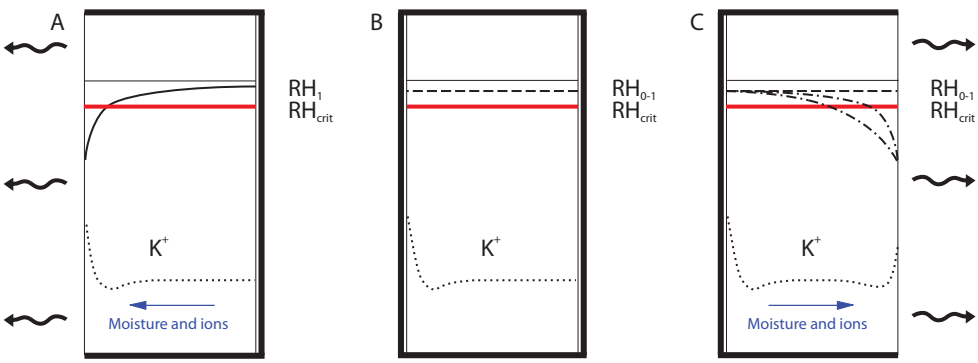

Figure 4.28: Illustration of the humidity and alkali distribution in a concrete specimen subjected to 1st (left) and 2nd (right) drying. The humidity level after redistribution, RH_{0-1}, is above the critical limit for ion transport.

The drying treatment does not generate a uniform distribution in terms of moisture content, see Figure 4.30B. In the left half of the specimen facing the earlier open side, the moisture content is on average less than the moisture content in the second half. The moisture content reaches its lowest level at the surface and increases with depth until reaching a maximum. This appearance is explained by the hysteresis and the scanning curves that govern the gain in moisture content when moisture is redistributed and reaches the earlier dry half.

On the contrary, the other half of the specimen has experienced only drying, see Figure 4.30B. This means that all parts in this half have reached their moisture state by tracking a pure desorption isotherm. Therefore both moisture content and RH distribution are uniform on this side. The point at which the material

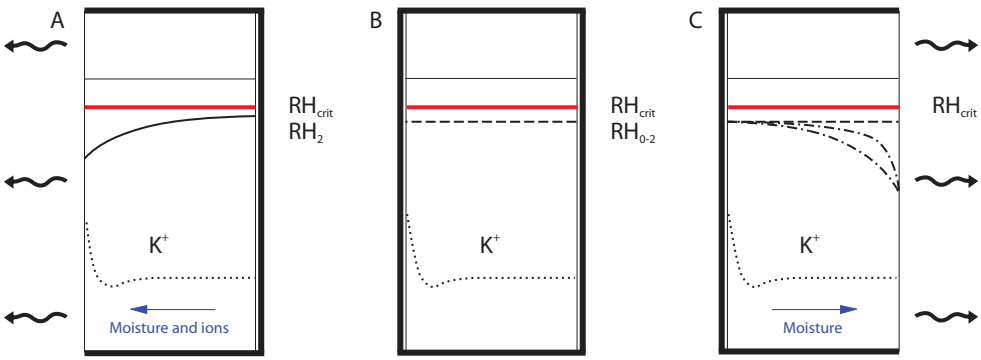

Figure 4.29: Illustration of the humidity and alkali distribution in a concrete specimen subjected to 1st (left) and 2nd (right) drying. The humidity level after redistribution, RH_{0-2}, is below the critical limit for ion transport.

has experienced both drying and wetting is about half of the specimens thickness. This fact is clearly demonstrated in Paper VI.

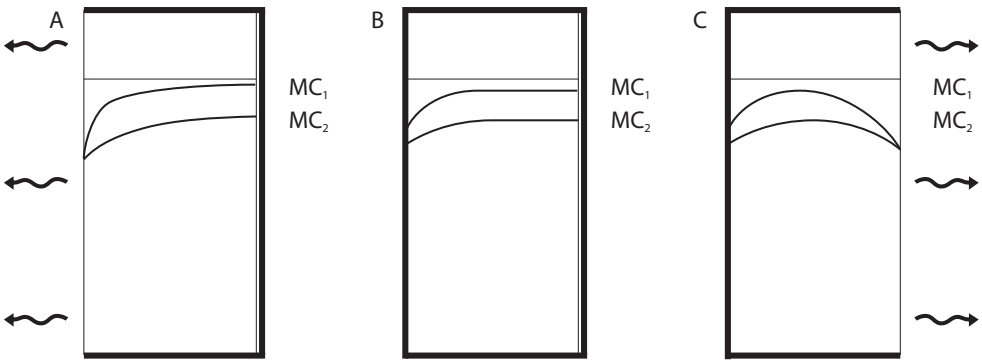

Figure 4.30: Illustration of the moisture content distribution, MC_1 and MC_2, in a concrete specimen subjected to 1st (left) and 2nd (right) drying at two humidity levels, RH_{0-1} and RH_{0-2}, shown in Figure 4.28 and Figure 4.29.

The drying treatment continues, on three of the five specimens, with a 2nd drying at 55 % RH and 20 °C. The 2nd drying is applied after establishing the end of moisture redistribution, but this time by opening the other side, see Figures 4.28C and 4.29C. At this point the flow of moisture is reversed. Drying

now occurs, to the right, from a lower moisture level. It is possible to obtain any humidity level lower than the humidity achieved by self-desiccation, by initial drying at various durations and climates.

The method used to redistribute moisture is designed to initiate alkali redistribution by convective moisture flow in two steps, the 2^{nd} being the most important. The 1^{st} applied drying causes an increase in alkali concentration at the drying surface, see dotted curve in Figures 4.28A and 4.29A. This increase is mainly the result of a moisture flow, since there is no driving potential for alkali diffusion at the start. As soon as the alkalis accumulate at the surface there will be a driving potential in the direction opposite to the moisture flow governed by RH differences. However, the moisture content is significantly reduced at this position and thereby limits the possibility of moving alkalis in the opposite direction by diffusion, see Figure 4.30A. The moisture content is still less than in the specimen half facing the sealed side, even after a complete redistribution of moisture, see Figure 4.30B. Therefore this limiting mechanism is still present after moisture redistribution, however to a slightly reduced extent.

The 2^{nd} drying step is applied to initiate alkali redistribution in the right half of the specimen via the moisture flow from a certain moisture state, see Figures 4.28C, 4.29C and 4.30C. As stated earlier, both moisture content and RH distribution are at first uniform in this part, see Figures 4.28B, 4.29B and 4.30B. In addition the alkali distribution is at first likely to be uniform, see dotted curve in Figures 4.28B and 4.29B. This assumption rests on the fact that moisture flow, up to this point, has only occurred at a low magnitude in this part of the specimen. Furthermore, there is no apparent cause of achieving diffusion of alkali ions because differences in alkali content in this half of the specimen are insignificant.

Alkali distribution was established by running four specimens for each mortar and RH level in an SEM-EDS instrument. One specimen was dried at one side only and this served as a reference. The data obtained from the SEM-EDS measurement was treated by using Matlab. This method is described in detail in Paper VII. One typical result after application of the data treatment is shown in Figure 4.31.

Figure 4.31 shows the alkali distribution in four different samples of w/c 0.65 mortar, one subjected to the 1^{st} drying only (upper left) and three specimens subjected to the whole drying treatment. The potassium content is shown on the y-axis and the x-axis represents the average position of the SEM-EDS analysis image, in mm, with reference to the surface subjected to the 2^{nd} drying (the right hand side in each diagram). The average potassium content in each image is represented by the thin solid curve and is quantified as the wt.-%. The average

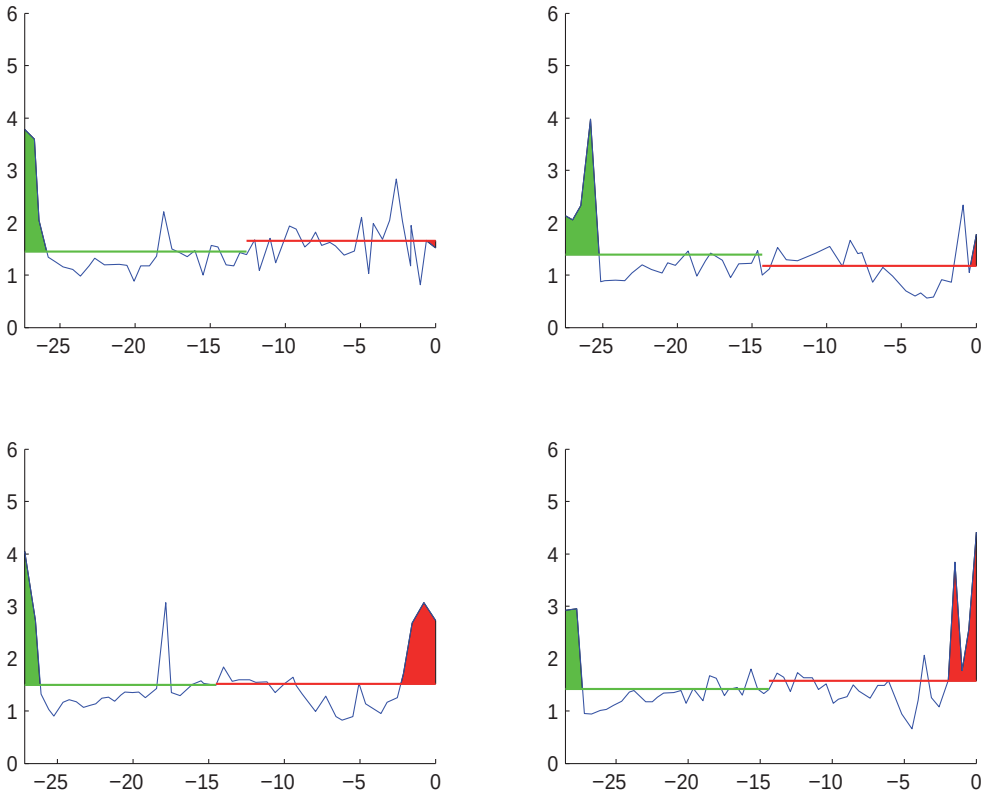

Figure 4.31: Alkali redistribution at 85 % RH, reference in upper left corner.

content through half of the specimen, right and left, is shown as a solid horizontal line. The green area to the left shows the accumulation of alkali achieved after applying the 1^{st} drying and the red area to the right the accumulation achieved after applying the 2^{nd} drying.

The study clearly shows that ions accumulated during the 2^{nd} drying at a humidity level of 78 % RH obtained by drying in w/c 0.65 mortar. This is strong evidence that the critical humidity level for convective ion transport is less than 78 % RH in w/c 0.65 mortar. Ion accumulation was also shown to occur in w/c 0.4 mortar at the 2^{nd} drying at a humidity level of 91 % RH obtained by drying. This implies that convective ion transport occurs at a level of 91 % RH in w/c 0.4 mortar.

For additional results of the ion content distribution after the 2^{nd} drying including the standard deviation see appendix.

Chapter 5

Model validation

Moisture distributions were determined for nine screeded slabs on several occasions before and after flooring, see Paper IV. The future moisture profiles were evaluated by using the proposed method in chapter 3. Each diagram in Figures 5.1 - 5.5 shows the screeded slab's moisture distribution before flooring, dashed lines, and after a certain time of redistribution, thick solid lines. In addition, the evaluated uniform RH level is shown as a thick dashed line in each diagram. In slabs 5-8 one additional moisture profile per each screeded slab was determined after the publication of Paper IV, therefore these do not appear in Paper IV. It was not possible to perform this analysis on the homogeneous slabs investigated in Paper VI, because of incomplete data.

The iteration procedure is shown in Table 5.1, where slab 4 serves as an example.

The moisture distribution in slab 4 determined before flooring application shows that the humidity varies between 75.5 % RH at section 0.00-0.02 m, and 86.5 % RH at section 0.06-0.08 m, see Table 5.1. The initial guess of the uniform moisture distribution according to the quantitative model is 83.75 % RH, see Table 5.1.

The determination of the moisture capacity in each section is dependent on both the moisture history and its level with reference to the initial guess. The moisture capacity in each section of material C is determined by using the desorption isotherm for sections where the determined RH is above the initial guess, see section 4.2 Figure 4.6, apart from section 0.04 - 0.06 m. Section 0.04 - 0.06 m has to be carefully investigated since it is close to the screed. This section is likely affected by application of the wet screed before reaching the obtained humidity.

Table 5.1: The calculation of the future uniform moisture distribution inside a screeded concrete slab is performed according to the quantitative model presented in section 3.3.

			1^{st} iteration		
Depth	d_i	$\overline{\varphi_i}$	$\left(\overline{\frac{dW_e}{d\varphi}}\right)_i$	$d_i \cdot \left(\overline{\frac{dW_e}{d\varphi}}\right)_i$	$d_i \cdot \left(\overline{\frac{dW_e}{d\varphi}}\right)_i \cdot \overline{\varphi_i}$
[m]	[m]	[% RH]	[kg/m^3]	[kg/m^2]	[kg/m^2]
0.00-0.02	0.02	75.5	0.06	0.0012	0.0906
0.02-0.04	0.02	82.5	0.02	0.0004	0.033
0.04-0.06	0.02	85	0.3	0.006	0.51
0.06-0.08	0.02	86.5	0.8	0.016	1.384
0.08-0.10	0.02	86.5	0.8	0.016	1.384
0.10-0.12	0.02	86.5	0.8	0.016	1.384
$\sum$=				0.0556	4.7856
φ_∞ =		83.75		$Eq.(3.6) \Rightarrow$	$\frac{4.7856}{0.0556} = 86.1$

Slab 4 was subjected to drying at 60 % RH for a duration of 110 days before application of the M material which dried 90 days prior to flooring, see section 4.1 Table 4.2. This most likely implies that the humidity in section 0.04 - 0.06 m has first decreased on drying and later increased as a result of the screed application, cf. qualitative model Figure 3.2 point b. As the moisture distribution was determined 90 days after this application it is likely that the moisture capacity for section 0.04 - 0.06 m should be determined from the desorption scanning curve of material C. Therefore, the moisture capacity for section 0.04 - 0.06 m is determined from the desorption scanning curves, see section 4.3 Figure 4.18.

Furthermore, the moisture capacity in each section of material M is evaluated by using the absorption scanning curves, see section 4.3 Figure 4.16, since both sections will gain moisture to reach the guessed humidity level.

Equation (3.6) in section 3.3, gives a uniform humidity distribution of 86.1 % RH which is significantly higher than the initial guess. This increase in uniform humidity means that section 0.04 - 0.06 m now becomes drier than the new uniform humidity distribution, hence a 2^{nd} iteration may be needed. However, the increase in uniform humidity distribution to 86.1 % RH leads to a change in evaluating the moisture capacity from a desorption to an absorption scanning curve in section 0.04 - 0.06 m. Such a change in scanning implies an insignificant change of moisture capacity. Therefore, in this case a 2^{nd} iteration is unnecessary and better precision is not obtainable.

The result of using the quantitative model in each slab is shown in Figures 5.1 -5.5. In each diagram RH is shown on the x-axis and the vertical distance in mm from the slab surface is shown on the y-axis, positive figures for an increasing depth. The line markers represent the RH level obtained in each section. Flooring installation is defined as day 0 (zero) and the legend indicates when the profile was obtained in relation to flooring.

The different materials used for each screeded slab are indicated in the diagrams, C representing w/c 0.65 concrete, C_{HCS} representing w/c 0.4 concrete, SFC representing Floor 4310 Fibre Flow, and M representing w/c 0.55 cement mortar.

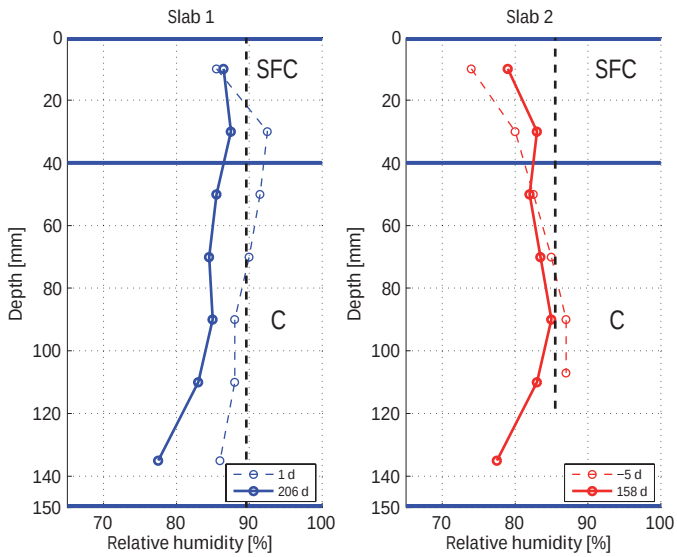

Figure 5.1: Moisture distribution determined for two SFC screeded concrete slabs on plywood at the time of flooring, thin dashed line, after complete redistribution predicted by the model, thick dashed line, and after x days of redistribution, thick solid line.

The humidity distribution determined 206 days after the flooring was laid in slab 1 indicates that the maximum RH is not yet reached, see Figure 5.1. The higher RH level obtained at the 30 mm level indicates that additional moisture will be transported upwards thus increasing the level by about 1 % RH. The results obtained from slabs 2 and 4, about 160 days after flooring, clearly demonstrate that moisture will be redistributed from the 30 mm level to the 10 mm level, see Figures 5.1 and 5.2. It is very likely that the future RH level be-

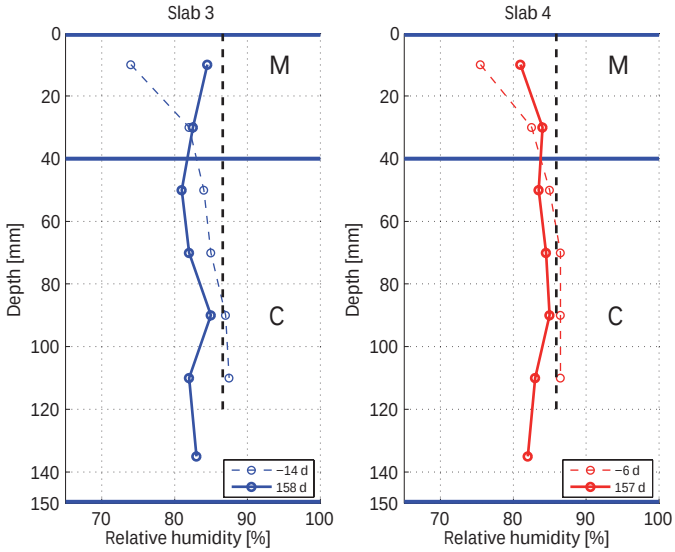

Figure 5.2: Moisture distribution determined for two M screeded concrete slabs on plywood.

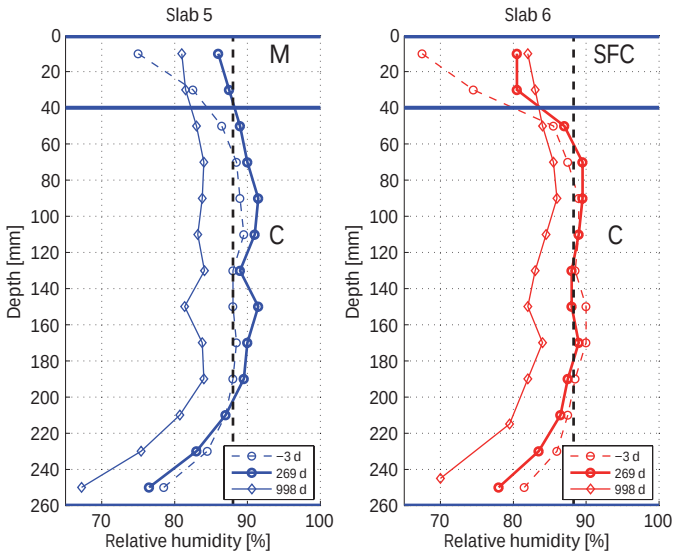

Figure 5.3: Moisture distribution determined for two of the M and SFC screeded concrete slabs.

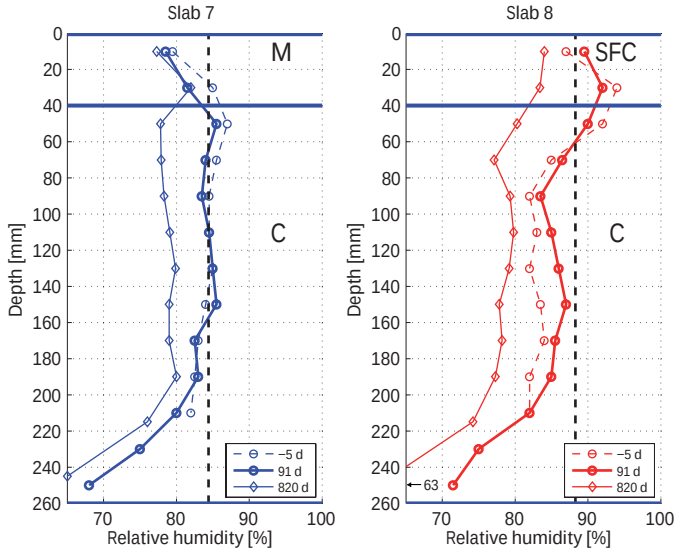

Figure 5.4: Moisture distribution determined for two of the M and SFC screeded concrete slabs.

neath the flooring will increase by about 3 - 5 % RH compared with the top RH levels obtained.

The determined RH distribution in slab 3 shows a higher RH level in the 0-20 mm section than in the 20-40 mm section, see Figure 5.2. This may be a consequence of measurement uncertainty as such an increase could not be explained by moisture redistributing from deeper sections.

Disregarding the expected future humidity increase, the proposed quantitative model gives results about 1 - 8 % RH on the safe side judging from slabs 1 - 4. However, including the expected future rise for slabs 1, 2 and 4 the overestimation drops to about 1 - 3 % RH.

Applying the quantitative estimation to slabs 5 and 6 results in a 2 - 7 % RH higher humidity at the 10 and 30 mm level determined 269 days after flooring, see Figure 5.3. However, on the basis of this moisture distribution a further increase in humidity is very likely to occur. Judging from the determined moisture distribution, the screed RH may increase by about 3 - 8 % RH. Including this future suggested increase the quantitative model underestimates the screed humidity by about 1 - 2 % RH.

When the quantitative model is applied to slabs 7 and 8, the screed humidity estimation is higher than that obtained for slab 7 and slightly lower for slab 8,

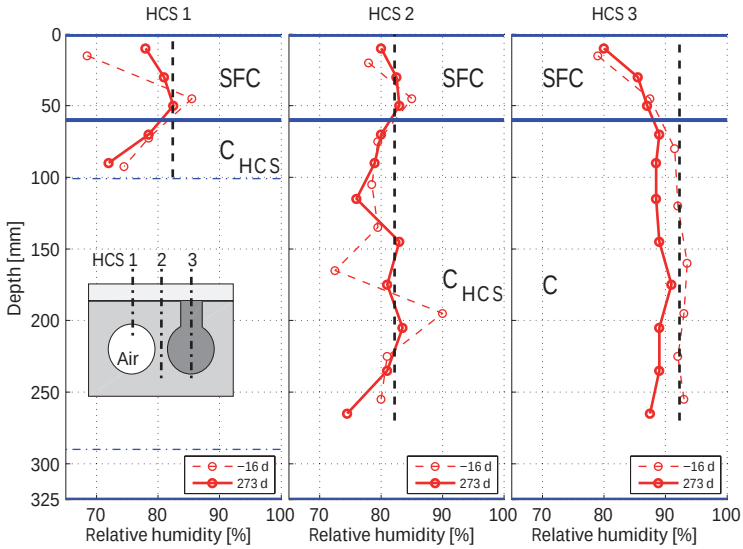

Figure 5.5: Moisture distribution determined for three separate sections of the SFC screeded HCS, with one core hole filled with material C. Sections 150-180 and 180-210 in vertical section HCS 2 were judged as outliers and therefore excluded from the estimation of future RH distribution.

see Figure 5.4. However, the maximum humidity of neither of the screeds has been reached yet. It may be expected that the humidity may increase by about 6 - 7 % RH for slab 7 and by about 2 - 3 % RH for slab 8. Incorporating these expected increases the future screed humidity in slab 7 will be underestimated by 1 - 2 % RH and by about 3 - 4 % RH in slab 8.

Comparison of the results from humidity distribution measurements with the estimated future uniform RH, the filled core, HCS3, shows about 5 - 10 % RH higher humidity level at the 10 - 30 mm level, see Figure 5.5. However, considering future upward moisture redistribution the final humidity level in the screed may increase to about 90 % RH, thus reducing the apparent overestimation to some 2 - 3 % RH. The moisture profiles determined for vertical sections HCS 1 and 2 are in addition to vertical moisture redistribution, also affected by horizontal moisture redistribution. The quantitative model is not designed for use in such cases and therefore the estimated future moisture distribution is uncertain in those two vertical sections.

Chapter 6

Discussion and conclusions

6.1 Moisture redistribution

The proposed model of moisture redistribution requires the initial moisture distribution through a screeded slab. Initial distribution may be determined before the application of flooring either in situ or under controlled conditions on samples extracted from the slab. In the study of moisture redistribution in screeded concrete slabs, samples were extracted from the slab, see Paper IV. In either case, the current status of the floor construction should be described in as much detail as possible in terms of constituent materials, layer thicknesses and moisture distribution before flooring. Furthermore, each material should be included in the determination.

In determining the moisture distribution, it may be beneficial to divide each material into a larger number of sections, since the higher resolution may reveal unexpected changes in moisture level. This high resolution would enhance the knowledge of the moisture history, thus perhaps reducing the uncertainty. In addition, by determining a number of moisture distributions in the slab it would be possible to reveal a scatter. Furthermore a rough determination of these parameters may give rise to a large uncertainty.

On the other hand, moisture may be lost during sampling by dividing the slab in too thin sections. This problem occurs as the determination of RH on thin material layers, below 10 mm, may be difficult both because of possible moisture losses during sampling and equipment installation requirements. Another limitation when deciding the possible number of sections, is the total thickness

of each material section. Each section should be treated separately, which means that mixtures of materials must be avoided.

The investigated screeded slabs were, in each case, divided into vertically discrete sections of a certain thickness. As the initial moisture distribution in the slab was unknown at the time of sampling it was determined on equally thick sections. However, as the moisture profile is very steep in certain sections the determined profile may be misleading, especially in sections close to the surfaces.

Due to limitations of the measurements techniques, a certain section size may be required to minimize uncertainties. Individual section depths could be assigned if the overall distribution is known from former measurements. If the moisture distribution is determined on material samples, these should be collected in such a way that enough material from each depth is obtained. If the moisture distribution is determined in situ using drilled in sensors, each sensor should determine the RH at the vertical midpoint of each section.

The developed quantitative model was compared with the previous model by performing a simulation of the redistribution under an impermeable seal. Initial moisture distribution to the quantitative model was obtained from a simulation of a concrete slab, with a w/c ratio of 0.65, exposed to single-sided drying at 55 % RH and 20 °C. Furthermore the calculation took into consideration moisture dependent transport properties and a sorption isotherm obtained for the material C, see section 4.2 Figure 4.6.

The moisture distribution obtained from the simulation is shown in Figure 6.1(solid curve). The input to the quantitative model was the moisture distribution obtained from the simulation and the moisture capacity for each section. Two values were assumed for the moisture capacity at the assumed RH interval, 0.1 kg/m^3 and 1.0 kg/m^3, where the humidity in the particular section is below and above respectively of the initial guess. The results from the quantitative model simulation showed that the equivalent depth increased from 0.4h in the previous model to 0.57h.

As the moisture capacity is about five to ten times higher in some parts, it is important to find those when the humidity distribution before flooring is determined. Hence, the parts at the base of a homogeneous slab have the largest effect on the result from the quantitative model. These parts should therefore be prioritized, if the number of measurements is limited.

The proposed qualitative model for estimating the moisture distribution in a screeded concrete slab fits the verifying experiments and serves as an illustration of how moisture may be redistributed inside such a slab. The quantitative estimations of moisture distribution after flooring indicate a similarity to the results obtained from the experiments. However, the humidity in the verifying screeded

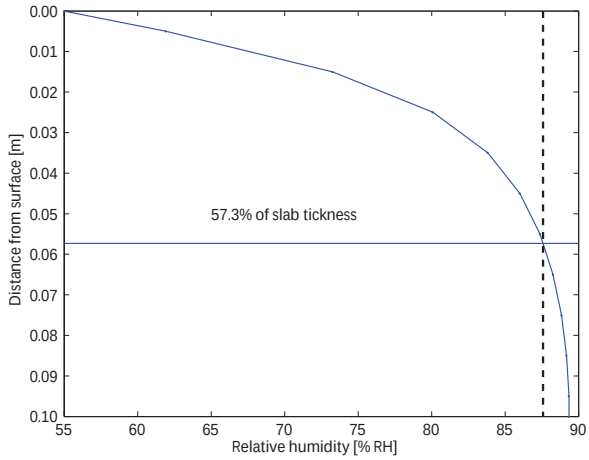

Figure 6.1: An estimation of the depth of intersection when applying the new proposed quantitative model of redistribution.

slabs has not yet been completely redistributed given the limited redistribution time.

Neither the time aspects nor possible drying are included in the model. This may lead to an overestimation of the RH level under the flooring when the screed is very dry at the time of flooring, which means a reduced risk of moisture damage. On the other hand, when the screed humidity is high, it is likely that the quantitative model underestimates the RH level under the flooring as the time needed for redistribution has a negative impact on the humidity obtained below the flooring. It may be higher than expected. The slow moisture transport in concrete is the key factor in reducing the rate of moisture redistribution. Drying from the floor construction through both flooring and slab base will favourably affect the obtained screed humidity level as the average humidity decreases, thus reducing the maximum humidity beneath the flooring.

In addition an uneven temperature distribution may affect the moisture distribution. Measurements performed on site show that the temperature, on average, is higher on the slab base than on the slab top, the report also shows that irregular temperature fluctuations are common on a construction site [50]. The lower average temperature in the floor top may have a negative effect on the humidity distribution as moisture is then transferred to the colder upper side, thus increasing the humidity.

The model uses an average moisture capacity to calculate the new moisture content at the estimated future RH distribution, see Figure 6.2.

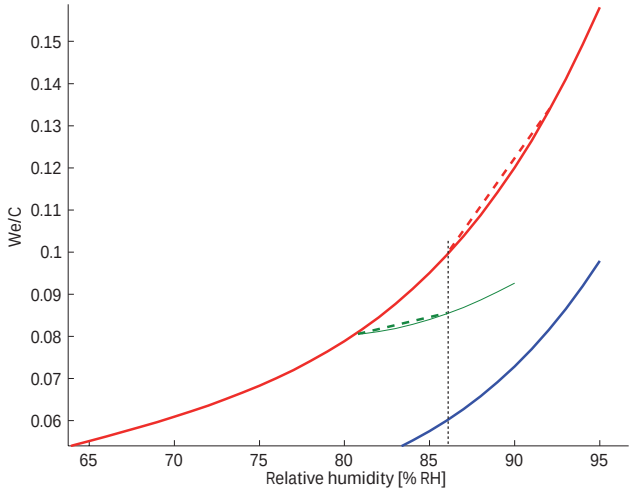

Figure 6.2: The average moisture capacity shown for two separate sections of a screeded slab, one for the desorption isotherm (red dashed line) and one for the scanning curve (green dashed line). The uniform RH after redistribution is shown as a vertical dotted line.

It is possible to develop software which is able to estimate the moisture distribution underneath flooring according to the proposed quantitative model. However, additional data on sorption isotherms for concrete mixtures and screed compounds, not included in this research, needs to be further investigated. The software would require a model for estimating scanning curves for different materials, as such are not available for all expected conditions.

Sorption isotherms and scanning curves

The sorption balance is very useful for determining sorption isotherms of cement-based materials [43, 51, 52]. Besides reduced labour costs, the speed of determining one desorption and absorption isotherm is increased by a factor of 10 compared with the previously used climate chamber method [53, 54]. Such high speed isotherm determination is beneficial as uncertainties arising from hydration are reduced. In addition, sorption balances are accurate enough to perform scanning curve investigations. The small samples of concrete and mortar are not representative and require chemical analysis of each sample. Sampling from dried slabs gave the 2^{nd} desorption isotherm. Testing is undertaken in a carbonate free environment thus preventing carbonation. However, one drawback is the high

initial cost of the sorption balance.

In Paper III, several scanning curves were presented for concrete, mortar and one self-levelling flooring compound. All these scanning curves were investigated by subjecting the material sample to a linearly increasing/decreasing RH in a sorption balance. This method has previously been used in [43]. However, small but significant time lag effects occurred as a consequence of the slow moisture exchange between the passing gas stream and the samples. These were minimized by linearly distributing the error originating from the start and the end levels on the scanning curve. After this linear error distribution the time lag effects were reduced.

The small time lag effect may be further reduced by using an RH step change sequence for evaluating scanning curves. In this way there is a possibility to extrapolate each step's final mass instead of using linearly distributed errors, thus further reducing possible time lag effects.

Results from the repeated scanning sorption isotherm investigations indicate that the moisture content is recovered when returning to the desorption isotherm after performing one scanning curve loop.

Redistribution of moisture after early drying

The redistribution of moisture was determined by inserting probes in plastic tubes perpendicular to the moisture flow. Since the plastic tubes were present during drying and later redistribution they affected the moisture flow. However, by inserting the probes at various depths from the surface 80 mm into the concrete cylinder, the flow of moisture at the centre part was left undisturbed. Installing RH probes vertically from the top would certainly hinder moisture flow as the probe itself would obstruct moisture transport during drying and redistribution. The obstruction leads to a higher RH than if measurements are performed horizontally from the side, since moisture accumulates below the probe. A larger opening facing the concrete from the top will have a greater impact on moisture transport. It is easily recognized that all desiccation would cease if the opening occupied the specimens' top surface completely. Instead, a redistribution would start. Another option of installation is to insert the RH probe from the cylinder base. This would imply that the material below the measurement point would be replaced by the plastic tube. This loss of material would also mean a moisture source loss. By performing the measurements from the side the moisture flow is disturbed only in the immediate vicinity of the tube opening.

When RH probes are installed perpendicular to the moisture flow other errors are introduced see Figure 6.3. One error is dependent on the position with

reference to the moisture distribution. The RH probe determines the humidity of the air in the sealed tube, and this air humidity is determined by the concrete's surface humidity facing the opening. Since the vertical opening is not sealed it will allow a moisture flow, a redistribution from humid surface areas to drier areas. The redistribution occurs through the surgical tape and the air in the tube. This means that the humidity in the air will end up at a level somewhere between the humidity at the bottom and the top of the tube opening. This error is dependent on the installation location with respect to the moisture distribution. A probe installed at a shallow depth faces a distribution that varies a lot with depth, while a probe installed deeper faces a moisture distribution with considerably less variation. It also means that a shallow probe will show a higher RH than is actually the case in a drying situation. However, when a seal is attached to the surface the depth dependent error decreases with time. After the moisture has been completely redistributed and the moisture flow has ceased this error no longer exists.

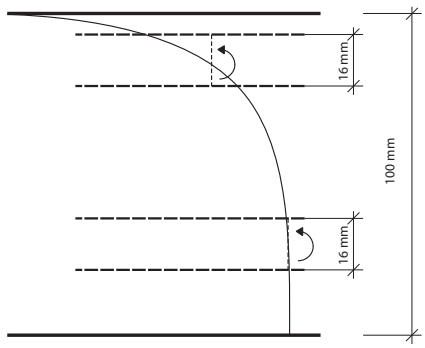

Figure 6.3: Two probes installed at different depths in a concrete specimen. Dashed lines represent the concrete surface facing the probe. The arrow indicates the direction of redistribution.

A flooring on a concrete slab is typically not completely impermeable, which means that drying continues after installation. In a less dense flooring material the humidity load on the adhesive is less than estimated by using the quantitative model of moisture redistribution. If the flooring is installed by using a water soluble adhesive a certain wetting of the concrete occurs, and this increases the RH load on the adhesive. These two factors affect the level of humidity exposure below the flooring and the duration of the estimated humidity.

The outcome of the study may have been different if drying had been performed at a lower RH. Additionally the type of cement used in the concrete specimens was rapid hardening and this may also contribute to the small differences achieved between the two drying treatments. Rapid hardening cement hydrates much faster than an ordinary Portland cement, hence possibly diminishing the expected difference between the two drying treatments.

6.2 Critical limit for ion transport

Potassium ion distribution was determined on mortar specimens subjected to a drying treatment described in Paper IV. The drying treatment generated a moisture distribution obtained through an equivalent moisture history. This is an important issue, as the proportion of empty capillaries is not consistent if the moisture history differs within the material, due to the hysteresis exhibited by the sorption isotherm. The moisture content at a particular RH is higher if it results from a decrease in humidity (drying) than if it results from an increase in humidity (wetting). Furthermore, the maximum moisture content at a particular RH is attained by drying a virgin concrete never exposed to any prior drying treatment. In addition the drying treatment applied to the sample should preferably not generate a non-uniform ion distribution, since it may cause diffusion, especially at high humidities.

In efforts to find the critical limit for ion transport it is vital to achieve the highest possible moisture content for the investigated humidity. In any other case the critical humidity would be underestimated, hence achieving a higher critical humidity than the ”true” one. If the investigated material exhibits a variation in moisture content, the achieved critical limit would be uncertain, regardless of a uniform RH distribution. The inconsistent moisture content would affect the ratio between the filled and emptied capillaries. This means that there would be a reduced opportunity for ion transport.

6.3 Other aspects

The moisture flow resistance of the flooring material and the slab material, influences the humidity increase achieved by the redistributed moisture. This increase becomes larger if the flooring material exhibits a higher moisture flow resistance than the slab material. Such floor constructions are commonly utilized in the construction industry. It is for instance common to apply a PVC flooring to a

high w/c ratio concrete slab, with the risk of severely increasing the humidity under the flooring. The low moisture transport resistance of high w/c ratio concrete enables a large moisture flow towards the flooring. The moisture flow allowed through the flooring material is far lower. This means that the inflow of water is higher than the out flow, hence increasing the humidity.

Redistributed moisture would have a much smaller impact on the humidity under a PVC flooring given a low w/c ratio concrete in the slab. The difference in moisture flow resistance between a low w/c ratio concrete and a PVC flooring is of equal magnitude. This means that the flow of moisture to the flooring and the flow from it is also of equal magnitude. Therefore the humidity increase in such a case is rather moderate because of redistributed moisture.

The suggested model of moisture redistribution presented in section 3.3, takes into account the effect of hysteresis. This changes the point of intersection between the moisture distribution prior to flooring installation and that after completion of redistribution. The consequence is that the point of intersection is located deeper than the previously suggested 0.4 of the slab thickness. This is clearly shown in the results in Paper VI where the point of intersection is located at about 0.5 - 0.55 of the slab thickness. It must however be borne in mind that this result was obtained when the slab was completely sealed at both the bottom and the top, which is seldom the case in practice.

Unsaturated concrete exists in both outdoor and indoor structures. Ion movement in these structures may have an adverse impact on the durability. For instance, chloride ion movement in unsaturated low w/c ratio concrete may occur in submerged constructions like caissons and concrete columns supporting bridges. Accumulation of chlorides may initiate corrosion of the reinforcement, hence reducing the durability. Another example where unsaturated concrete occurs, is the splash zone in marine constructions where the moisture conditions change frequently. Also in this application the chloride ion is the adverse species. In addition, onshore constructions like the walls of a swimming pool contain unsaturated concrete, with a potential of chloride transport with the risk of reinforcement corrosion.

Furthermore, unsaturated concrete is more or less the natural condition in indoor applications. Ion transport may in this case contribute to a reduction in the durability of a flooring. The alkali ions in concrete contribute to material deterioration when redistributed moisture conveys them to the adhesive. The adhesive is degraded and the bond between the concrete and flooring is reduced. Apart from the disagreeable odour, the degradation products, VOC, they are believed to have an adverse effect on peoples' health.

Chapter 7

Future research

The results from this research have raised a number of questions that need to be investigated to develop the proposed models further.

Additional input, such as sorption isotherms including scanning curves for other concrete mixes and screeds are needed to decrease uncertainties of the proposed model. Desorption isotherms determined for samples extracted from shallow parts of concrete showed a decrease with time in their ability to bind moisture by absorption. Samples extracted from deeper lying parts also showed a decrease in the ability to bind moisture by absorption. These two findings may have an impact on moisture redistribution.

As the sorption isotherm is temperature dependent and low temperatures regularly occur during construction, additional sorption isotherms should be determined for temperatures other than 20 °C.

The model does not take into consideration time lag effects and drying that may occur through the flooring material and an open base surface. Drying will decrease the humidity beneath flooring, thus reducing the risk of moisture related damage.

A detailed analysis of the uncertainties involved and the way in which they may affect the estimated maximum humidity level is not performed in this work. However, uncertainties originating from a lot of sources are briefly mentioned in the next four paragraphs.

First of all, the uncertainty involved in RH determinations of each section will affect the overall uncertainty. However, when a complete distribution throughout an entire screeded slab is determined, the overall uncertainty in moisture distribution decreases. Sections may be regarded as outliers, disqualifying

them from further analysis.

Secondly, by performing a detailed moisture distribution determination throughout the entire slab by subdividing it into many horizontal sections, a lower uncertainty may be obtained. The converse, a higher uncertainty, will follow if a non-sufficient, poor, low resolution, or incomplete moisture distribution determination is performed. In such a case it is not possible to disregard outliers.

Thirdly, possible non-uniform temperature distributions may also add to the uncertainty, since such are not included in the model. Such a non-uniform temperature distribution will redirect moisture flow from warmer towards colder sections inside the screeded slab, with a non-uniform moisture distribution as the result.

A fourth source of uncertainty is drying that may occur through the slab base and flooring. Further drying will reduce the humidity level underneath the flooring and thus reduce the maximum humidity beneath the flooring.

The magnitude of the above uncertainties needs to be further investigated in future research. Some of the above sources of uncertainty affect the maximum humidity more than others. Some may even possibly be disregarded.

Bibliography

[1] L.-O. Nilsson. Moisture measurements Excess moisture in concrete slabs on grade. Drying and measurement methods. (in Swedish). Technical Report TVBM-3008, Div Building Materials, Lund University, 1979.

[2] RBK. *Moisture measurement in concrete (in Swedish)*. Sveriges Byggindustrier, Stockholm, Manual 3^{rd} edition, 2001.

[3] E.O. Kraemer. *A treatise on Physical Chemistry*. Van Nostrand, New York, 1931.

[4] J.W. McBain. An explanation of hysteresis in the hydration and dehydration of gels. *Journal of American Chemical Society*, 57:699–700, 1935.

[5] S. Diamond and K.O. Kjellsen. Resolution of fine fibrous C-S-H in backscatter SEM examination. *Cement and Concrete Composites*, 28(2):130–132, 2006.

[6] R.F. Feldman and P.J. Sereda. A new model for hydrated portland cement and its practical implications. *Engineering Journal*, 53(8-9):53–59, 1970.

[7] H.M. Jennings. A model for the microstructure of calcium silicate hydrate in cement paste. *Cement and Concrete Research*, 30(1):101–116, 2000.

[8] I.G. Richardson. The calcium silicate hydrates. *Cement and Concrete Research*, 38(2):137–158, 2008.

[9] V. Baroghel-Bouny. Water vapour sorption experiments on hardened cementitious materials. Part I: Essential tool for analysis of hygral behaviour and its relation to pore structure. *Cement and Concrete Research*, 37(3):414–437, 2007.

[10] I. Langmuir. The adsorption of gases on plane surfaces of glass, mica and platinum. *Journal of the American Chemical Society*, 40:1361–1403, JUL-DEC 1918.

[11] S. Brunauer, P.H. Emmett, and E. Teller. Adsorption of gases in multimolecular layers. *Journal of the American Chemical Society*, 60 (2):309–319, 1938.

[12] R.W. Dent. A multilayer theory for gas sorption. Part I. Sorption of a Single gas. *Textile Research Journal*, 47(3):188–199, 1977.

[13] T.C. Powers and T.L. Brownyard. Studies of the physical properties of hardened portland cement paste, bulletin 22. *Res. Lab. of Portland Cement Association, Skokie, IL, U.S.A., reprinted from Journal of the American Concerete Institute (Proc.), vol. 43*, pages 101–132, 249–336, 469–504, 549–602, 669–712, 845–880, 933–992, 1947.

[14] T. Young. An essay on the cohesion of fluids. *Philosophical Transactions of the Royal Society of London*, 95:65–87, 1805.

[15] P. S. Laplace. *Traité de mécanique céleste*, chapter Supplément au dixième livre du Traité de mécanique céleste, Sur l'action capillaire, pages 1–67. Courcier, Paris, 1806.

[16] P. S. Laplace. *Traité de mécanique céleste*, chapter Supplément au dixième livre du Traité de mécanique céleste, Supplément a la théorie de l'action capillaire, pages 1–78. Courcier, Paris, 1807.

[17] W. Thomson. On the equilibrium of vapour at a curved surface of liquid. In *Proceedings of the Royal Society of Edinburgh*, volume 42, 1871.

[18] D.H. Everett. Adsorption hysteresis. In E.A. Flood, editor, *The Solid-Gas interface Vol. 2*, pages 1055–1113. Marcel Dekker, New York, 1967.

[19] P.C. Carman and P. le R. Malherbe. Diffusion and Flow of Gases and Vapours through Micropores. II. Surface Flow. *Proceedings of the Royal Society of London. Series A. Mathematical and Physical Sciences*, 203(1073):165–178, 1950.

[20] R.M. Barrer and J.A. Barrie. Sorption and Surface Diffusion in Porous Glass. *Proceedings of the Royal Society of London. Series A. Mathematical and Physical Sciences*, 213(1113):250–265, 1952.

[21] P.C. Carman. Diffusion and Flow of Gases and Vapours through Micropores. IV. Flow of Capillary Condensate. *Proceedings of the Royal Society of London. Series A. Mathematical and Physical Sciences*, 211(1107):526–535, 1952.

[22] E. Samson, J. Marchand, K. A. Snyder, and J. J. Beaudoin. Modeling ion and fluid transport in unsaturated cement systems in isothermal conditions. *Cement and Concrete Research*, 35(1):141–153, 2005.

[23] A.T.C. Guimar aes, M.A. Climent, G. de Vera, F.J. Vicente, F.T. Rodrigues, and C. Andrade. Determination of chloride diffusivity through partially saturated portland cement concrete by a simplified procedure. *Construction and Building Materials*, 25(2):785 – 790, 2011.

[24] M.A. Climent, G. de Vera, J.F. López, E. Viqueira, and C. Andrade. A test method for measuring chloride diffusion coefficients through nonsaturated concrete: Part I. The instantaneous plane source diffusion case. *Cement and Concrete Research*, 32(7):1113 – 1123, 2002.

[25] G. de Vera, M.A. Climent, E. Viqueira, C. Antón, and C. Andrade. A test method for measuring chloride diffusion coefficients through partially saturated concrete. Part II: The instantaneous plane source diffusion case with chloride binding consideration. *Cement and Concrete Research*, 37(5):714 – 724, 2007.

[26] M.A. Climent, G. de Vera, J.F. López, C. Garcia, and C. Andrade. Transport of chlorides through non-saturated concrete after an initial limited chloride supply. In Andrade, C and Kropp, J, editor, *2^{nd} International RILEM Workshop on testing and modelling the chloride ingress into concrete*, volume 19 of *RILEM Proceedings*, pages 173–187, 2000.

[27] A.V. Saetta, R.V. Scotta, and R.V. Vitaliani. Analysis of chloride diffusion into partially saturated concrete. *ACI Materials Journal*, 90(5):441–451, SEP-OCT 1993.

[28] O. Francy. *Modélisation de la pénétration des ions clorures dans les mortier partiellement saturés en eau*. PhD thesis, Université Paul Abatier, 1998.

[29] E.P. Nielsen and M.R. Geiker. Chloride diffusion in partially saturated cementitious material. *Cement and Concrete Research*, 33(1):133–138, 2003.

[30] U. Angst, B. Elsener, R. Myrdal, and Ø. Vennesland. Diffusion potentials in porous mortar in a moisture state below saturation. *Electrochimica Acta*, 55(28):8545 – 8555, 2010.

[31] T.Q. Nguyen. *Modélisations physico-chimiques de la pénétration des ions chlorures dans les matériaux cimentaires*. PhD thesis, L'ecole nationale des ponts et chaussees, 2007.

[32] T.Q. Nguyen, J. Petkovic, P. Dangla, and V. Baroghel-Bouny. Modelling of coupled ion and moisture transport in porous building materials. *Construction and Building Materials*, 22(11):2185–2195, 2008.

[33] P. Castro, O.T. De Rincon, and E.J. Pazini. Interpretation of chloride profiles from concrete exposed to tropical marine environments. *Cement and Concrete Research*, 31(4):529–537, 2001.

[34] L.-O. Nilsson. A numerical model for combined diffusion and convection of chloride in non-saturated concrete. In Andrade, C and Kropp, J, editor, *2nd International RILEM Workshop on testing and modelling the chloride ingress into concrete*, volume 19 of *RILEM Proceedings*, pages 261–275, 2000.

[35] E. Bastidas-Arteaga, A. Chateauneuf, M. Sánchez-Silva, Ph. Bressolette, and F. Schoefs. A comprehensive probabilistic model of chloride ingress in unsaturated concrete. *Engineering Structures*, 33(3):720–730, 2011.

[36] H. Wengholt Johnsson. *Chemical emissions from flooring systems - the effect of different concrete grades and moisture loads (in Swedish)*. Licentiate thesis, Chalmers University of Technology, 1995.

[37] A. Anderberg. *Studies of moisture and alkalinity in self-levelling flooring compounds*. PhD thesis, Div of Building Materials, Lund University, 2007.

[38] G. Hedenblad and L.-O. Nilsson. Critical moisture levels of some building materials - preliminary study (in Swedish). Technical Report TVBM-3028, Div of Building Materials, Lund University, 1987.

[39] T.C. Powers. A discussion of cement hydration in relation to the curing of concrete. In *Proceedings 27*, pages 178–188, Washington, D.C., 1947. Highway Research Board.

[40] M. Gerstig and L. Wadsö. A method based on isothermal calorimetry to quantify the influence of moisture on the hydration rate of young cement pastes. *Cement and Concrete Research*, 40(6):867–874, 2010.

[41] H. H. Willems and K. B. Van Der Velden. A gravimetric study of water vapour sorption on hydrated cement pastes. *Thermochimica Acta*, 82(1):211–220, 1984.

[42] l. Zhang and F.P. Glasser. Critical examination of drying damage to cement pastes. *Advances in cement research*, 12(2):79–88, 2000.

[43] A. Anderberg and L. Wadsö. Moisture in self-levelling flooring compounds. Part II. Sorption isotherms. *Nordic Concrete Research*, 32(2):16–30, 2004.

[44] L. Greenspan. Humidity fixed point of binary saturated aqueous solutions. *Journal of research of the national bureau of standards - A. Physics and Chemistry*, 81 A(1):89–96, 1977.

[45] A. Anderberg and L. Wadsö. Moisture in self-levelling flooring compounds. Part I. Water vapour diffusion coefficients. *Nordic Concrete Research*, 32(2):3–15, 2004.

[46] A. Sjöberg. *Secondary emissons from concrete floors with bonded flooring materials - effects of alkaline hydrolysis and stored decomposition products*. PhD thesis, Chalmers University of Technology, 2001.

[47] A. Sjöberg and O. Ramnäs. An experimental parametric study of VOC from flooring systems exposed to alkaline solutions. *Indoor Air*, 17(6):450–457, 2007.

[48] L.-O. Nilsson and J. Aavik. Drying of residual moisture in vaccuum treated concrete floors on ground on thermal insulation. Part C: Drying of residual moisture - Validation in a laboratory. Part D: Drying of residual moisture - In situ measurements(in Swedish). Technical Report P-93:13, 1993.

[49] A. Sjöberg and L.-O. Nilsson. Moisture measurements in heated concrete floors. Part II: Impervious floorings (in Swedish). Technical Report TVBM-3140, Div of Building Materials, Lund University, 2008.

[50] M. Åhs. Remote monitoring and logging of relative humidity in concrete. In *Proceedings of the 7th symposium on building physics in the nordic countries*, volume 1, pages 181–187, Reykjavik, Iceland, 2005. The icelandic building research institute.

[51] B. Johannesson and M. Janz. Test of four different experimental methods to determine sorption isotherms. *Journal of Materials in Civil Engineering*, 14(6):471–477, 2002.

[52] R. M. Espinosa and L. Franke. Inkbottle pore-method: Prediction of hygroscopic water content in hardened cement paste at variable climatic conditions. *Cement and Concrete Research*, 36(10):1954–1968, 2006.

[53] V. Baroghel-Bouny and T. Chaussadent. Pore structure and moisture properties of cement-based systems from water vapour sorption isotherms. In Diamond, S and Mindess, S and Glasser, FP and Roberts, LW and Skalny, JP and Wakeley, LD, editor, *Microstructure of Cement-Based Systems/Bonding and Interfaces in Cementitious Materials*, volume 370 of *Materials Research Society Symposium Proceedings*, pages 245–254, 1995.

[54] L. Ahlgren. *Moisture fixation in porous building materials (in Swedish)*. PhD thesis, Div of Building Materials, Lund University, 1972.

Appendix

Ion redistribution in mortar specimens

Ion distribution in the mortar specimens is shown in the following figures. The potassium content is shown on the y-axis and the x-axis represents the average position of the SEM-EDS analysis image, in mm, with reference to the surface subjected to the 2^{nd} drying (the right hand side in each diagram). The average potassium content in each image is represented by the thin solid curve and is quantified as the wt.-%. The average content through half of the specimen, right and left, is shown as a solid horizontal line. The midpoint is at around -14 mm, depending on the specimen thickness. The error bars represent the standard deviation of the potassium content at each image (point).

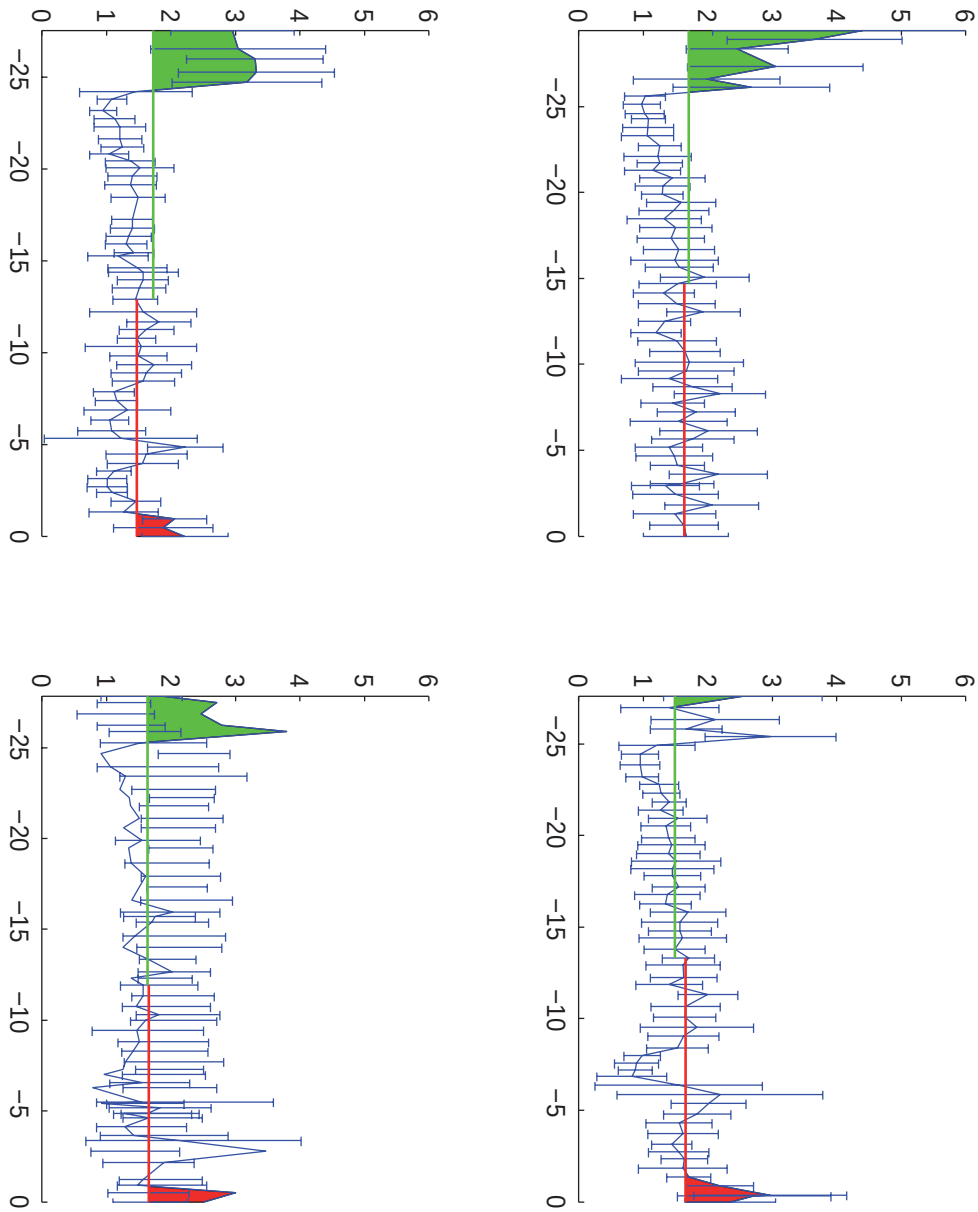

Figure A.1: Standard deviation of the potassium content at each image(point) of the w/c 0.65 mortar conditioned to 78% RH before 2nd drying.

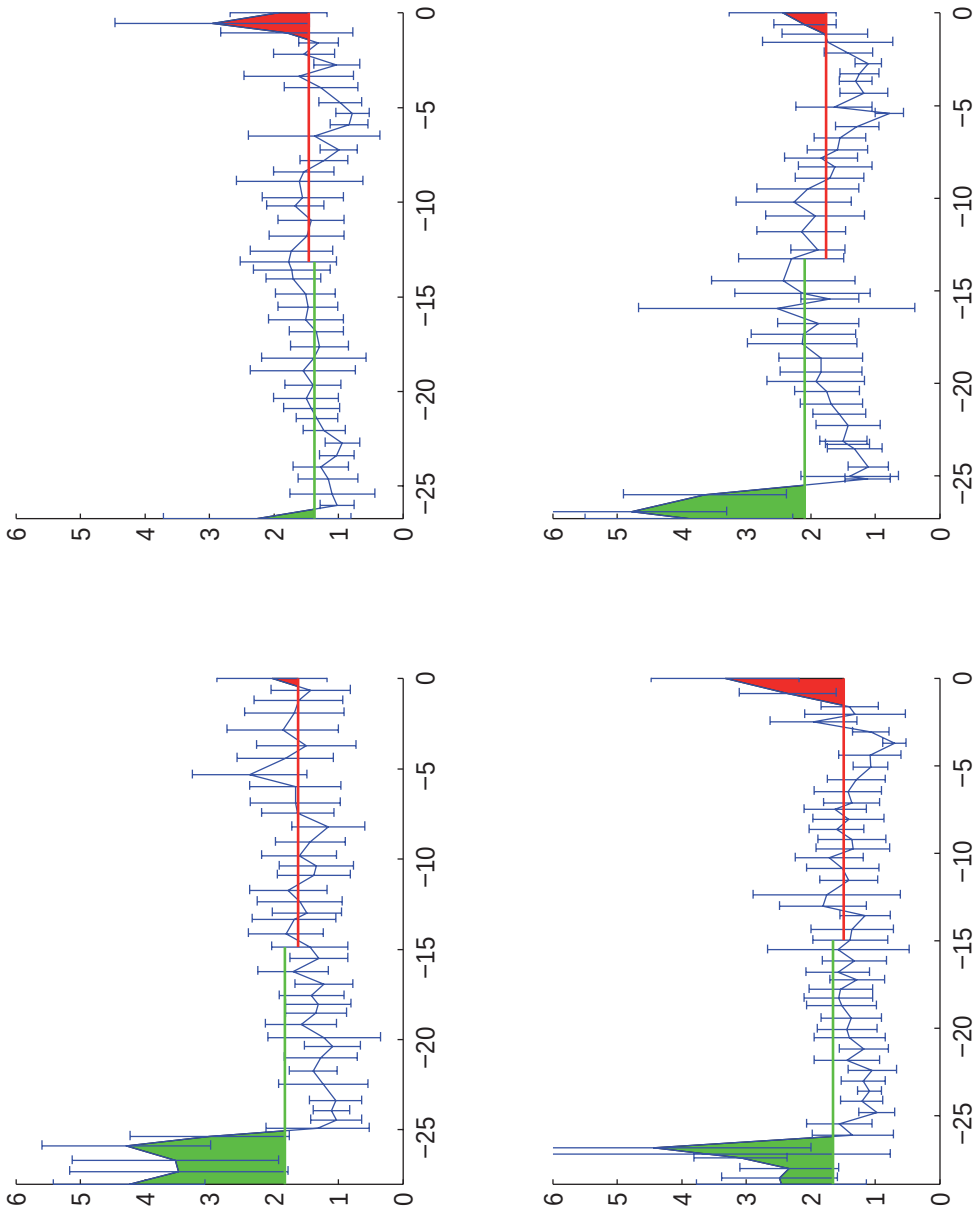

Figure A.2: Standard deviation of the potassium content at each image(point) of the w/c 0.65 mortar conditioned to 83% RH before 2nd drying.

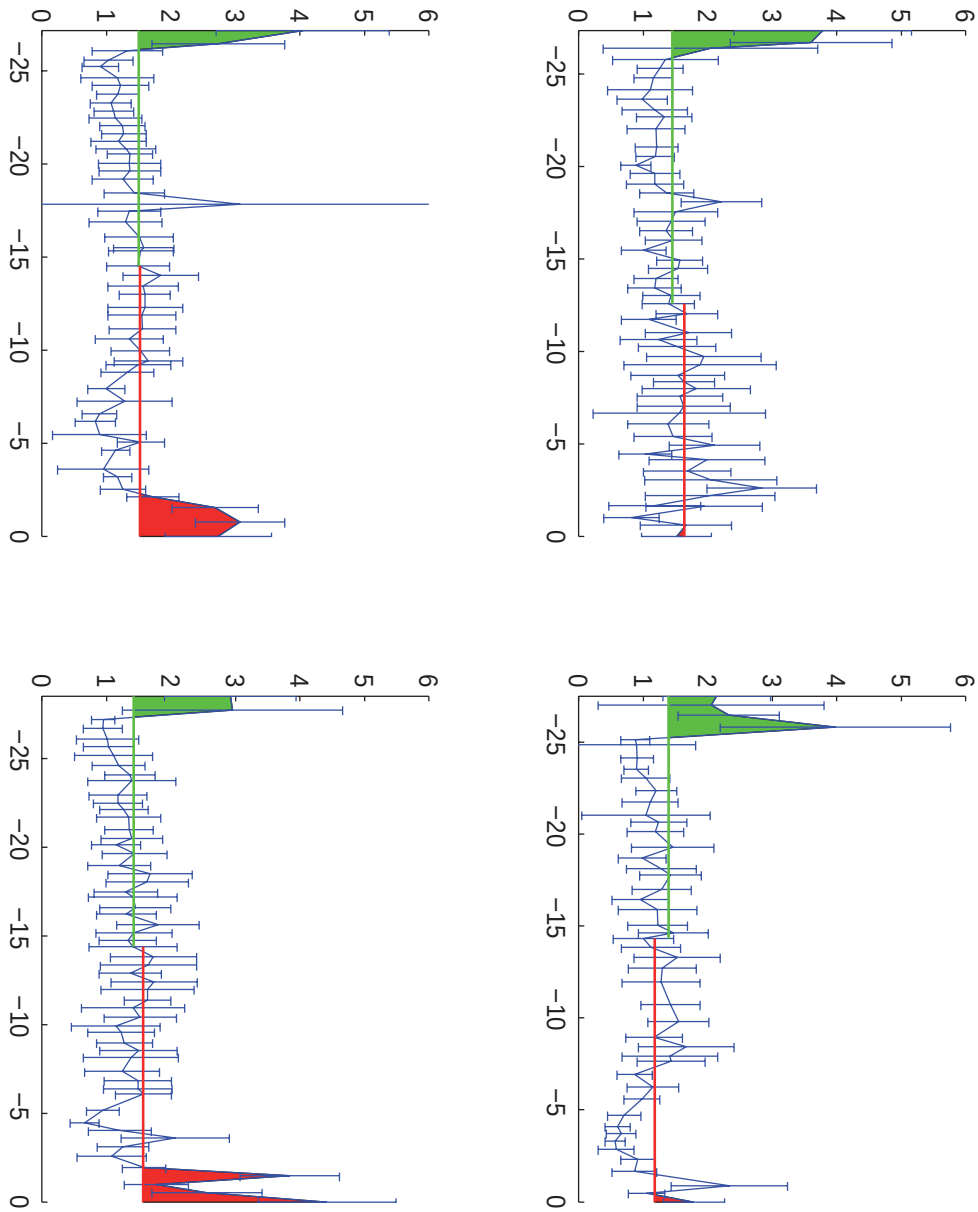

Figure A.3: Standard deviation of the potassium content at each image(point) of the w/c 0.65 mortar conditioned to 85% RH before 2nd drying.

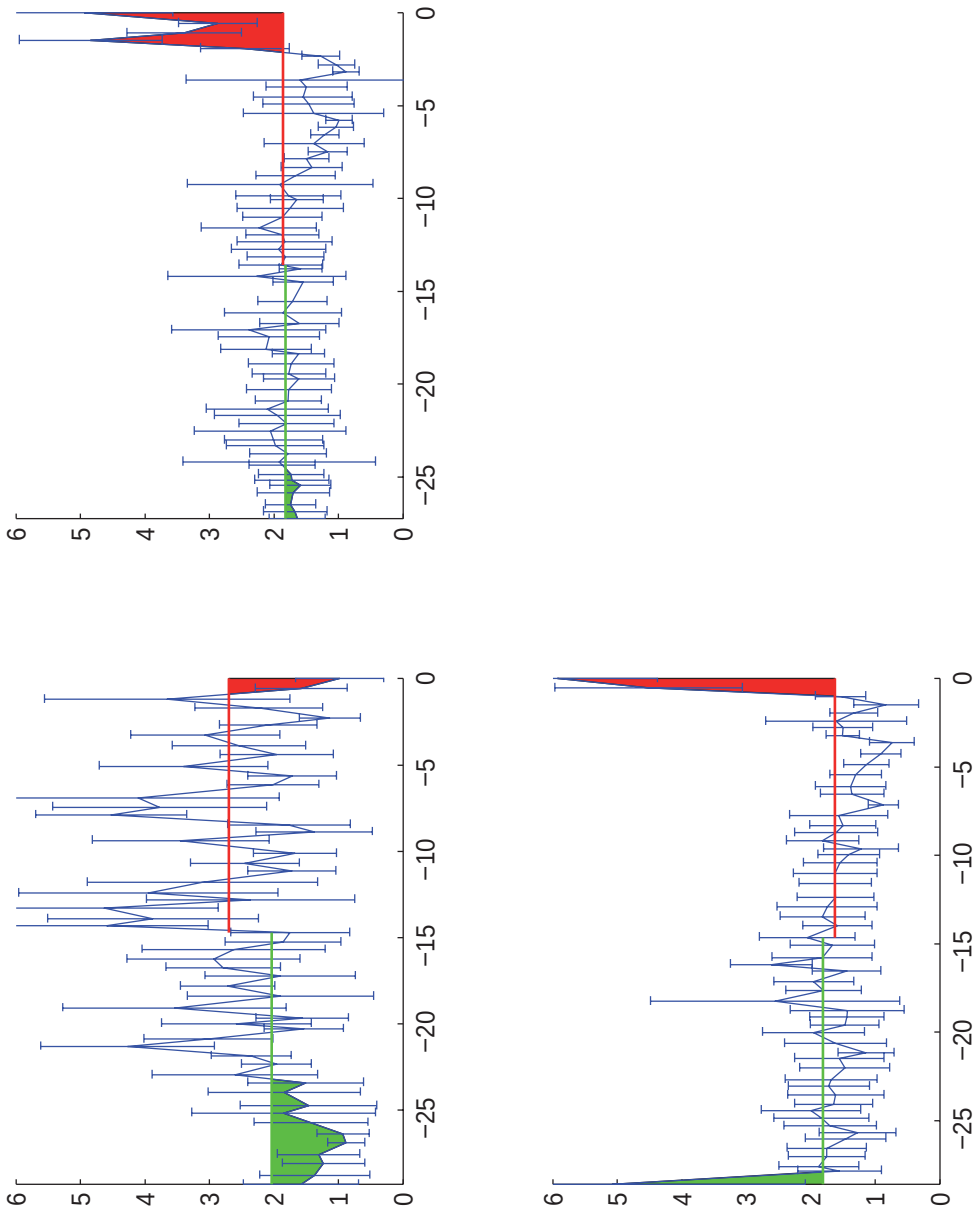

Figure A.4: Standard deviation of the potassium content at each image(point) of the w/c 0.65 mortar conditioned to 93% RH before 2nd drying.

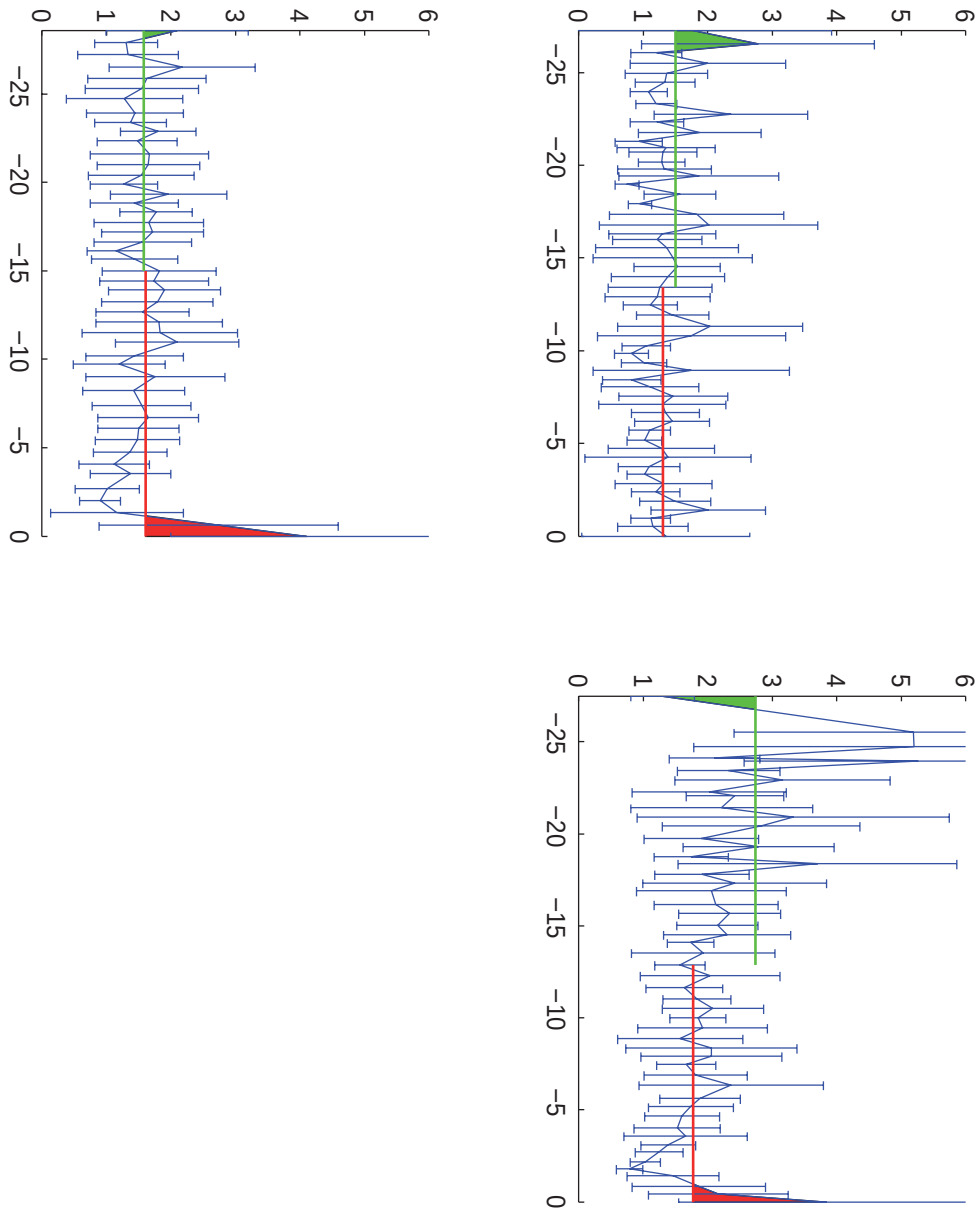

Figure A.5: Standard deviation of the potassium content at each image(point) of the w/c 0.4 mortar conditioned to 91% RH before 2nd drying.

I

Proceedings of the 7th Symposium on Building Physics in the Nordic Countries.
Reykjavik, June 13-15 2005. Vol 1 pp 181-187.

Remote monitoring and logging of relative humidity in concrete

M Åhs, Ph.D. student, Div. of Building Materials,
Div. of Building Materials, Lund University, Lund, Sweden;
magnus.ahs@byggtek.lth.se
http://www.byggnadsmaterial.lth.se

KEYWORDS*: relative humidity, concrete, remote monitoring, in-situ measurements.*

SUMMARY*:*
It is important to measure the relative humidity, RH, level in a concrete slab before applying semi permeable flooring to the surface. If the moisture level in the concrete is too high when the flooring is applied the high alkali level in combination with the moisture will degrade the adhesive.

This paper describes a new system used to continuously measure and monitor RH in situ during the construction stage. The paper includes descriptions of the method, an authentic measurement, and also how to evaluate results given by the measuring equipment. The presented results are taken from measurements performed on a construction site where the RH has been monitored, via the mobile phone network.

1.Introduction

Drying of concrete is a slow process and frequent measurements appear redundant. However, there are benefits to be achieved from frequently measuring RH. First of all frequently performed measurements make it possible to follow how fast the concrete is drying in existing climate and secondly it is possible to estimate the remaining drying time until the flooring may be applied.

This paper describes a newly developed system for logging and monitoring in-situ measurements of RH. The system is called Betongdatorn Fukt 5.0. In short, an RH sensor, Humi-Guard, is installed in a hole drilled into the concrete slab. When the RH sensor is installed it is connected to an instrument that transmits readings to a data logger. Measurements from both temperature and RH are stored at an optional rate in the data logger which is located indoors on the building site. The data logger is connected to a GSM-link. The software Betongdatorn Fukt 5.0, is installed on a computer with a modem. The modem is used to connect to the data logger via the GSM-Link. Data from the data logger is accessed and transmitted to the computer via the mobile phone network. Evaluations of the measurements are performed on a specially designed Excel spread sheet. Calculations of the uncertainties involved when measuring are performed for each in-situ measurement individually in the specially designed Excel spread sheet.

There are many different methods for measuring RH in concrete in-situ, e.g. measurements in drilled holes using instruments from Humi-Guard, Vaisala, Testo, RBK (2001), e.g. measurements in drilled holes using a metal rod with wood and metal discs to measure a complete RH profile through a slab, Sjöberg (2004). Today in Sweden, the main part of RH measurements in concrete are performed manually. RH is, in best cases, measured about once or twice each month about two months before the flooring is applied. More commonly RH measurements are carried out about one week or less before the flooring. The actual measurements are carried out either as in-situ measurements or as measurements on samples removed from the concrete.

Measuring RH of a concrete slab in-situ is rather time consuming. When measurements are performed in situ, the RH sensor needs up to 4 days after installation to reach equilibrium according to RBK (2001). However, after this initial phase of reaching equilibrium, the RH and temperature can be measured anytime. In Sweden building companies purchase these measurements from other companies. In order to get a regular day-by-day follow up of the drying process of a concrete slab a computerized data acquisition system was developed by Skanska Sweden AB in 2002, Åhs (2002).

Today the high rate of construction demands carefully planning of forth coming activities as accurately as possible in order to optimize construction. When planning applying semi-permeable flooring, e.g. PVC, to a concrete slab, time for drying needs to be taken into account, since time is often a critical parameter during construction. Very often construction time is limited and drying of concrete is slow, this makes it important to be able to estimate the time needed for the concrete to reach a certain level of RH.

If the RH is too high, there is a risk to create future moisture related problems. The adhesive may degrade due to the high moisture and alkali levels and create harmful emissions Sjöberg (1999, 2001a). These emissions are believed to have an essential role in the sick building syndrome Kumlin *et al* (1994), Sjöberg (1999, 2000), Hall (2003).

The common way to determine RH in concrete slabs is to measure RH just before attaching flooring. If requirements are not fulfilled the contractor often has no time to let the concrete dry further and the flooring is applied anyhow.

This may cause problems in the future since the moisture redistributes after flooring is applied. Moisture moves from areas with high moisture content to areas with lower moisture content and thus increases RH in the former dry areas. This process continues until equilibrium is established, if ever, and takes many months or even years. Underneath the flooring, the RH increases until it reaches a maximum level. The adhesive will degrade if the obtained RH level is too high. The problem is hidden on a short time basis since the problem with degrading adhesive does not occur until about 1 or 2 years.

If the RH on the other hand would be measured frequently, starting a long time before applying PVC flooring, then the contractor can take measures to speed up the drying process. This could lead to a faster and more reliable prognosis making of when the earliest possible date of flooring could be identified.

One other problem when measuring RH in-situ is the temperature stability during construction. In many cases temperature stability during construction is very poor because the building is not finished yet. Often doors, windows and insulation in walls and roof are not installed when the measurements are to be performed. The unstable temperature results in very uncertain measurement results. If the temperature has recently been very high and suddenly decreases fast, the reading shows to high RH and vice versa.

The newly developed system of logging RH has revealed unknown behaviour of how the Humi-Guard RH-sensor is working and how the actual temperature in concrete changes in time.

2.Method

This method for measuring RH in concrete is based on in situ measurements performed in a concrete slab.

A Ø16 mm hole is drilled in the concrete to a certain depth minimum 35 mm from surface. The depth of the hole is determined depending on the drying situation.

The depth of the hole is measured to ensure that you have reached the desired depth. Then the hole is carefully cleaned from concrete particles and dust using a vacuum cleaner or an air pump. A cylindrical brush is used to remove dust from the holes inner surface. A special manufactured measurement tube with a rubber sealing in the bottom is after cleansing inserted in the hole. The rubber sealing is open to the concrete surface and fitted tight to the sides of the hole. Sealing paste is put in between the measurement tube and the top of drilled hole to both fix the tube and also to prevent air movements from interfering with the measurements.

A leak detector is used to find out if the installation of the measurement tube is air tight fitted to the hole. If a leak is detected, the leak should be sealed and new tests are performed until no leak is detected.

After this a RH sensor, Humi-Guard shown in figure 1, is attached/fixed to a rubber plug contact, see figure 1, and promptly, approximately within 30 s, inserted in the measurement tube using a special rubber plug installing device. The RH sensor is read using a conductance meter shortly after installing it in the measurement tube. If the reading from the sensor is above 2 µS, the installation of the sensor has been carried out promptly enough. If the reading is below 2 µS then the sensor shall be replaced with a new sensor. After a successful sensor installation a rubber plug is inserted in the measurement tube to ensure that the whole installation is air proof.

The RH sensor is sensitive to RH changes and for one time use only. Its operating range in RH is (75 – 95) %. Sensors must be kept in a moisture controlled environment during storing. The RH sensor is sensitive to low RH, if the sensor has been exposed to below 75% RH for more than 30 seconds it may be damaged.

The RH sensor is constructed from two thin electrodes made of silver that are attached on the opposite sites of a small plastic core. The RH sensor is approximately Ø2 mm and 14 mm long. A fibrous body of polypropene containing a hygroscopic electrolyte is spun like a web close-coiled around both the plastic core and the two silver threads. The electric conduction of the hygroscopic electrolyte is dependent on the moisture and to some extent the temperature in the ambient air and the conductance between the two electrodes changes accordingly.

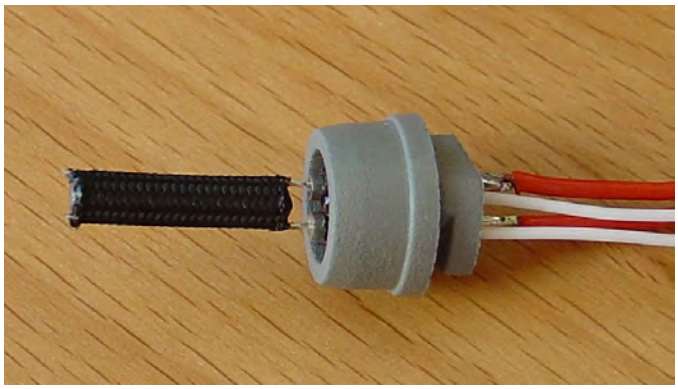

FIG. 1. Humi-Guard sensor attached on a rubber plug contact.

In close proximity to the RH sensor a temperature sensor is fixed on the rubber plug which is fitted into the measurement tube. The measurement tube and rubber plug contact, sealing, and concrete create an air tight space. Another rubber plug is inserted in the top of the measurement tube to prevent dirt and large air movements from interfering with the measurement. Four thin wires from the sensors are squeezed tight using the top rubber plug. The wires are connected to a specially designed transmitter, which is fixed on a steel frame next to the drilled hole, see figure 2.

The temperature sensor is a thermistor with an operating range between (0 - 40) °C.

Mineral wool with a thickness of about 70 mm covering (250*250) mm^2 is placed on top of the concrete as insulation to reduce temperature fluctuations from affecting the RH results.

FIG. 2. Transmitter and insulation on top of concrete at the measuring position

The instrument in the transmitter measures the conductance between the two silver threads and the temperature from the thermistor. The transmitter sends the data at an optional rate to the receiver via an antenna. It is able to transmit data to the receiver at a distance of 3 km if free sight in between the transmitter and the receiver. The data logger stores data at an optional rate ranging from 1 s up to once a month.

The software receives data from the data logger. The data is compared to data that is obtained from a reference system. The reference system is constructed from an insulated aluminium block. Inside the aluminium block 2-4 RH generating cells from a uniform batch are installed. The cells are made of a small glass container filled with a roll of cloth wetted in hygroscopic water solution. These cells generate a very accurate RH of about 85.1 %. Each batch of reference cells are inspected at an UKAS accredited laboratory. Above these cells RH sensors from the same batch are positioned. The software is used to calculate the RH values from the sensor in the concrete using a special algorithm that includes how the sensors from the same batch reacts to a known RH which is provided by the reference system.

3.Test results

In the in-situ measurement the RH and temperature were measured for a concrete layer cast on top of a hollow core slab. The top layer concrete was never subjected to any additional water in terms of rain since it was cast after the roofing was completed.

Data has been logged at an hourly rate during a period of 3.5 months starting from late April and ending in mid August 2004.

The RH (thick line) is represented on the left hand y-axis and the temperature (thin line) is represented on the right hand y-axis, see figure 3. The x-axis represents time.

During the first 5 weeks no insulation was on top of the concrete where the measurement was performed. In this period both the temperature and the RH fluctuates quite much and the mean RH is about 90% and the mean temperature is about 15 °C. The heating system was not running during this period. The drying rate is low during this period. A piece of mineral wool was put on top of the measuring point after 5 weeks and at the same time the heating system was turned on. The purpose of placing insulation on top of the measuring point was to reduce the amplitude of the fluctuations of the temperature. The amplitude of the temperature

and RH were both reduced very much and the insulation served its purpose. During the following 15 weeks the mean temperature was about 20 °C and the mean RH was about 85 % RH.

During the measuring period the RH in the concrete has varied between 83.9 % to 94.4 % RH and the temperature has varied between 8.5 °C to 24.7 °C

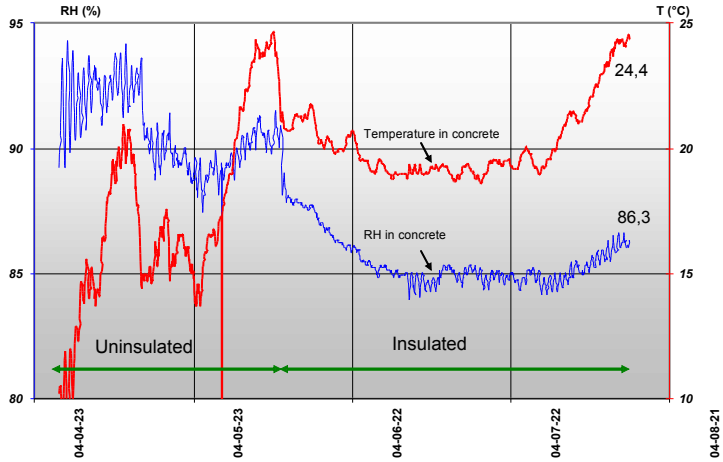

FIG. 3. Relative humidity (thick line) and temperature (thin line) measurements performed during a period of 3.5 months in a concrete slab w/c 0.38.

4.Discussion

The RH and temperature both fluctuate on a daily basis, see figure 3. This fluctuation is probably corresponding to the temperature outdoors, however the outdoor temperature was not measured during the period. During the first part when the measured spot is uninsulated both curves shows larger fluctuations than during the latter part.

During the first month with no insulation the RH sensor does not measure RH in the concrete accurately. The result is affected by the temperature changes to some extent. Since RH rises each time the temperature drops it is obvious that the RH sensor is affected by the surrounding air. When the temperature in air suddenly drops, the RH level increases instantaneously, a temperature drop of 1 °C in air leads to approximately a rise in RH of 5 % RH. In contradistinction to air, the RH in a material drops when the temperature decrease however the drop of RH is small, less than 0.3% RH, Nilsson (1980, 1987), Sjöberg et al (2002).

The amplitude of RH fluctuations declines from ±2.5 %-units down to ±0.5 %-units, when the measurement spot is insulated. The result is now in harmony with established theories for moisture mechanics in material and earlier research performed in laboratory. In laboratory it has been shown that the RH rises between 0.1 – 0.5 %-unit/°C depending on w/c-ratio and RH level. The insulation is interfering with the drying process. The insulation put on top acts as an additional obstacle for the water to pass through when the concrete slab is drying. The resistance for the water to pass through the mineral wool insulation corresponds to about 2-3 mm of extra concrete put on top.

It is possible to explain the behaviour in the uninsulated period in two different ways.

The materials in the drilled hole i.e. air, concrete, plastic tube, RH sensor, temperature sensor, sealing paste and rubber plug absorb moisture at different rates. When the temperature suddenly drops in the system the equilibrium is no longer present. The RH in the air instantly increases and the materials in the system suddenly all has a lower RH than the air. The materials respond to this increase of RH by absorbing surplus moisture from the air by diffusion. The rate of absorption is both dependent on the geometry of the

measurement system and how quick the materials absorb water. The concrete at the bottom of the hole is quite slow to absorb water both because of a small exposing area and because of the concretes moisture properties. The RH sensor, however, which both has a larger exposing area and absorbs water quicker than concrete, reacts immediately and therefore a rise in RH, is measured. Another possible explanation is that differences in temperature or differences in how fast the temperature changes in concrete, air, temperature sensor and RH sensor affects the results.

The newly developed system of logging RH has enlightened this behaviour of the measuring sensor and how the actual temperature in concrete changes in time.

To detect fast changes of a studied parameter a high frequency in data acquisition is required. On the other hand long term measurements produce large amounts of data if the frequency is high.

One advantage of logging data from an RH sensor is that when measuring RH manually you are not able to determine if you have measured during a time when the RH is increasing or if it is decreasing. When logging data you may notice fluctuations.

The data acquired in many cases gives a better view of changes which is not possible to detect manually. Slow changes on the other hand are also hard to monitor if the changes are too small to determine on a day by day basis. Unexpected events are also much easier to detect when the measurements are performed by an automatic system.

5.Conclusion

Betongdatorn Fukt 5.0 logging system compared to manually performed measurements gives a better view of how the drying process is proceeding in a concrete slab, e.g. on a construction site.

The system presents both temperature and RH in a diagram and this makes it easy to follow how the drying in the concrete is progressing. The diagram also shows if the temperature is stable enough to make a reading of RH. The drying rate of concrete is clearly shown in the diagram and this gives you an instrument to evaluate if the existing drying climate conditions are satisfactory.

The diagram also makes it quite easy to make a prognosis of when the RH is low enough to apply the flooring.

There is a risk that manually performed measurements are made when the temperature has recently peaked, e.g. when the sun has warmed the measured spot. Measurements performed just after a temperature peak shows a much lower RH than the actual RH. Betongdatorn Fukt 5.0 makes it possible to distinguish misleading results of this kind.

6.References

Hall T. 2003. The physical status of an existing building and its components – special emphasis on future emissions. Chapter in “Improving Construction Competitiveness”. Blackwell Science, Oxford, England

Kumlin A., Åkerlind L-O., Hall T. 1994. Method to solve indoor air quality problems: a practical Swedish strategy. Proceedings of Indoor Air – An Integrated Approach ’94. Gold Coast, Australia. 27 Nov – 1 Dec 1994. Vol 1. pp 329-332.

Nilsson L-O. 1980. Hygroscopic moisture in concrete – Drying measurements & related material properties. Report TVMB-1003, Lund Sweden 1980, pp 24 – 37.

Nilsson L-O. 1987. Temperature effects in RH measurements on concrete – some preliminary studies. Proceedings of the Symposium and day of Building in Lund Sweden, August 24 – 27, 1987 pp 456-462

RBK, 2001. Manual for measuring moisture in concrete (in Swedish), third edition 2001, The Swedish Council for Building Competence.

Sjöberg A. 1999. Transport Processes in covered concrete floors. Proceedings of the XVII Symposium on Nordic Concrete Research. Reykjavik, Iceland. 4 – 6 August 1999. pp 122-124.

Sjöberg A. 2000. Concrete floors as secondary emission source. Healthy Buildings 2000. Espoo, Finland. 6-10 August 2000.

Sjöberg A. 2001a. Secondary emission from concrete floors with bonded flooring materials. Department of building Materials, Chalmers University och Technology, Göteborg, Sweden. Publication. P – 01:2. www.bm.chalmers.se/research/publika/p012.htm

Sjöberg A., Nilsson L-O., Rapp T., 2002. Measuring relative humidity in concrete slabs with floor heating system Stage I, (in Swedish). Publication P – 02:1 Göteborg 2002. www.bm.chalmers.se/research/publika/p021.htm

Sjöberg A. 2004. A method for measuring moisture distribution in concrete structures. Experimental evaluation of the OE-method. (in Swedish) Report TVBM-3122, Division of Building Materials, Lund Institute of Technology, Lund 2004. www.byggnadsmaterial.lth.se/tvbm-3122.htm

Åhs M. 2002. Remote monitoring of relative humidity in concrete. Betongdatorn 5.0 a new system for measuring relative humidity in concrete structures – evaluation of new system and methodology. SBUF Rapport 11105. Malmö 2002.

II

A METHOD FOR STUDY SORPTION PHENOMENA

M Åhs[1,2,*], A Sjöberg[1,3] and A Anderberg[1,4]

1 Division of Building Materials, Lund University, Lund, Sweden
2 Skanska Sverige AB, Malmö, Sweden
3 Fuktdimensionering AB, Malmö, Sweden
4 maxit Group, Stockholm, Sweden.

ABSTRACT
Sorption of humidity in surface materials is a crucial parameter for the moisture balance in the indoor air. In a similar way, sorption of indoor pollutants in surface materials is important for the level of, for example, VOCs and other compounds in the indoor air. Knowledge of sorption capacity and sorption rate is of fundamental importance when indoor air quality is modeled.

This paper describes studies of sorption phenomena made with a sorption balance. It includes descriptions of the method and one measurement, and it shows how the evaluation is performed. In the study, steady state sorption phenomena have been measured for a surface material used in furniture and clothes. The procedure for water vapor sorption has been studied.

INDEX TERMS
Sorption phenomena, sorption balance, steady state, dynamic state

INTRODUCTION

During the last decade, several models for simulating indoor air quality have been developed of different scientists all over the world, for example Damain *et al.* (2002) and Murakami *et al.* (2003). To imitate the reality as close as possible the user is in great need for material properties that are actually used in the simulating model.

These models require different input parameters like air flow, surfaces, dimensions of the room and the properties of the surface materials. In order to simulate the surface material interaction with the surrounding atmosphere and thus the indoor air quality, the materials ability to absorb, desorb and store substances from the air in the room has to be known.

One method to evaluate sorption phenomena for a material is described in this paper. This method, based on a sorption balance, has been used in pharmaceutical and food industry for organic materials for a long period of time. The sorption balance has in these cases been used to study sorption of water vapor on *e.g.* protein inhalation powders by Maa *et al.* (1998), morphine sulphate by Wadsö and Markova (2001), durum wheat semolina by Hébrard *et al.* (2003) Plant lipases by Caro *et al.* (2002). Inorganic materials used in buildings has also been studied such as, self leveling flooring compounds by Anderberg (2004), and the outcome has proved to be satisfactory. The method is fast in comparison to other methods and generates the important material properties involved when modeling indoor environments. In addition to studies made on water vapor, both absorption/desorption and the diffusion rate of volatile organic compounds (VOC) in surface materials are properties that can be studied in measurements performed with a sorption balance. Measurements on VOCs have been performed on polyurethane foam by Cox *et al.* (2001) and on vinyl flooring by Zhao *et al.* (2004).

This paper also presents how a sorption isotherm for water vapor in natural wool was achieved. Natural wool can be found in many applications *e.g* as a part of a weave in furniture fabric or in clothes used in the indoor environment. The method described can easily be applied on VOCs and other volatile substances instead of water vapor, since the sorption balance used in this study is designed for organic compounds as well.

The content of for example moisture in a material depends, among others, on the vapor pressure of the substance in the surrounding atmosphere. The material has a certain content of the substance when in equilibrium with

* Corresponding author email: magnus.ahs@byggtek.lth.se

surrounding atmosphere. If the vapor pressure in the atmosphere surrounding the material changes, the equilibrium state is no longer present. The material responds either by an uptake or a loss of content of the substance to the surrounding atmosphere to reach equilibrium once more. This process is a continuously ongoing process. Therefore it is important to know the equilibrium content of a substance at a corresponding vapor pressure and how much and how fast it changes when modeling indoor air environments.

RESEARCH METHODS

The method described in this paper is based on a sorption balance. The sorption balance, figure 1, is a high performance balance arranged in a climate cabinet equipped with a stable and reliable climatic control unit. The temperature is adjustable well within a range that may be expected in an indoor environment *e.g.* 0-50 °C. Vapor pressure of a substance is generated by mixing different proportions of a saturated gas stream and a dry gas stream, and is adjustable between completely dry to completely saturated gas. The saturated gas is generated by bubbling dry gas through a liquid substance.

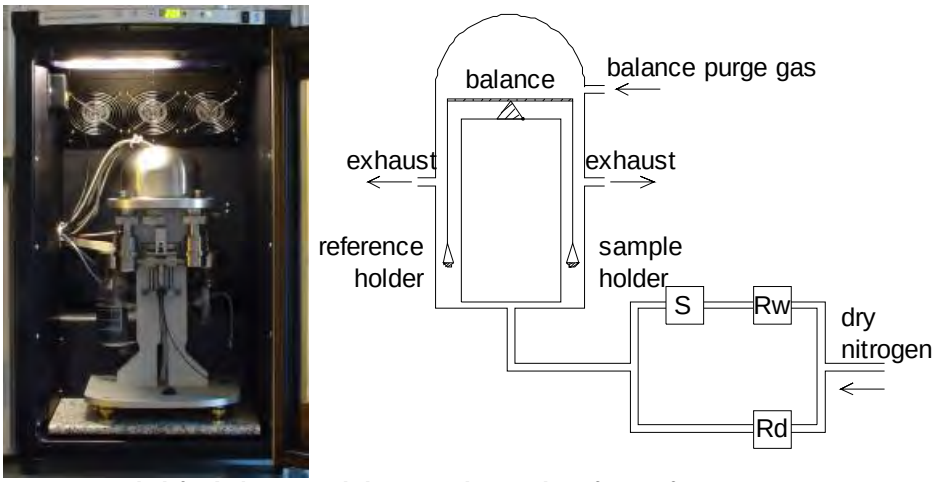

***Figure 1**. On the left side the sorption balance in a climate cabinet from Surface measurements System, SMS, is shown on the right side a sorption balance principle is shown*

The balance, which is the key component in the system, monitors the sample mass as a function of time. It is continuously weighing the sample which is subjected to different vapor pressure levels of the active substance. The sample mass is digitally recorded on a computer at a predefined rate.

A carrying gas is conveyed through a mass flow control unit which distributes the gas in two separate tubes which are equipped with very accurate gas flow control meters. One gas tube runs through a glass vial which is filled with a liquid substance, *e.g.* water or VOCs that generates a saturated gas. The second gas tube works as a dry mixing gas which is mixed in different proportions with the saturated gas by the mass flow control unit to achieve the desired level of vapor pressure. The mixed gas flows past both the reference pan, (reference holder in figure 1), and the sample pan (sample holder in figure 1) at a constant speed.

Two identical glass pans hang in a symmetric microbalance which detects very small differences in sample mass, *e.g.* mass changes of as little as 0.1 µg is possible to recognize for sample sizes as big as 1.5 g. The material sample is put in one glass pan and the other one is empty called the reference pan. These pans should always be used in pairs to avoid systematical errors. The symmetric setup minimizes disturbances from absorbed substance on the glass pans.

The vapor pressure, in the gas stream passing the pans, is defined in a test cycle and runs in a predefined order, called a sequence. The level of vapor pressure is either set to a constant level, stepwise change or continuously increasing/decreasing level (ramping or sinusoidal). Each step runs for either a predefined time period or when a predefined maximum mass change per time unit is reached. A scanning curve is measured by ramping up or down from different levels at a low speed. This ramping application would result as a curve starting from either the

desorption or the absorption isotherm, reaching towards to the opposite isotherm.

The balance is placed in a temperature stable climate cabinet since partial pressure is strongly temperature dependent. If the substance used in the sorption balance is water a rise in temperature of 1 °C leads to a variation of up to 10% in saturated vapor pressure. Therefore fans are installed in the cabinet which circulates the air inside to prevent temperature gradients on the instrument from influencing the test.

RESULTS

In a study by Svennberg (2005) a sorption balance of the brand DVS 1000 from Surface Measurement Systems at Lund University, has been used. In that study the absorption and desorption isotherm on 100 % natural wool for water vapor was measured.

As the study was made for water vapor, de-ionized water was used for saturating the carrying gas, which in this case was N_2. The wool sample were exposed to step changes in vapor pressure ranging from 0 % relative humidity, (RH), up to 95% RH down to 0 % RH in 10 % RH steps and the equilibrium moisture content was determined for each step. The sorption isotherm for water vapor is shown in Figure 2.

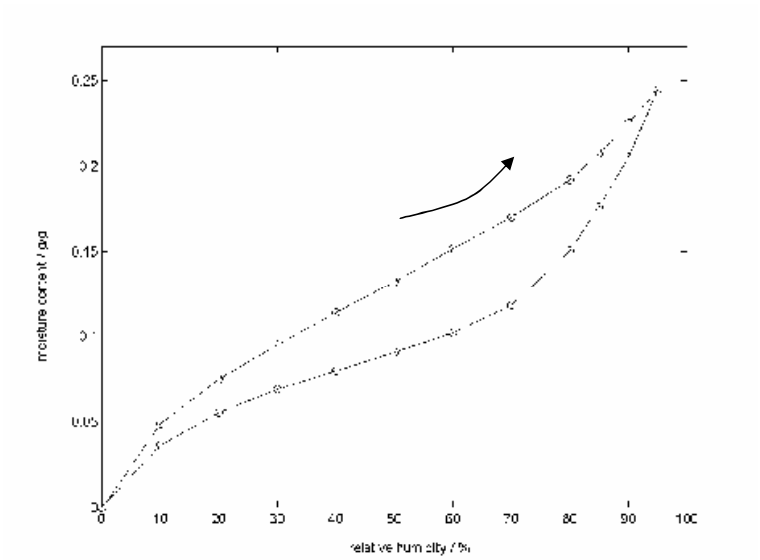

***Figure 2**. Water sorption isotherm for 100% natural wool (felt, density 176 kg/m^3).*

The rings in figure 2 shows the result from each step in the sequence and represent the ratio between equilibrium mass at a certain generated vapor pressure and the dry mass. In figure 2 it is possible to see the difference between the absorption and the desorption isotherm. If the desorption sequence is not followed through to the bottom but turns upwards again lets say from 70 % RH and slowly going up to 90 % RH, the curve would start from 70 % and finish at the 90 % RH level. This would result as a scanning curve, see arrow, figure 2.

DISCUSSION

The method is quite fast, for instance the whole sorption isotherm for wool fibers was measured during a time of approximately 72 hours. This makes it possible to run several tests after each other to make a statistical analyze of the material properties studied.

The time required for achieving one complete sorption isotherm lasts from a couple of hours for low density porous materials, such as glass wool insulation, up to about two weeks for high density porous materials such as concrete.

Comparing the obtained results with existing sorption isotherms shows that there is a strong reliability in the

material properties extracted through a sorption balance. However there are some requirements that must be met and errors to be aware of.

The sample size is limited due to two conditions, firstly the total maximum load of the sample is limited to a few grams and secondly the total mass change in the test cycle is limited to about a hundred milligrams. This makes it in some cases difficult to select a representative sample of a dense inhomogeneous material such as concrete.

The temperature in the climate cabinet is very stable. However it is possible that large and rapid fluctuations in the room temperature may influence the climate in the cabinet. This may in some cases have an effect on the results. Disturbances of this kind may be taken into account since the temperature of the climate cabinet is recorded in the data file.

The set point vapor pressure is controlled via the gas flow controllers which are very accurate. However there is a small potential error in the gas mass flows distributed. The volume of the gas is dependent on two factors, the actual vapor pressure level and the temperature. Both the vapor pressure level and the temperature dependencies are managed via a preset table which provides the correct mass flow settings. There is a possibility to validate the generated water vapor pressure by measuring the mass change of a saturated salt solution in the sorption balance. Ramping from a vapor pressure above to below the equilibrium vapor pressure level should validate that the requested vapor pressure level is the same as the generated vapor pressure level.

Other potential sources of error in this method are for instance those connected to the sample pans. It is of uppermost importance to clean the sample pans in between the tests *e.g.* by flushing the pans using de-ionized water. The results might otherwise be affected by the previous material. The cleaning of the sample pan also minimizes the build up of static electricity. Otherwise that will be shown as a slow but significant weight drift.

The sample pans and the reference pans should be kept in pairs to minimize errors due to different behavior during a test cycle. If sample and reference pan are made of glass they should be handled with care since glass easily cracks. If a small crack occurs, in the sample pan or the reference pan, it may be difficult to observe that with the naked eye however it may influence the result. If a crack is suspected then one way to detected it is to run a test cycle with clean empty pans and monitor the mass change. A feared crack in either of the glass pans will show as a substantial mass change during the test cycle with the empty pans.

The wire hanging down from the balance has to run free and the sample pan may not touch surrounding surfaces when in measuring position. The position of the wire may be disturbed when putting the sample pan on the hook of the wire. If the wire or sample pan touches a surface inside the instrument the balance readings are inaccurate and the mass of the sample is very unstable.

Another source of error occurs if the time defined for a vapor pressure step is too short. Then the sample mass increase/decrease per time unit at the end of the step has not yet reached a reasonably low level. If the time step at a certain vapor pressure is too short then equilibrium has not yet occurred. There is a possibility to extrapolate the results to evaluate the mass for the sample in equilibrium with belonging vapor pressure. The accuracy on the equilibrium mass is depending on many parameters *e.g.* how precise your extrapolation imitates the reality, how to chose sufficient number of values from the measuring for the extrapolation and so on. If the sample mass in a step has not leveled out at all it is not possible to make an extrapolation with a decent accuracy.

CONCLUSION AND IMPLICATIONS

The sorption balance has proved to be an important instrument to use when producing sorption isotherms, which is an important material property input in many applications regarding indoor air quality simulations.

This instrument has the potential to be widely used in future research on material properties regarding different compounds *e.g.* VOC's and others. This will be of great importance in order to achieve better input values in order to improve the accuracy in the results from the simulations.

With the sorption balance there is a possibility to measure the diffusion coefficient in the same measurement as the sorption isotherms are measured. The study of sorption kinetics is performed on a specimen with a well defined geometry. However this possibility has not been used very often yet.

In addition to this, details in the sorption phenomena such as the scanning curves may be studied by continuously increasing/decreasing the vapor pressure level, *i.e.* ramping. In certain sorption balances there is a possibility to make the vapor pressure perform a sinusoidal variation. This may also be used as an interesting tool to study how a material responds to continuously changing vapor pressures in the surrounding environment.

ACKNOWLEDGEMENTS
Funding was provided by both SBUF, the Development Fund of the Swedish Construction Industry and FORMAS, the Swedish Research Council for Environment, Agricultural Sciences and Spatial Planning.

REFERENCES

Anderberg A. 2004. Moisture properties of Self-levelling Flooring Compounds. Report TVBM-3120, Lund 2004

Caro Y., Pina M., Turon F., Gilbert S., Mougeot E., Fetsch DV., Attwool P. and Graille J. 2002. Plant Lipases: Biocatalyst Aqueous Environment and Enzyme Activity, Biotechnology and Bioengineering, Vol 77, NO. 6, March 20, 2002

Cox SS., Zhao D. and Little JC. 2001. Measuring Partition and Diffusion Coefficients for Volatile Organic Compounds in Vinyl Flooring, Atmospheric Environment, Vol. 35, 2001, pp 3823-3830.

Damain A., Blondeau P. and Tiffonet AL. 2002. Investigating the Influence of the Wall Materials and the Thickness on the Reversible Sink Effect, *Proceedings of the 9th International Conference on Indoor Air Quality and Climate- Indoor Air '02*, Monterey: Indoor Air '02**,** Vol 3, pp 564-569

Johannesson B. 2000. Paper 4, A Test of Four Different Experimental Method to Determine Sorption Isotherms., Ph. D. Thesis, Lund University, Lunds institute of technology,

Maa YF., Nguyen PA., Andya JD., Dasovich N., Sweeny TD., Shire SJ. and Hsu CC. 1998. Pharmaceutical Research, vol 15, NO. 5, 1998, pp 768-775.

Murakami S., Kato S., Ito K. and Zhu Q., 2003. Modeling and CFD prediction for diffusion and adsorption within room with various adsorption isotherms, Indoor Air 2003, Vol 13, Supplement 6, pp 20-27.

Svennberg K. 2005. Sorption isotherms for textile fabrics and foam used in the indoor environment. Report TVBH-7227, Lund 2005

Wadsö L. and Markova N. 2001. Comparison of three methods to find the vapor activity of a hydration step. European journal of Pharmaceutics and Biopharmaceutics 51, 2001, pp 77-81.

Zhao D., Little JC. and Cox SS. 2004. Characterizing Polyurethane Foam as a Sink for or Source of Volatile Organic compounds in Indoor Air, Journal of Environmental Engineering, ASCE, Vol. 130, 2004, pp 983-989.

III

Available online at www.sciencedirect.com
ScienceDirect
Construction and Building Materials 22 (2008) 2228–2234
Construction and Building MATERIALS
www.elsevier.com/locate/conbuildmat

Sorption scanning curves for hardened cementitious materials

Magnus Sören Åhs *

Division of Building Materials, Lund Institute of Technology, Lund University, P.O. Box 118, 221 00 Lund, Sweden

Received 29 November 2006; received in revised form 14 August 2007; accepted 15 August 2007
Available online 24 October 2007

Abstract

Drying of screeded floor slabs is an important issue for the building industry. However, virtually no attention is paid in prediction models to the hysteresis of sorption isotherms, mainly because of lack of data. Disregarding the hysteresis in prediction models will generate inaccurate predictions of future moisture distribution and remaining drying time. This paper presents a method for fast determination of scanning sorption isotherms and sorption isotherms by using a gravimetric vapour sorption balance. A sorption balance continuously determines the mass of a small sample subjected to a sequence of predefined vapour pressures and temperatures. Sorption isotherms and two examples of sorption scanning curves at 20 °C are presented. Results from three materials commonly used in screeded slabs are included, *viz* concrete W/C 0.65, concrete W/C 0.55, and a screed, Floor 4310 Fibre Flow. Absorption scanning curves obtained for concrete show a significant moisture history dependence as a consequence of the hysteresis of the desorption isotherm itself. Desorption scanning curves originating from the absorption isotherms indicate little influence of the moisture history.

Keywords: Cementitious material; Vapour sorption hysteresis; Sorption isotherm; Sorption scanning curve

1. Introduction

Drying of residual moisture and moisture distribution in screeded floor slabs are important concerns for today's building industry. Residual moisture is here defined as water in a material above a threshold known to cause damage to an adjacent material. Moisture coming from different sources, *e.g.* mixing, screeds, adhesives, and air, influences the vertical moisture distribution in the floor slab. Estimations of moisture distribution therefore require, apart from initial and boundary conditions, determination of various moisture related properties. The amount of water physically bound in the pore system corresponding to the relative humidity, RH, in the surrounding air, the sorption isotherm, plays a significant role in estimations of moisture distribution. However, the moisture history dependence of sorption isotherms, hysteresis, is often overlooked when such estimations are performed. Sorption isotherms are indeed central to estimating residual moisture and later drying–wetting processes, *e.g.* when screed and flooring are applied.

Moisture distribution in single layer concrete floor slabs [1] can be estimated with a fair degree of certainty. However, further research is needed to evaluate moisture distribution in two-layer slabs with a comparable accuracy. This lack of knowledge may result in moisture related damage to materials and combinations of materials where residual moisture may be the key factor indirectly responsible for health problems. For example, degradation of adhesive in a moist and high alkali environment may release volatile organic compounds, VOCs, such as 1-butanol and 2-ethyl-hexanol. High concentrations of VOCs are suspected to cause health related problems including runny noses and eyes [2]. The residual moisture may also cause visual damage to the flooring such as axial deformations, discolouration, and blisters.

Prediction models currently used to estimate drying and moisture distribution do not take into account the hysteresis phenomenon of the sorption isotherm [3–5]. Disregarding

* Tel.: +46 46 222 49 20; fax: +46 46 222 44 27.
E-mail address: magnus.ahs@byggtek.lth.se

0950-0618/$ - see front matter © 2007 Elsevier Ltd. All rights reserved.
doi:10.1016/j.conbuildmat.2007.08.009

hysteresis will lead to inaccurate moisture distribution estimations, *e.g.* the RH level in the screed top layer adjacent to PVC-flooring. When screed and flooring are applied, small amounts of water coming from the adhesive will substantially increase the RH in the upper part of the floor slab. Underestimating this increase in RH will, in turn, amplify the risk of moisture damage. An increased awareness of this problem is needed, especially since a prolonged concrete drying time is unattractive to building contractors.

For modelling of two-layer combinations, it is particularly important to recognize the hysteresis phenomena of the sorption isotherm, since sorption scanning curves profoundly affect the moisture redistribution. Prediction is straightforward for initial drying of a concrete slab when the moisture content at all depths of the first slab is determined from the desorption isotherm. However, when a second layer is applied to the slab, predictions of the future moisture distribution become more complex since hysteresis needs to be taken into account. As moisture penetrates the dry slab, moisture content is determined from a sorption scanning curve, commencing from the desorption isotherm. These sorption scanning curves will start from low moisture content levels on the desorption isotherm (Fig. 1, curves 1 and 3) and end up at successively higher moisture content levels. When the screed eventually dries and moisture load in turn decreases, moisture content is determined from sorption scanning curves, (Fig. 1, curves 2 and 4) commencing from the endpoint of the previous sorption scanning curves.

There is little previous research into determining sorption scanning curves in cementitious materials [6–8]. Research by Ahlgren [8] was not systematically carried out and variations within a material were never investigated. In addition, the experimental setup using climate boxes was time-consuming, with one year needed to determine a complete isotherm. As a consequence of the long testing period significant hydration took place during the experiment and had to be considered. A detailed description of the climate box method is published in [9]. Sorption balances have been widely used in other research areas such as the pharmaceutical and food industries [10–12]. Johannesson and Janz used a sorption balance on porous glass and sedimentary calcareous sandstone [13]. Additionally, Anderberg and Wadsö [6] used a sorption balance to determine both sorption isotherms and scanning curves of self-levelling flooring compounds. An inkbottle pore-method to predict sorption scanning curves on cement based materials was recently published [14].

This research has focused on experimental determination of isothermal sorption scanning isotherms for three different cement based materials: concrete W/C 0.65, concrete W/C 0.55, and a screed Floor 4310 Fibre Flow, SFC. A description of the method used and the investigated materials is presented as well as an estimation of the obtained accuracy of the performed measurements. Sorption isotherms have been obtained as well as two scanning sorption isotherms for each sample by using a sorption balance [15].

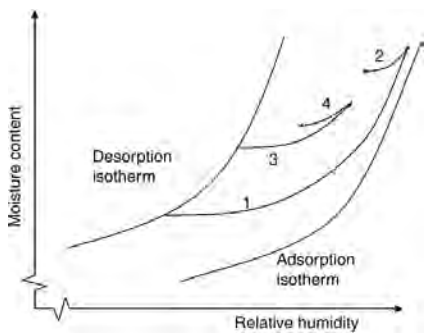

Fig. 1. Illustration of sorption scanning curves. Absorption scanning curves are marked 1 and 3 and desorption scanning curves are marked 2 and 4.

2. Materials

Three cement-based materials were used in this study, two concrete mixes with a W/C 0.65 and W/C 0.55, and a screed Floor 4310 Fibre Flow, SFC. Ordinary Portland cement, CEM II/A-LL 42,5 R according to 197-1 European Standard, was used in the two concretes tested. The basic binder of the SFC was alumina cement. For a detailed material description, see Table 1.

All samples were obtained from a full scale floor construction at different stages of drying in a room at 60% RH and 20 °C. The samples were never subjected to levels below 60% RH. To avoid effects of carbonation, at least 5 mm of the surface layer was chiselled off immediately prior to sampling. Samples were chiselled out from the floor construction at a specific time after casting, about 1–7 days prior to testing. The actual RH level of the samples was not determined at sampling. However, the RH lev-

Table 1
Mixture description for each material

Material	W/C 0.65	W/C 0.55	SFC[a]
CEM II/A-LL 42,5 R	250	400	
Water	162	220	320
Sand 0–8 mm	976	1672	
Sand 8–12 mm	489		
Gravel 8–16 mm	489		
Portland cement			15–80
Alumina cement			80–320
Gypsum			30–160
Dolomite 0.002–0.1 mm			490
Sand 0.1–1 mm			740
Polymer			15–80
Glenium 51	1.5	2.9	

Quantities are in kg/m^3.
[a] Mixture according to manufacturer.

els reached prior to sampling were expected to decrease with time since samples were removed during a period of over a year. Considering that all samples were selected close to the surface and the youngest samples were older than one month, the actual RH level of the samples should be closer to 60% RH.

Sample mass varied within a range from 20 mg to 100 mg due to the limitations of the sorption balance. Concrete samples of this size may contain a comparatively large fraction of aggregates that are close to inert in sorption processes, apart from the interfacial transition zones, ITZ. The amount of sorbed water in the ITZ of the larger aggregates is insignificant when the sorption isotherms are compared. However, a difference in aggregate fraction between samples significantly alters the sorption isotherm obtained. In order to eliminate aggregate fraction differences, the cement content was determined for each sample, thus obtaining comparable sorption isotherms.

The cement ratio of the concrete samples was indirectly determined by analyzing the samples in an inductively coupled plasma atom emission spectroscope, IPC-AES, thus obtaining the calcium content. The cement ratio, C_{ratio}, of each sample was calculated by using the following equation:

$$C_{\text{ratio}} = \frac{m_{\text{Ca}} \cdot M_{\text{CaO}}}{M_{\text{Ca}} \cdot 0.63}, \tag{1}$$

where m_{Ca} represents the calcium content, M_{CaO} the molar mass of calcium oxide, M_{Ca} the molar mass of calcium, and 0.63 an assumed mass ratio of CaO in the cement used. Two different batches of cement were used. Sorption isotherms for each sample were evaluated as mass of sorbed water per mass of cement.

3. Method

Scanning curves and sorption isotherms were studied using a gravimetric vapour sorption balance. The balance continuously measures the mass of a material sample subjected to a test cycle of variable RH and temperature conditions. A mix of dry and saturated nitrogen was used to achieve the set point RH level. Nitrogen was used to prevent carbonation of the cementitious material. Data consisting of RH, temperature and sample mass necessary for evaluating the sorption isotherms of the samples were recorded on a computer. A detailed description of the sorption balance is found in [15]. By subjecting the samples to linearly increasing and decreasing levels of RH, ramping, sorption scanning curves were determined. The sorption isotherm was determined at the same time by step changes of RH.

Screeds may be applied on both dry and wet slabs with a unique moisture history. In order to capture data from various moisture histories, samples were removed from parts that dried in a 60% RH climate for different time periods. Subsequently samples were put in a glass jar on a wetted cloth to soak in deionized water for minimum 6 h to fill the capillary pores. However, to achieve a sufficient degree of saturation for the concrete samples, soaking continued for at least 48 h. Soaking time could be reduced to about 6 h for SFC samples. Immediately after soaking the sample was placed on a sample glass pan and put in the sorption balance. Initial conditions in the sorption balance were set to 95% RH and 20 °C. As the balance was unstable a short while after loading, the test sequence was started after about 10–15 s, to avoid oscillating recordings.

Several test cycles, all including constant RH levels and ramps, were arranged in a sequence at a constant temperature of 20 °C (Fig. 2). This test method has previously been used on screeds [6]. Test cycles were essentially based on constant steps, starting from 95% RH down to 10% RH, up to 95% RH and finally a 0% RH step at the end of the cycle. During this cycle two ramps were included, thus allowing investigation of the scanning phenomenon. Both absorption and desorption scanning were examined between 70% RH and 95% RH at a rate of 40–115 min per % RH. Absorption scanning started from an initial desorption phase and desorption scanning started after an initial desorption phase down to 10% RH and a continuing absorption phase up to the start level at some 90–95% RH. Before and after the scanning, constant RH steps were set in order to quantify the degree of equilibrium obtained from the sample. Test cycles to determine a complete sorption isotherm including two scanning curves lasted about 10–15 days.

Mass equilibrium was almost reached for each RH step. The final part of each step was subjected to curve fitting using the following equation:

$$m_0(t) = m_{\text{f}} - (m_{\text{f}} - m_0(0))\mathrm{e}^{-k(t-t_0)}, \tag{2}$$

where $m_0(t)$ represents the recorded sample mass at the time t, m_{f} represents the final mass, $m_0(0)$ is the initial mass at time $t = 0$, k is a curve fitting constant and t_0 is the initial

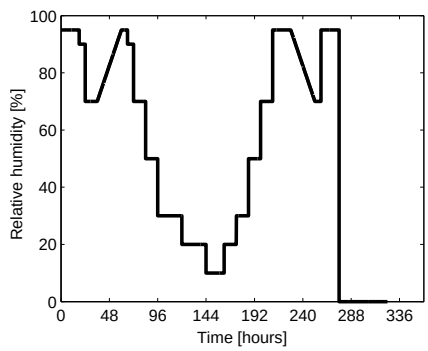

Fig. 2. A typical test cycle for determining the sorption isotherm and scanning curve for the studied materials. The x-axis represents time in hours and y-axis represents set point relative humidity in % RH. The absorption ramp is located between 36 and 60 h and the desorption ramp between 228 and 252 h.

time for each curve fitting. The best fitting curve was obtained by the method of least squares.

Two definitive points on the scanning curve, the beginning and the end, are determined by two constant RH steps before and after the ramp using Eq. (2). In between those points it is not possible to exactly calculate the equilibrium mass due to time lag effects. The difference between the last recorded sample mass and the extrapolated mass never exceeded 0.14% of total mass change in each step excluding the step at 0% RH.

This difference was evenly distributed, see Fig. 3, to the recorded mass with maximum difference in the beginning and zero in the end, using the following equation:

$$m_1(t) = m_0(t) - \frac{(m_0(0) - m_f) \cdot (t_{end} - t)}{t_{end}}, \quad (3)$$

where $m_1(t)$ represents the resulting sample mass with the evenly distributed difference added, $m_0(t)$ the recorded mass, $m_0(0)$ the recorded mass at the beginning of the ramp, m_f the extrapolated final mass before the ramp, t_{end} the ramp's ending time point, and t represents time.

Finally, the resulting mass of the scanning has been adjusted using the following equation:

$$m_{fr} = m_1(t) + \frac{(m_{fe} - m_0(t_{end})) \cdot t}{t_{end}}, \quad (4)$$

where m_{fr} represents the resulting sample mass with the evenly distributed difference added, $m_1(t)$ from Eq. (3), m_{fe} the extrapolated equilibrium mass at the end of the step succeeding the ramp, $m_0(t_{end})$ the recorded mass at the end of the ramp, t represents time, and t_{end} represents the ramp's ending time point.

The difference between the recorded and the extrapolated final mass is calculated using Eq. (2). This difference has the largest impact at the beginning of the scanning curve due to time lag effects. However, the difference at the end of the scanning curve is most affected by the difference between the recorded and the extrapolated final mass at the end of the scanning curve. To minimize the time lag effects Eqs. (3) and (4) were used.

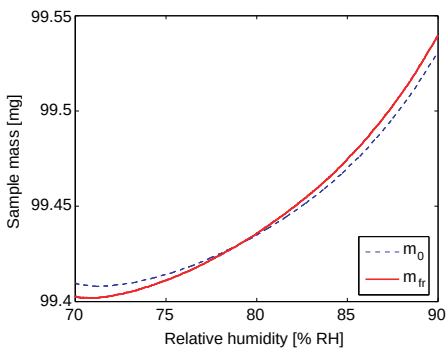

Fig. 3. Illustration of the recorded sample mass m_0 (dashed line) in comparison with the m_{fr} (solid line) obtained by using Eqs. (3) and (4). The x-axis represents relative humidity in % pH and y-axis represents sample mass in mg.

4. Results

The results of this study are divided into two parts. The first part, Figs. 4–6, presents sorption isotherms of W/C 0.65, W/C 0.55, and SFC, respectively. The second part, Figs. 7–9, shows sorption isotherms of individual samples including adsorption and desorption scanning curves and the difference in the amount of sorbed water depending on when the samples were removed from the slab.

The x-axis in Figs. 4–9 represents the relative humidity in % RH. The y-axis in Figs. 4, 5, 7 and 8 represents the moisture content, quantified as the evaporable moisture content, We, divided by cement content, C. The y-axis in Figs. 6 and 9 represents the moisture content per mass of material as a fraction of mass at 10% RH.

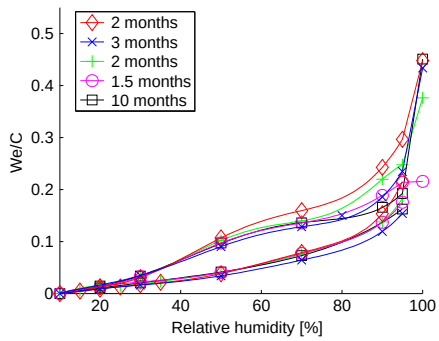

Fig. 4. Sorption isotherms for concrete W/C 0.65, samples removed at different times from the floor slab.

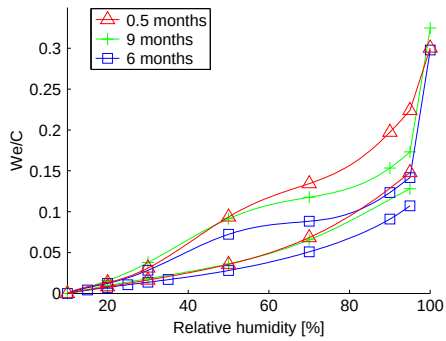

Fig. 5. Sorption isotherms for concrete W/C 0.55, samples removed at different times from the floor slab.

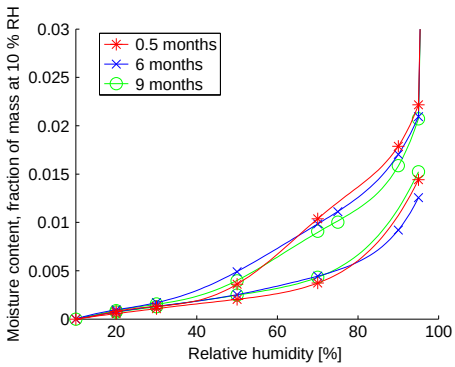

Fig. 6. Sorption isotherms for Floor 4310 Fibre Flow, samples removed at different times from the floor slab.

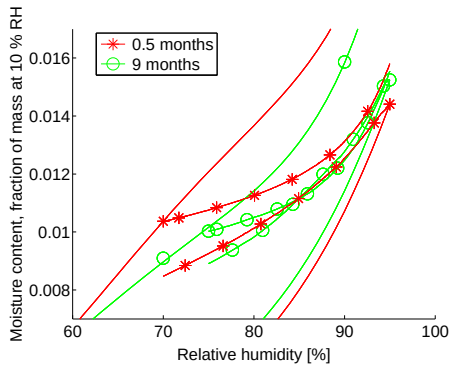

Fig. 9. Sorption isotherms including absorption and desorption scanning curves for Floor 4310 Fibre Flow.

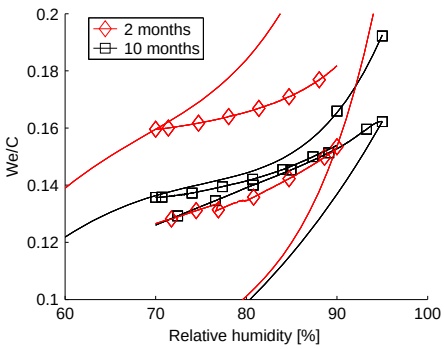

Fig. 7. Sorption isotherms including absorption and desorption scanning curves for W/C 0.65.

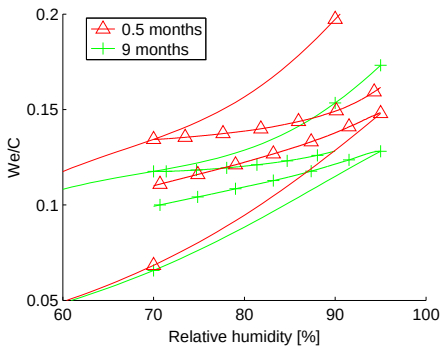

Fig. 8. Sorption isotherms including absorption and desorption scanning curves for W/C 0.55.

Sorption isotherms are presented for both concrete and SFC (Figs. 4–6). The results clearly show a hysteresis between desorption and absorption isotherms in all investigated materials. The obtained absorption isotherms show a significantly lower scatter than the obtained desorption isotherms.

One remarkable finding is the significant history dependence, hysteresis, in the desorption isotherm itself. Desorption isotherms for concrete W/C 0.65, determined 2 months after the casting, are significantly higher, between 45% RH and 95% RH, than subsequently removed samples (Fig. 4). This is also the case for the W/C 0.55 concrete (Fig. 5).

An important remark has to be made regarding the results of the 1.5 months sample and one of the 2 months old W/C 0.65 samples. Their moisture contents at saturation are significantly lower than the remaining three samples, showing a We/C of about 0.22 and 0.35 compared with 0.43–0.45.

Desorption curves for the SFC indicate minor time dependency. The hydration degree does not increase much between 1 and 9 months since the main binder component in the SFC is alumina cement.

All materials are regarded as dry at 10% RH. Markers on the sorption isotherms represent the extrapolated water gain at each RH step. The solid lines represent a general polynomial curve fit of the markers for each sorption isotherm.

Four scanning curves for each material are presented in Figs. 7–9. Two obtained absorption scanning curves are shown for each material; these mainly start from the desorption isotherms at 70% RH. Two obtained desorption scanning curves are shown for each material; these mainly start from the absorption isotherms at 95% RH.

All measurements are performed at 20 °C.

5. Discussion

Sorption isotherms and scanning curves were determined for samples of concrete W/C 0.65, W/C 0.55 and

SFC. Significant hysteresis was observed for desorption isotherms for concrete W/C 0.65 and W/C 0.55, between 60% RH and 95% RH (Figs. 4 and 5). The moisture content for the desorption branch decreased with an increased drying time. As a consequence the adsorption scanning curve decreased considerably (Figs. 7 and 8). This does not agree with previous findings of the desorption isotherm [16]. However, this disagreement may originate from a different sample preparation. Powers first water cured the samples and then dried them to 0% RH before determining absorption and subsequently the desorption isotherm. In addition, later research has shown that there is a risk of damage to the pore structure when the specimen is dried to levels below 10% RH [17].

To prevent structural and physical damage to the hydrates, all sorption isotherm data were obtained without exposing samples to levels below 10% RH. However, the most important finding is that the longer a concrete is kept in a 60% RH environment the larger the decrease of the desorption isotherm (Figs. 4 and 5). Only minor changes were observed in the absorption isotherm above 80% RH. A small but noticeable decrease in desorption isotherms above 60% RH with curing time was shown for the SFC material (Fig. 6). Both sorption isotherms and scanning curves for SFC agree well with previous research on similar material [6].

The absorption scanning curves show that the moisture content increases at a low rate at an early stage. A loss of mass was recorded in the beginning (not visible in the diagram) due to time lag effects. As the relative RH level increases, the moisture content increases and the curve ascends towards the absorption isotherm. In this first phase the moisture is probably accumulated mostly as adsorption on the pore walls made available after previous drying. As the scanning curve approaches the boundary absorption isotherm, it curves upwards more and more. This curving upwards is most probably due to a gradual transition from adsorption on the pore walls to capillary condensation in the pores. When the RH level increases, the absorption scanning curve comes closer to the boundary absorption isotherm. However, the curve appears never to cross the boundary defined by the absorption isotherm. Most likely the absorption scanning curve reaches the boundary absorption isotherm at 100% RH, as stated earlier by Powers and Brownyard [16].

Desorption scanning curves, starting from the absorption isotherm, are for a minute period parallel to the x-axis and then descend and softly turn towards the desorption isotherm. From the results of this study it is not possible to suggest if the desorption scanning curve meets the desorption isotherm above 0% RH. However, the results clearly demonstrate that an ascending absorption scanning curve could cross a descending desorption scanning curve (see Fig. 8).

The decrease of sorption isotherms in concrete through aging is often explained as structural changes of the material due to hydration. In this study, however, hydration could not completely explain the decrease of desorption isotherm branches with an increased drying time. A rough estimate showed that all samples taken from the large specimens had an equal degree of hydration, about 0.8. The degree of hydration was estimated judging from both the total porosity based on water content at saturation, see Figs. 3 and 4, and the drying conditions of the samples. Below 80% RH hydration of cement grains virtually ceases [18].

An equal hydration would imply an equal amount of physically bound water at the desorption branch in the range from 60% RH to 95% RH. However, the desorption isotherm decreased significantly with drying time in that range. It is not possible to completely eliminate differences in hydration degree since it was never determined. There is a possibility that the desorption isotherm is affected by the moisture history of the material itself, an indication of a hysteresis effect previously not found in literature.

A comparison of the amount of sorbed water at saturation showed a relatively small spread for the samples (see Figs. 4 and 5). However, two samples, 1.5 and 2 months old, respectively, showed significantly lower moisture content at saturation. One probable cause of this difference is that these samples were removed too early from the wet cloth, and thus did not reach a saturated state. This is clearly seen on comparing the water content at 100% RH, see Fig. 4, where the We/C is about 0.22 and 0.37 for the two samples compared with 0.43–0.45 for the remaining samples.

Since the boundary sorption isotherms and scanning curves were determined at the same time the sample mass was checked before and after scanning to see whether the process was reversible. The results from this examination indicated that both absorption scanning starting from the desorption isotherm and desorption scanning starting from the absorption isotherm were reversible.

References

[1] Nilsson L-O. Hygroscopic moisture in concrete – drying measurements & related material properties. In: Division of building materials, Lund; 1984. p. 170.
[2] Wolkoff P et al. Are we measuring the relevant indoor pollutants? Indoor Air 1997;7(2):92–106.
[3] Holm AH, Kuenzel HM. Practical application of an uncertainty approach for hygrothermal building simulations – drying of an AAC flat roof. Build Environ 2002;37(8–9):883–9.
[4] West RP, Holmes N. Predicting moisture movement during the drying of concrete floors using finite elements. Constr Build Mater 2005;19:674–81.
[5] Obeid W, Mounajed G, Alliche A. Mathematical formulation of thermo-hygro-mechanical coupling problem in non-saturated porous media. Comput Meth Appl Mech Eng 2001;190(39):5105–22.
[6] Anderberg A, Wadsö L. Moisture in self-levelling flooring compounds. Part II. Sorption isotherms. Nord Concrete Res 2004;32(2):16–30.
[7] Baroghel-Bouny V, Chaussadent T. Texture and moisture characterization of hardened cement pastes and concretes from water vapour sorption measurements. In: The modelling of microstructure and its potential for studying transport properties and durability. Kluwer Academic Publishers.; 1996.

[8] Ahlgren L. Fuktfixering i porösa byggnadsmaterial (in Swedish). In: Division of building technology. Lund: Lund University; 1972. p. 197.
[9] Atlassi E, Nilsson L-O, Xu A. Moisture sorption properties of concrete with admixtures and industrial by-products – implications for durability. In: Durability of concrete: aspects of admixtures and industrial by-products, 2nd international seminar. Stockholm: Svensk Byggtjänst; 1989.
[10] Maa Y-F et al. Effect of spray drying and subsequent processing conditions on residual moisture content and physical/biochemical stability of protein inhalation powders. Pharm Res 1998;15(5): 768–75.
[11] Costantino HR. Water sorption behavior of lyophilized protein-sugar systems and implications for solid-state interactions. Int J Pharm 1998;166:211–21.
[12] Hébrard A et al. Hydration properties of durum wheat semolina: influence of particle size and temperature. Powder Technol 2003;130: 211–8.
[13] Johannesson B, Janz M. Test of four different experimental methods to determine sorption isotherms. J Mater Civil Eng 2002;14(6):471–7.
[14] Espinosa RM, Franke L. Inkbottle pore-method: prediction of hygroscopic water content in hardened cement paste at variable climatic conditions. Cement Concrete Res 2006;36(10):1954–68.
[15] Åhs M, Sjöberg A, Anderberg A. A method for study sorption phenomena. In: Proceedings of the 10th international conference on indoor air quality and climate, Beijing, China; 2005. p. 1969–73.
[16] Powers TC, Brownyard TL. Studies of the physical properties of hardened portland cement paste. Bulletin 22. Research Laboratories of the Portland Cement Association, Skokie, IL, U.S.A., reprinted from J. Am. Concr. Inst., (Proc.), vol. 43 (1947). pp. 101–32, 249–336, 469–504, 549–602, 669–712, 845–80, 933–92.
[17] Zhang l, Glasser FP. Critical examination of drying damage to cement pastes. Adv Cement Res 2000;12(2):79–88.
[18] Powers TC. A discussion of cement hydration in relation to the curing of concrete. In: Proceedings, vol. 27. Washington, DC: Highway Research Board; 1947. p. 178–88.

IV

Moisture distribution in screeded concrete slabs

Magnus Åhs
Licentiate in Engineering
Div. of Building Materials, Lund University
P.O. Box 118, 221 00 Lund
E-mail: magnus.ahs@byggtek.lth.se

Ph.D. Anders Sjöberg
Division of Building Materials, Lund University
P.O. Box 118, 221 00 Lund
E-mail: anders.sjoberg@byggtek.lth.se

ABSTRACT

A qualitative model of moisture distribution in screeded concrete slabs is presented. From this model it is possible to identify humidity changes in each material and thus determine corresponding moisture properties. The distribution of relative humidity, RH, was determined in nine screeded concrete slabs before flooring and after a certain time of redistribution. Moisture redistribution is clearly demonstrated in the results section, where the increase in humidity beneath the flooring is exemplified. The initial moisture distribution and subsequent changes agreed with the presented qualitative model. This model may be used to develop current moisture distribution prediction tools further by introducing a more complex interrelation between moisture changes and corresponding changes in moisture related properties.

Key words: moisture redistribution, qualitative model, relative humidity, screeded concrete slab

1. INTRODUCTION

Drying of residual moisture in concrete floor slabs has been brought into focus during the last decade. Residual moisture in concrete is water that remains after the requirements associated with pouring and curing are fulfilled. Depending on the water/cement ratio and environmental conditions, different quantities of water will be released to the surroundings until moisture equilibrium is achieved. If a moisture barrier such as PVC flooring is installed on the top of the slab, residual moisture will be redistributed and increase the humidity at the surface. To reduce the humidity level attained beneath the flooring, drying of residual moisture in concrete slabs is crucial.

Insufficiently dried concrete slabs in the presence of high alkali levels have been accused of promoting and sustaining degradation of adhesives beneath PVC floorings [1]. Degrading adhesives are known to emit volatile organic compounds, VOC, to the indoor environment [2]. Exposure to such VOC in high concentration has a negative health impact on people living or working in such environments [3]. Emissions originating from the damaged floor constructions

are of rather low concentration. The impact on health due to long term exposure to such low concentrations is not yet established [4]. However, research has shown that there is a higher frequency of diffuse health related symptoms among people who live or work in buildings in which such damage has occurred. These symptoms are hard to correlate to moisture damaged floor constructions as they appear as ***e.g.*** runny nose and irritated respiratory passages.

Moisture distribution determination in concrete floor slabs, especially screeded concrete slabs, is difficult. Irrespective of the applied method, the outcome is affected by uncertainties originating from e.g. sampling methods, equipment or unforeseen moisture losses from samples prior to testing. One recently developed method to determine the relative humidity, RH, in a concrete slab is based on long term monitoring and logging of the RH. Temperature effects on in-situ measurements of RH are recognised by examining the results obtained through long term in-situ measurements [5].

Prediction of moisture distribution in screeded concrete slabs is even more difficult. It is strongly dependent not only on precise characterization of the constituent materials but also a detailed knowledge of moisture/material interactions, drying time, drying conditions and concrete/screed moisture interactions. One of the common drawbacks in current models [6-8], apart from simplification of the moisture related properties of materials used in floor constructions, is the often incomplete description of moisture interactions between flooring, screed, and concrete. Current models may therefore generate predictions subject to large uncertainties.

This study presents a model for qualitative analysis of the moisture distribution in a screeded concrete slab. The model is described in section 2, where the moisture distribution is shown for two cases through four phases. A brief description of vital moisture related aspects of each phase is included. In order to verify the model, moisture distribution was determined on a number of screeded slabs before flooring and after redistribution. The experimental set up is described in section 3 and the moisture distribution before and after flooring in each slab is presented in section 4. In section 5 the results obtained are discussed and compared with the qualitative model. Conclusions from the presented works are presented in the last section.

2. QUALITATIVE MODEL

This section presents a qualitative model which describes moisture distribution in screeded concrete slabs during construction. The model covers the time from pouring of the structural slab, continues with screed casting and finishes after flooring installation.

Moisture is evenly distributed in a freshly poured concrete slab. During early hydration, the humidity level decreases uniformly as a result of chemical binding of moisture to the cement. Further drying occurs when the external humidity is lower than that in the slab. The surfaces dry first as this moisture must be released before that inside. This variation through the slab is presented as a moisture distribution profile that shows humidity at the centre of the slab in relation to the surfaces.

When a screed is laid on the slab, moisture from the screed will rewet the slab surface and initiate redistribution of interior moisture. Owing to the wet screed the humidity at the top surface of the slab will increase. However, drying at the slab base and screed top continues. The

humidity of the screed decreases as some moisture becomes chemically bound. Finally, impermeable flooring is laid on the screed and as a result residual moisture is redistributed.

Figure 1 show two cases of screeded concrete which represent important events related to moisture distribution.

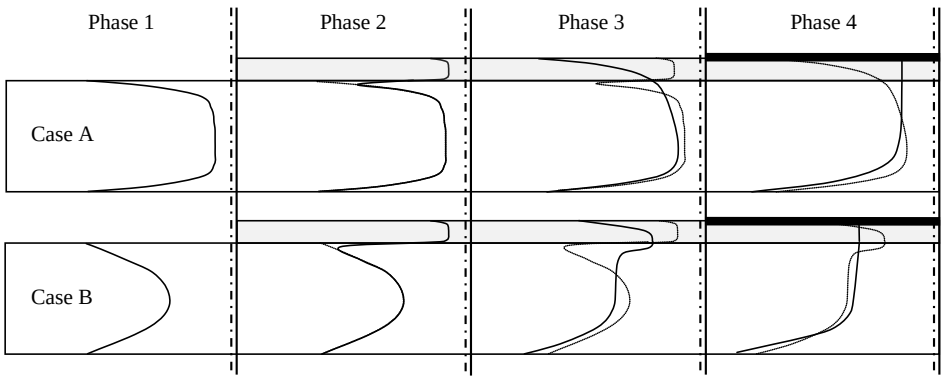

Figure 1. Phase 1 shows the distribution of residual moisture in a concrete slab. A wet screed is applied in phase 2. The applied screed dries in phase 3, and finally in phase 4 flooring is installed.

The top figure illustrates a screed applied on a newly poured concrete slab and the figure below when screed is applied on a slab subjected to years of drying. In each phase the dotted line represents initial moisture distribution and the solid line represents the moisture distribution prior to entering the next phase. The double dashed/solid line separates each phase; in addition it also indicates the highest attainable moisture level. It may be used for comparing the difference in absolute level between both cases and phases.

Phase 1. Drying of residual moisture in a concrete slab

A. This profile illustrates the moisture distribution in a slab during initial drying. It occurs as a result of vertical moisture flow from the centre of the humid slab through the bottom and top surfaces. The slab surfaces have lost a lot of moisture in relation to the slab interior. A steep gradient on the moisture profile indicates a larger moisture flow in relation to a flat gradient.
B. Like case A. However, this illustration shows a slab where drying has proceeded further. The moisture level in the central parts of the slab has significantly decreased.

Phase 2. Application of screed on top of the slab

A. In this phase a screed is laid on the concrete slab. The top surface of the screed dries through moisture release to the less humid surroundings. Moisture flow at the top surface of the slab is reversed and as a consequence the screed base dries. However, this occurs at the expense of the slab top surface becoming increasingly humid. Just above the slab centre moisture transport is still directed towards the screed. However, the direction of moisture flow at the slab base remains unaffected. Additionally, drying in the screed occurs owing to chemical moisture binding of the cement.

B. Like case A. However, the moisture level difference between slab and screed is significant, implying that the slab has a larger capacity to receive moisture from the screed than in case A.

Phase 3. Drying of the screed's residual water

A. A significant amount of moisture has dried from the screed. Near the slab surface a considerable increase in humidity is evident. Humidity at the top surface of the screed is lower than at the base. This is a result of moisture redistribution from the interior parts of the slab.
B. Like case A. However, the moisture level in the slab is substantially lower than in the screed. Moisture is still being transferred down from the screed into the slab.

Phase 4. Installation of an impermeable flooring and redistribution of moisture

A. The surface is covered with moisture impermeable flooring, an efficient barrier which reduces moisture transport from the screed surface. The screed no longer dries but becomes increasingly humid as a result of redistribution of moisture from interior parts of the slab to the top surface. Drying will follow when the moisture flow from the screed becomes larger than the flow towards it. Future moisture profiles will never exceed this last phase, unless moisture is supplied from the outside.
B. Like case A. Further drying of the central parts of the screed occurs as additional moisture is relocated down into the slab and up towards the flooring. Yet some moisture is transferred from the slab centre towards the screed.

3 EXPERIMENTAL SET UP

3.1 Material

Nine screeded slabs, covering an area of 800*1200 mm^2, with PVC flooring on top, were used in this study. Eight solid slabs were cast and preconditioned in the laboratory, the ninth, a hollow core slab, HCS, was cast in a factory. The solid slabs were made of concrete C, see table 1, and separated into two batches by their thickness, see table 2. Batch 1 consisted of slabs 1-4, 110 mm thick and batch 2 of slabs 5-8, 220 mm thick. Batch 3, the HCS, was manufactured with C_{HCS}, 265 mm thick with 5 longitudinal core holes.

Two different screeds were applied on the slab surfaces; cement mortar M, and a self levelling flooring compound SFC. The SFC labelled Floor 4310 Fibre Flow, manufactured by Maxit, was delivered as a dry powder mix in 25 kg bags. A detailed description of concrete, mortar and SFC mixes is given in table 1.

Table 1. Mixture description of the materials used. The quantities are in kg/m^3.

Material	**C**	**M**	**C_{HCS}***	**SFC***
w/c ratio	**0.65**	**0.55**	**0.4**	
CEM II/A-LL 42,5 R	250	400		
CEM I 52,5 R			390	
Portland Cement				1-5
Aluminous cement				5- 20
Gypsum				2 -10
Water	162	220	147	20
Dolomite 0.002-0.1 mm				31
Sand 0.1-1 mm				47
Sand 0-8 mm	976	1672	973	
Sand 6-13 mm			851	
Sand 8-12 mm	489			
Gravel 8-16 mm	489			
Polymer				1-5
P30			1.2	
Glenium 51	1.5	2.9		

* Mixture according to manufacturer, mass-% of dry powder, density~1900 kg/m^3

All surfaces and material connections around the circumference were sealed with self adhesive bitumen alumina sheets; alumina tape without bitumen was also used. Cavities remaining after sampling for RH distribution were filled with a self expanding foam, DANA Joint - & insulation foam 591.

3.2 Methods

Formwork

Coated plywood, 13 mm, was used as formwork for the solid concrete slabs. Each form was put on a pallet, 800*1200 mm^2. Before pouring the forms were prepared with form oil, using an ordinary paint brush. No reinforcement bars were put inside the form. However, lifting tools were fixed on one vertical plywood sheet prior to pouring, to facilitate handling of the heavy concrete slabs in the laboratory. The web above the HCS mid core hole was cut off forming a 100*800 mm slit. Coated plywood sheets prepared with form oil were used as formwork on each side of the mid core.

Pouring of slab

Concrete pouring was carried out in laboratory conditions, in formwork prepared for each of the three different batches. The HCS mid core hole was filled with material C through the slit. All castings were cured for 2 days covered by a plastic sheet, thereafter the formwork was stripped. Subsequently the vertical edges on each slab were sealed with self adhesive bitumen coated alumina sheets to obtain one dimensional moisture flow.

First drying

All slabs were drying in a climate room at 20 ºC and 60 % RH. Batch 1 was dried laying flat on coated plywood and Batch 2 was vertically tilted.

In order to accelerate drying, slabs 7 and 8 were put in a climate box for 269 days at 32 ºC, 39 days after pouring. The humidity in the climate box was obtained with a saturated solution of Sodium Bromide, NaBr, which generates an equilibrium humidity of 55 % RH at 32 ºC, [9].

Pouring of screed
Prior to screed application, a primer, Optiroc 6000, was evenly spread on the top surface of each slab by using an ordinary paint brush. Mixing was carried out in the laboratory by using a concrete mixer. On slabs 1, 2, 6, and 8 40 mm of material SFC was laid, and on slabs 3, 4, 5, and 7 40 mm of material M, see table 2. On the HCS 60 mm of material SFC was poured. All screeds were cured for 2 days, covered by a plastic sheet. The vertical screed edges were sealed subsequent to curing, by using self adhesive bitumen coated alumina sheets.

Second drying
After curing the screed, all slabs were put in a 20 ºC and 60 % RH climate for additional screed drying. Slabs in batch 2 were once again vertically tilted.

Installation of flooring
On the day flooring was laid, adhesive was applied to the screed top surface. The quantity of applied adhesive is shown in table 2.

Table 2. Description of drying and material application sequence

Batch No.	1				2				3
Slab	1	2	3	4	5	6	7	8	9
Material	C	C	C	C	C	C	C	C	C_{HCS}
1st Drying [days]	105	105	110	110	9	11	408	408	28[1]
Screed	SFC	SFC	M	M	M	SFC	M	SFC	SFC
2nd Drying [days]	48	96	98	90	261	259	40	40	138
Adhesive [m^2/l]	3.6	3.6	3.5	4.3	3.1	3.0	3.3	3.0	3.0
Flooring	PVC	PVC	PVC	PVC	PVC	PVC	PVC	PVC	PVC
Redistr.[days]	206	158	149	157	269	269	91	91	273

[1] Initial drying time of the C filling of the mid core. The HCS was cast approx. 60 days earlier.

Flooring installation was completed within 10 minutes after adhesive application. Immediately after flooring, additional aluminum tape without bitumen was used to seal the flooring rim to the previously installed aluminum sheets on the vertical slab edges.

Determination of moisture distribution
The RH profile in all nine slabs was determined prior to flooring and after a certain time of moisture redistribution. All samples were obtained at least 100 mm from the vertical alumina sealing on the slab to avoid possible edge effects. To avoid possible drying disturbances, moisture profiles were always obtained not less than 260 mm from previous sampling.

Samples were obtained vertically through the slab using a 90 mm core drill which gradually penetrated the concrete in sections of 20 – 30 mm. Each section was chiselled off and crushed into gravel size pieces. Immediately after crushing, pieces of 5-15 mm size were put in glass test tubes, instantly sealed with elastic rubber plugs. Pieces considered to contain a high degree of cement paste were selected in order to maximize the quantity of moisture.

The RH was measured by using a carefully calibrated RH sensor, Vaisala HMP-44, inserted in the test tube. These sensors were connected to a computer logging system displaying the readings as curves in a diagram on a screen. When the curve in the diagram had levelled out the actual reading was performed, some 12-48 hours after inserting the sensor in the test tube. The RH sensors were preconditioned at 20 ºC and 55 % RH prior to measurements.

One day after drilling, the cavities were filled with self expanding foam DANA 591. No water was used for cooling the core drill when sampling.

4. RESULTS

Moisture distribution was determined in each slab prior to flooring, thin dashed lines, and after redistribution, thick solid lines, see fig 2. RH is shown on the x-axis in % RH and the y-axis represents the vertical distance in mm from the slab surface, positive figures for increasing depth. Each line marker represents the RH level obtained in each section. Flooring installation is defined as day 0 (zero) and each legend states when the profile was obtained in relation to flooring. The screed/concrete boundary is visualized at the top of each figure by a horizontal thick solid line. Dashed lines in the HCS figure represent edges of the longitudinal mid core hole.

The diagram representing slab 1 displays the RH distribution 1 day and 206 days after flooring. Each RH measurement has an uncertainty of 1 - 2 % RH, therefore changes within this range may not be significant. Drying of the screed base at the 30 mm level has decreased the RH from 93 to 87 % RH; a virtually uniform moisture profile in the screed is shown. Throughout the concrete slab, a considerable decrease exceeding 5 % RH is shown after moisture redistribution.

The moisture distribution in slab 2 was obtained 47 and 5 days prior to flooring and after 158 days of redistribution. Before flooring significant drying in excess of 10 % RH is shown in the top 60 mm of the slab. The increase in screed humidity after 158 days of redistribution is about 5 % RH. The humidity decrease of nearly 10 % RH in the concrete base indicates significant drying through the coated plywood.

In slab 3 the RH distribution is shown 56 and 14 days prior to and 158 days after flooring. Duplicate samples were obtained from different locations in the slab, 56 days before flooring. Screed humidity drops considerably by about 7 -10 % RH during the first 42 days of drying. After flooring the humidity level increases significantly, from 74 to 86 % RH in the top 20 mm of screed. Additionally, after 149 days of redistribution, slab humidity has decreased by about 4 % RH almost uniformly.

The moisture distribution in slab 4 is shown 48 and 6 days prior to flooring, and 157 days after redistribution. The screed humidity has decreased substantially during the initial 42 days of drying, by about 7 - 5 % RH. The moisture level 50 mm below flooring has decreased by about 2 - 4 % RH, showing larger decrease at the base, compared with the moisture profile obtained 6 days prior to flooring with 157 days of redistribution. The screed humidity has increased by about 2 - 7 % RH after redistribution, the larger increase was found at the 10 mm level close to the flooring.

After 269 days of redistribution shown in slab 5, humidity increases considerably by about 10 % RH in the screed compared with the profile obtained 3 days before flooring. A minor humidity increase in the slab top section is also indicated. The measurements also suggest a humidity decrease in the slab base after redistribution.

In slab 6, measurements made on day -3 and 269 clearly show an increase in humidity in the screed from 68 to 81 % RH. A humidity decrease of 5 % RH is shown at the slab base. Note that

the moisture level is nearly unchanged around the slab centre. There has been overall moisture redistribution and drying of the slab base has occurred.

Moisture distribution determined for the drier slab 7 shows a slight decrease of about 1 - 4 % RH at the screed top after 91 days of redistribution. Overall, the moisture profile obtained after redistribution is more or less equal to the moisture distribution obtained prior to flooring. However, the RH profile has flattened out in the screed layer and the slab bottom surface has dried further.

After 91 days of redistribution, the RH level in slab 8 increases 10 mm beneath the flooring. A moisture level decrease is shown both 30 mm and 50 mm below the screed top surface. The RH has increased between the 70 mm and 190 mm level.

The last three moisture profiles, HCS 1-3, show the moisture distribution in samples obtained from the HCS, 16 days prior to flooring and 273 days after. HCS 1 represents the humidity above the core hole next to the concrete filled mid core hole. A significant humidity increase, from 68 to 78 % RH, is shown in the screed surface and a minor decrease from 75 to 72 % RH in the HCS web at 90 mm level.

HCS 2 displays the results from RH determination performed on material from the wall separating the mid core hole from the neighbouring core hole. Top screed humidity has increased by some 3 - 5 % RH. The results from the slab mid section, at 175 mm depth, show a strange looking profile before flooring and after redistribution. This could be a result of the horizontal moisture distribution. However, a clear 5 % RH decrease in humidity is shown at the slab base.

HCS 3 diagram shows the moisture profiles on samples obtained from the concrete filled mid core hole. A minor increase by 1 - 2 % RH is shown in the top screed. Throughout the concrete filling, 60 mm and below, the moisture level has decreased from about 4 - 5 % RH, to slightly lower levels in the HCS base.

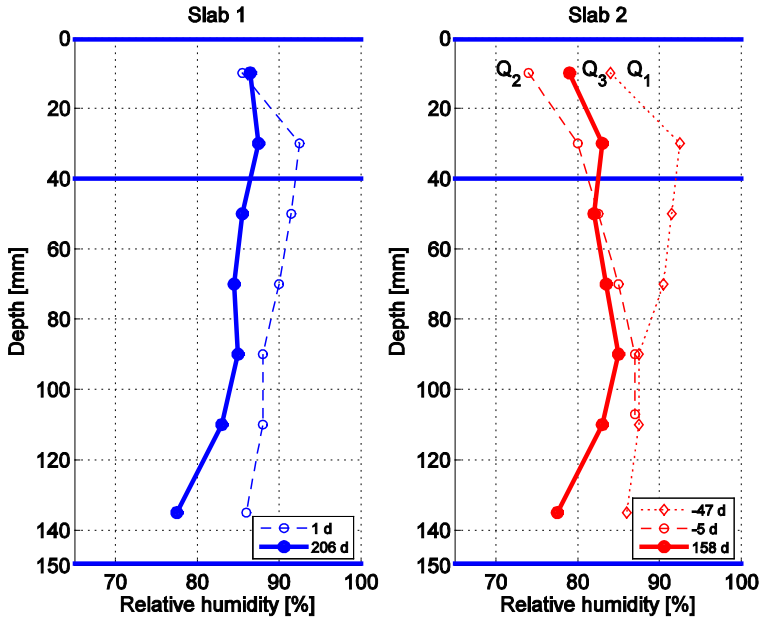

Figure 2. Moisture distribution determined for two SFC screeded concrete slabs on plywood before flooring (dashed lines) and after a certain time of redistribution (solid lines).

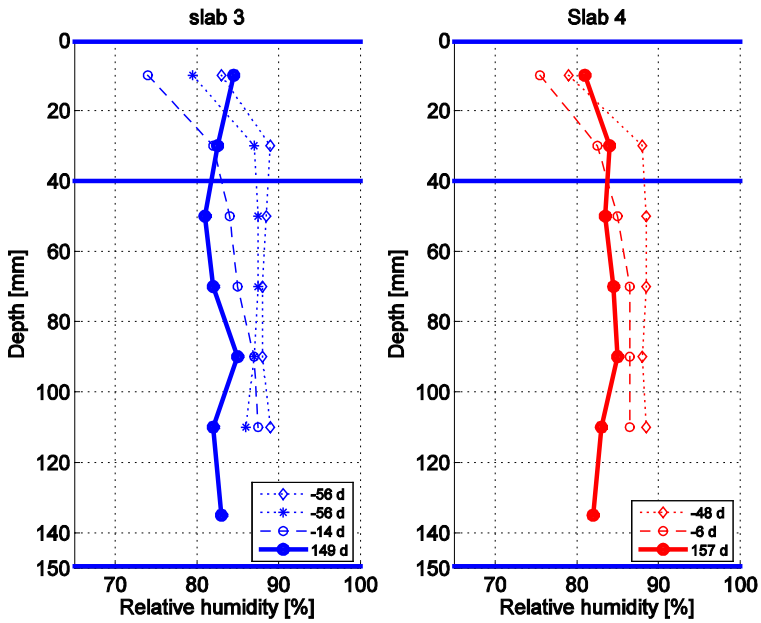

Figure 3. Moisture distribution determined for two M screeded concrete slabs on plywood before flooring (dashed lines) and after a certain time of redistribution (solid lines).

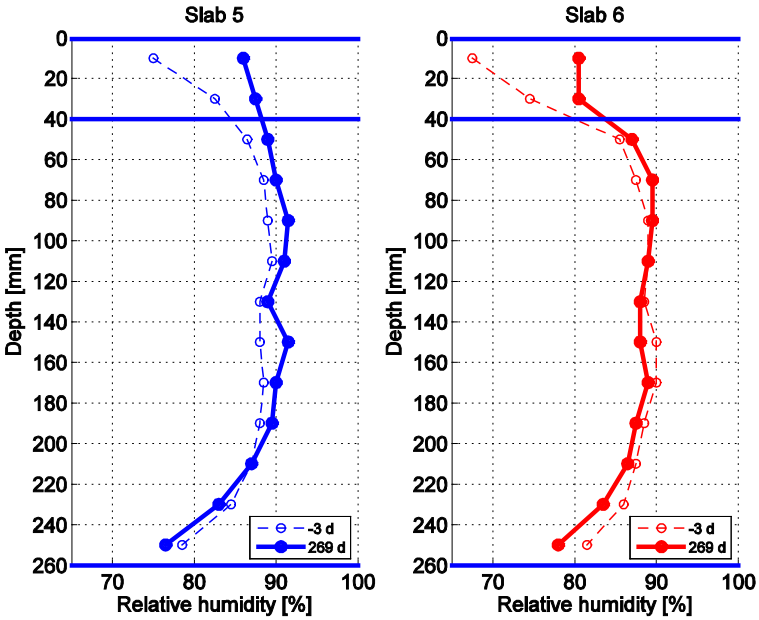

Figure 4. Moisture distribution determined for one M (left) and one SFC (right) screeded concrete slab before flooring (dashed lines) and after a certain time of redistribution (solid lines).

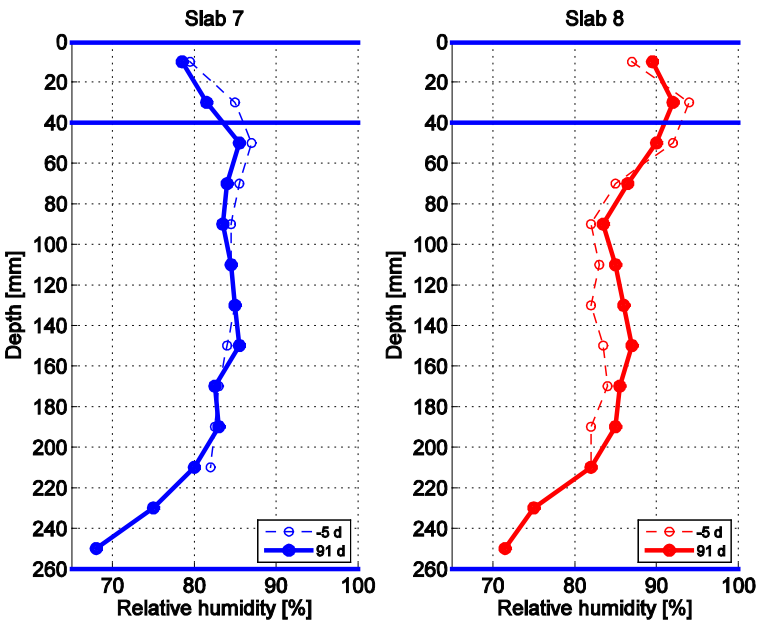

Figure 5. Moisture distribution determined for one M (left) and one SFC (right) screeded concrete slab before flooring (dashed lines) and after a certain time of redistribution (solid lines).

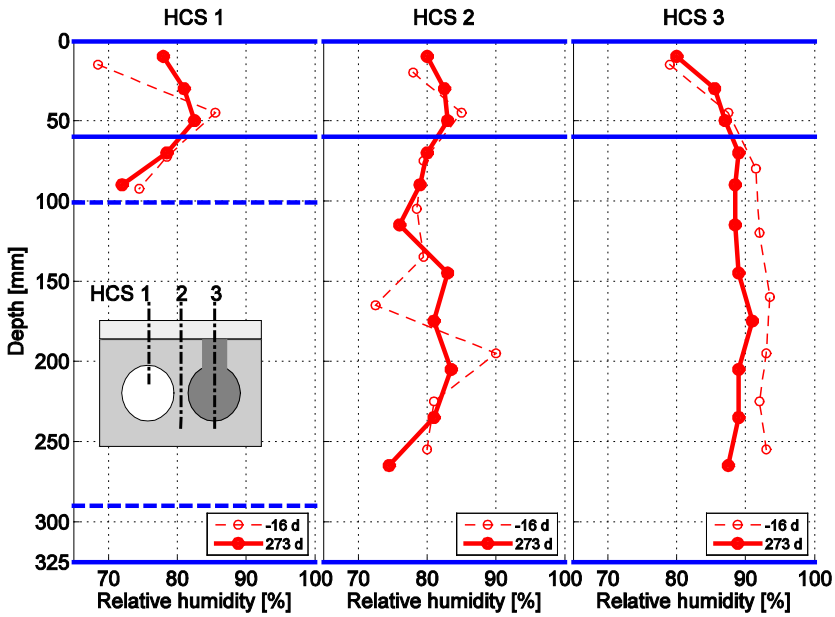

Figure 6. Moisture distribution determined in three sections of the SFC screeded hollow core slab, with one hollow core filled with material C, before flooring and after a certain time of redistribution.

5. DISCUSSION

5.1 Comparison of slabs 1 and 2, Case B

The influence of screed drying time on redistribution is discussed by comparing slabs 1 and 2. The screed on both slabs 1 and 2 had dried for 48 days, see table 2, when moisture profile 1 d and -47 d were obtained. Both these profiles are therefore almost identical and show an elevated RH level in the screed/concrete corresponding to Case B phase 3 in the qualitative model. Slab 2 dried for a further 42 days before a new RH profile -5 d was obtained. Judging from this moisture profile, drying has occurred mainly through the screed. The profiles 206 d and 158 d were obtained on the same day. Slab 1's shorter drying and longer moisture redistribution resulted in a more uniform screed moisture profile compared to slab 2. The moisture profile obtained in slab 1 after redistribution corresponds to phase 4 case B in the qualitative model. Further drying before flooring in slab 2 was accompanied by 158 days of moisture redistribution. This time was insufficient to achieve complete moisture redistribution in the screed. The moisture levels in slabs 1 and 2 are almost equal from slab centre and below, both before flooring and after redistribution, clearly demonstrating that equal drying conditions were achieved through the coated plywood at the base.

5.2 Comparison of slab 2 with 3 and 4, Case B

The influence of different screed materials with respect to moisture redistribution is discussed by comparing slab 2 with slabs 3 and 4. The screed dried for 48 days before the moisture profiles were determined on slab 3, -56 d, and slab 4 ,-48 d. Almost identical moisture profiles were obtained from slabs 3 and 4. The elevated screed humidity in slab 2 is not seen in slabs 3 and 4, this may be a result of further chemically bound moisture in the mortar. Additional moisture profiles -14 d and -6 d were obtained on the same day as profile -5 d for slab 2. These three moisture profiles are rather similar indicating that moisture has dried mainly through the screed as for slab 2 and that the moisture transfer rate is higher through hardened SFC than through hardened mortar. They also indicate that drying through further hydration diminishes with time as hydration mainly occurs early after pouring. The moisture distribution was finally determined after 149 and 157 days of redistribution in slabs 3 and 4, on the same day as slab 2. Moisture in the screed of slab 4 still needs additional time to achieve a uniform distribution. The lower parts of slabs 3 and 4 show equal moisture profiles, with allowance made for uncertainties. Finally, further drying of the slabs may occur mostly through the slab base as this is more open to moisture transport than PVC flooring. Therefore it is likely that the future profile will correspond to phase 4 in the proposed qualitative model.

5.3 Comparison of slab 7 with 8, Case B

The effect on residual moisture redistribution due to long drying before screeds are laid is discussed by comparing slabs 7 and 8. Screed drying on slabs 7 and 8 lasted for 35 days prior to determination of the moisture profiles, -5 d. The achieved RH profiles demonstrated the elevated moisture levels in the screed, corresponding to Case B phase 3 in the qualitative model. However, drying through cement hydration may have reduced the elevated screed moisture level in slab 7 compared to slab 8. In addition the benefits of the open SFC did not occur as a result of the short drying time. Both slabs were showing, within uncertainties, equally dry slab centres and bases. Flooring was applied on both slabs 40 days after screed application followed by 91 days of redistribution. A complete redistribution was not obtained. The moisture distribution after flooring of slab 7 shows drying of the screed and slab top. This may be a consequence of the unfavourable impact of uncertainties on the achieved results. The humidity determined after redistribution may be too low at the 10 mm level and too high before flooring, compared to a true humidity. In slab 8, moisture from the screed centre has redistributed to the bottom, but also upwards to the screed top. Both slabs, particularly slab 8, correspond to Case B's 4th phase in the qualitative model.

5.4 Comparison of slab 5 with 6, Case A

The influence that early flooring application on two different screed materials has on moisture redistribution is discussed by comparing slabs 5 and 6. Drying of the mortar in slab 5 and SFC in slab 6 lasted for 258 and 256 days respectively until the moisture profiles, -3 d, were obtained. The moisture profiles determined agree well with phase 3 Case A in the qualitative model as the moisture profile for slabs 5 and 6 both show pronounced drying of the screed and an equally pronounced drying of the slab base. The SCF has dried more than the mortar, possibly an effect of the hardened mortar that becomes less open to moisture transport compared to the SFC. The moisture profile after flooring was determined after 269 days of redistribution. The increase in humidity in the mortar is considerable and clearly shows the effect of moisture

redistribution from the slab centre and up. The moisture level increase seen in the upper 200 mm of slab 5 is within the uncertainties and may therefore not be significant. In slab 6, moisture from the slab centre has been redistributed to the top and increased the screed humidity, thus giving a uniform moisture profile. However, besides the continuing drying of the slab base, additional moisture will be redistribute to the screed top as the maximum level is not yet achieved after 269 days of redistribution. Moisture profiles determined for slabs 5 and 6 after the achieved redistribution correspond to phase 4 Case A in the qualitative model.

5.5 HCS1-3

Moisture profiles obtained from the HCS in section HCS1-3 are not compared with the qualitative model owing to significant horizontal moisture transfer that occurred as a consequence of the non solid slab. However, HCS3 obtained in the filled core hole could, judging from the results obtained without too much trouble, be compared with the qualitative model Case B.

Moisture profiles labelled -16 d in HCS1-3 were obtained 122 days after screed application. Flooring was applied 16 days after obtaining the first moisture profile. Redistribution continued for 273 days until the humidity profiles after flooring were obtained. The -16 d profile of HCS1 clearly shows significant drying from the screed base and down into the HCS top as well as drying upwards. The significant downward drying may be a consequence of the reduced cross section above the empty core hole. The HCS1 redistribution profile demonstrates a significant increase in humidity at the screed top originating from both vertical and horizontal moisture redistribution. Downward drying through the web top is also seen.

The moisture profile HCS2 determined for the web segment dividing the empty and the filled core hole showed some drying upwards, some moisture was also drying through the slab base. HCS2 profile shows disturbances in the slab centre presumably originating from horizontal moisture redistribution. The HCS2 screed top shows an increase as a consequence of 2-dimensional moisture redistribution. Top web centre profiles are less disturbed by the horizontal redistribution. Significant drying through the web base is seen in HCS2.

HCS3 moisture distribution 16 days before flooring shows drying through the screed top. The uniformly distributed moisture profile in HCS3 may be explained both by horizontal drying through the web to the neighbour core holes and vertical drying through the web base. HCS3 is showing a small increase at the top as a result of mainly vertical moisture redistribution from the filling. Further uniform drying is seen in the filling as a result of the horizontal drying through the web walls. The profile HCS3 shows lower humidity levels at the base than at the filling centre as a result of further downward drying.

6. CONCLUSIONS

Comparison of the qualitative model of moisture redistribution with the results obtained before application of flooring and after a certain time of redistribution indicates that moisture after flooring will be redistributed according to the proposed model. This is useful with regard to moisture redistribution simulations, as simulating tools should include the hysteresis concrete exhibits. If hysteresis is not included the simulations should be performed stepwise in order to incorporate the scanning phenomenon, thus reducing the uncertainty.

REFERENCES

1. Wessén, B. and T. Hall. Directed Non-Destructive VOC-sampling: A method for source location of indoor air pollutants. In Proceedings of the 7:th International Conference on Indoor Air Quality and Climate. 1999. Edinburgh, Scotland: Construction Research Communications Ltd, pp. 420-425.
2. Sjöberg, A. and C. Engström, Measurements of stored decomposition products from flooring adhesives in a concrete floor, as a basis for choosing a new floor surface construction, in Building Physics 2002 - 6th Nordic Symposium. 2002.
3. Salthammer, T., Organic Indoor Air Pollutants. Occurrence, Measurement, Evaluation, ed. T. Salthammer. 1999, Wienheim, Germany: WILEY-VCH. 329.
4. Andersson, K., et al., TVOC and Health in Non-Industrial Indoor Environments. Indoor Air, 1996. 7(2): pp. 78-91.
5. Åhs, M. Remote monitoring and logging of relative humidity in concrete. In Proceedings of the 7th Symposium on Building Physics in the Nordic Countries 2005. Reykjavik, Iceland: The Icelandic Building Research Institute pp. 181-187.
6. West, R.P. and N. Holmes, Predicting moisture movement during the drying of concrete floors using finite elements. Construction and Building Materials, 2005. 19: pp. 674-681.
7. Obeid, W., G. Mounajed, and A. Alliche, Mathematical formulation of thermo-hygro-mechanical coupling problem in non-saturated porous media. Computer Methods in Applied Mechanics and Engineering, 2001. 190(39): pp. 5105-5122.
8. Leivo, V. and J. Rantala, Moisture behaviour of a massive concrete slab with a low temperature floor heating system during the initial drying period. Construction and Building Materials, 2005. 19: pp. 297-305.
9. Greenspan, L., Humidity fixed point of binary saturated aqueous Solutions. Journal of Research of the National Bureau of Standards- A. Physics and Chemistry, 1977. 81(1): pp. 89-96.

V

A quantitative model of moisture redistribution in dual layer concrete slabs with regards to hysteresis

Magnus Åhs, Licentiate in Engineering,
Div. of Building Materials, Lund university, Lund, Sweden;
magnus.ahs@byggtek.lth.se
http://www.byggnadsmaterial.lth.se

KEYWORDS: *model, moisture redistribution, hysteresis, concrete.*

SUMMARY:
Moisture in a drying concrete slab redistributes subsequent to applying semi-permeable flooring, hence increasing the humidity beneath the flooring. Such a humidity increase may be substantial in terms of relative humidity, RH, even though the redistributed moisture content appears insignificant. This comparably large increase originates from the hysteresis, moisture history dependence, exhibited by sorption isotherms for cement based materials. In contrast to retracing the desorption isotherm pursued when drying, the material's moisture content traces a scanning curve, when the humidity increases. Scanning curves give a lower change of moisture content in relation to RH, moisture capacity, compared with the desorption isotherm.

A qualitative and quantitative model of moisture redistribution in a dual layer concrete slab with regards to initial RH distribution and scanning curves is presented. The model is validated by determining the RH distribution in a number of screeded concrete slabs, before flooring and after a certain time of redistribution. Sorption isotherms and scanning curves for three cement based materials are shown.

1. Introduction

Redistribution of moisture occurs in building materials, *e.g.* concrete, because of internal and external moisture potentials. This process is self-sustaining and continues until reaching equilibrium with environmental or internal conditions. The relative humidity, RH, is here used as a moisture potential governing redistribution. Because of its hygroscopicity concrete absorbs and releases moisture depending on the surrounding RH and temperature. Moisture content in concrete is therefore commonly expressed in relation to the surrounding RH, the sorption isotherm, see FIG. 1. In FIG. 1 desorption, absorption and scanning curve branches are represented by the solid, dashed and dash dotted lines, respectively, in the 10 - 95 % RH range. The x-axis represents relative humidity in % RH and the y-axis represents the mass ratio of evaporable moisture relative to cement. The shaded area in FIG. 1 illustrates all attainable mass ratio RH relationships.

Sorption isotherms for cement based materials exhibit hysteresis (Baroghel-Bouny and Chaussadent 1996; Baroghel-Bouny et al. 1999; Espinosa and Franke 2006; Baroghel-Bouny 2007). This means that the moisture content fails to retrace its values back when reversing the prior sorption process. Instead, a new path is pursued and the conceived pathway, a scanning curve, is dependent on the preceding desorption/absorption sequence. The hysteresis feature has to be accounted for in estimations of moisture redistribution in screeded slabs, as moisture is both released and gained during construction.

Building materials, *e.g.* floor coverings, adjacent to screeded concrete slabs may be negatively affected from moisture redistribution. Besides dimensional instability, wood floors may experience fungal growth (Pasanen et al. 2000) on surfaces adjacent to concrete if not properly protected. Adhesives beneath low permeable floorings may deteriorate and release volatile organic compounds, VOC, to the indoor air (Sjöberg 2001; Sjöberg and Engström 2002; Björk et al. 2003). In addition, mould may grow on the organic fibres in linoleum floorings. Such moisture related damages, may occur if the humidity level exceeds a certain critical humidity. Preventive measures should therefore be considered to avoid ending up above such levels. Allowing the screeded concrete slab sufficient drying before applying moisture sensitive material is one such method. This decreases the amount of physically bound moisture, thus limiting effects from redistribution.

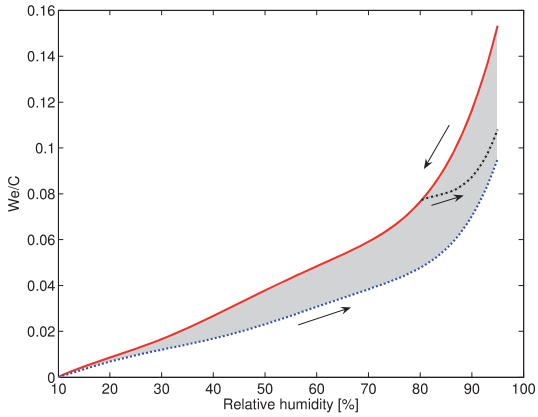

FIG. 1 Illustration of a sorption isotherm for concrete determined in the range between 10-95 % RH

At present there are a few models to estimate moisture distribution and drying of porous materials (Nilsson 1980; Holm and Kuenzel 2002; West and Holmes 2005). However, these models lack considering the hysteresis phenomenon and the reversal of sorption occurring when redistributing moisture. Therefore these models are not suitable to use for such applications. At screeding, moisture penetrates the slab's top surface, hence increasing the water content in the former dry concrete. As moisture is added the corresponding RH increase is not obtained by reversing the desorption process. Moisture from the screed will affect the relationship between moisture content and RH.

The main objective in this article is to describe a quantitative moisture redistribution model including the hysteresis phenomenon. The model is verified with RH measurements performed before flooring and after a certain time of moisture redistribution on a number of screeded concrete slabs. Material properties essential to the model were determined by using a sorption balance (Åhs 2005), including sorption isotherms and scanning curves (Åhs 2007) for w/c 0.65 concrete, C, w/c 0.55 mortar, M, and Floor 4310 Fibre flow, SFC, a self levelling flooring compound.

2. Qualitative model

Moisture redistribution in a screeded concrete slab is described in a qualitative manner for three distinct phases in order to display each horizontal section's moisture history, FIG. 2. Each phase represents important construction stages and the diagram shows current (solid line) and prior (dashed) moisture distribution. This model may work as a guide for determining each section's moisture capacity from a sorption isotherm based on previous moisture history. A sorption isotherm is located below phase 2 and 3, showing the complex interaction between redistributing moisture and concrete.

The first phase shows a homogenous concrete slab, experiencing single sided drying. Moisture distribution is characterised with a low surface humidity and a high slab base humidity. In the second phase a screed (shaded area) has been applied and started to dry. Moisture from the screed penetrates the slab surface hence increasing its humidity and screed surface humidity decreases because of drying. The final phase displays moisture distribution (vertical solid line) after flooring (thick solid horizontal line).

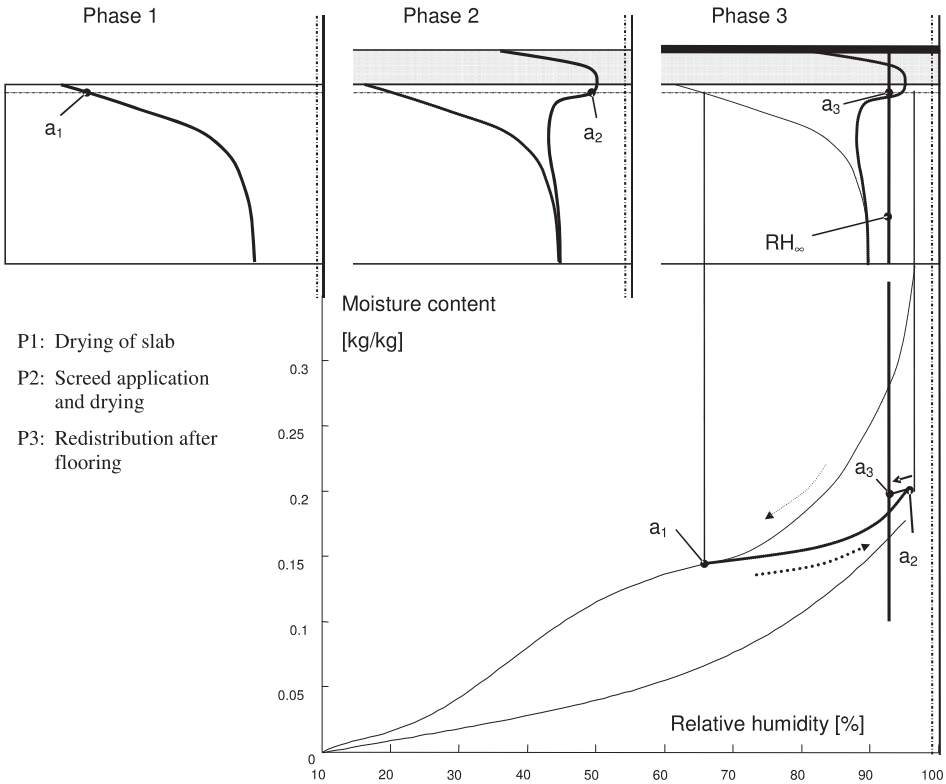

FIG. 2 Moisture redistribution in a concrete slab including a sorption isotherm with scanning curves

One particularly interesting horizontally oriented level, marked **a**, is indicated in the screeded slab, FIG. 2. This section's moisture content change is tracked with respect to RH variations in the sorption isotherm. The moisture content decreases in the concrete at drying, hence following the desorption curve (thin dashed line), until reaching $\mathbf{a_1}$, FIG. 2. In phase 2, the moisture content increases as a consequence of moisture being supplied from the screed application. Because of hysteresis the moisture content increase traces an ascending scanning curve to $\mathbf{a_2}$. As the humidity level is reduced in phase 3 during redistribution, a descending scanning curve is followed until settling at $\mathbf{a_3}$.

3. Quantitative model

Future moisture distribution in a screeded concrete slab is estimated by proposing a theoretical model, suggesting how to redistribute residual moisture after flooring. Four assumptions are made:

A) no further drying of the slab occurs after flooring
B) isothermal conditions
C) moisture transport is not considered
D) no additional chemical moisture binding during redistribution

Moisture redistributes in a sealed screeded slab until ultimately attaining a uniform vertical RH distribution, RH_∞, see FIG. 2. Provided each section's moisture history, RH change and moisture capacity are known their moisture content change is given. The preceding moisture history may be determined from the qualitative model. Moisture capacity is defined as the ratio of moisture content change relative to RH change. As no moisture is lost

through drying it is possible to determine RH_∞. Therefore the total moisture content change from flooring to a complete redistribution is 0 (zero). Moisture from wet sections redistributes to dryer conditions, and vice versa, until a uniform RH distribution is attained throughout the screeded slab. RH_∞ is achieved by iteration, as the moisture capacity is dependent on it.

RH_∞ will reach a level in between the extremes of the distribution as a consequence of assumption A. Therefore the midpoint of the two extremes may serve as a reasonable initial guess. Subsequently it is necessary to determine each section's moisture history in order to assign a realistic moisture capacity.

Based on the qualitative model, the slab base and screed solely undergo drying until flooring. Therefore such regions are assumed to have attained their moisture content and corresponding RH level through tracing the desorption isotherm. In contrast, other sections experienced drying and wetting cycles thus pursuing scanning curves. Such a qualitative analysis is fundamental when determining the proper moisture capacity for each section.

This theoretical analysis could be interpreted into an arithmetic expression, equation 1,

$$\sum_{\Delta x_i} (\overline{RH_i} - RH_\infty) \cdot d_i \cdot \left(\overline{\frac{\partial w}{\partial RH}} \right)_i = 0 \qquad (1)$$

where $\overline{RH_i}$ represents average RH level in [% RH], and RH_∞ represents the future uniform humidity level in [% RH], d_i represents the vertical thickness of each material section in [m], $\left(\overline{\frac{\partial w}{\partial RH}} \right)_i$ represents the average moisture capacity in [kg/(m^3 % RH)] evaluated from sorption (scanning) isotherms between current and future RH.

Equation 1 is based on the assumption that the total moisture content change within the screeded slab with respect to change from $\overline{RH_i}$ to RH_∞ is (zero). By a number of rearranging steps equation 1 gives equation 2, thoroughly explained in Åhs (2007)

$$RH_\infty = \frac{\sum_{\Delta x_i} \overline{RH_i} \cdot d_i \cdot \left(\overline{\frac{\partial w}{\partial RH}} \right)_i}{\sum_{\Delta x_i} d_i \cdot \left(\overline{\frac{\partial w}{\partial RH}} \right)_i} \qquad (2)$$

The obtained RH_∞ is compared with the initial guess. A new iteration is executed by substituting the initial guess with the achieved RH_∞, until obtaining an acceptable deviation.

4. Results

This section presents results from using the quantitative moisture redistribution model on four screeded concrete slabs, FIG. 3. Four floor structures were manufactured by using 220 mm of concrete C for the supporting slab, and 40 mm of mortar M as screed in slab 5 and 7, and 40 mm of self-levelling flooring compound SFC as screed in slab 6 and 8. The x-axis represents RH and the y-axis represents the distance from the top surface. The thin dashed line, solid line and thick dashed line represents moisture distribution before flooring, after a certain time of redistribution and calculated RH_∞ respectively. Moisture distribution measurements were performed relative to the flooring day, day 0 (zero), noted in each graph legend FIG. 3.

Sorption isotherms including several scanning curves were determined, in the range 10-95 % RH, for three cement based materials C, M, and SFC, FIG. 4-FIG. 6, (Åhs 2007). In FIG. 4 and FIG. 5 the x-axis represents RH in % RH. The y-axis, in FIG. 4, represents the mass ratio of evaporable moisture relative to cement content. In FIG. 5, the y-axis represents the mass fraction of evaporable moisture relative to mass at 10 % RH. FIG. 6 shows a detailed diagram of several ascending and descending scanning curves determined from three material C

samples. In FIG. 6 the x-axis represents change in RH and the y-axis represents the change in moisture content (We/C).

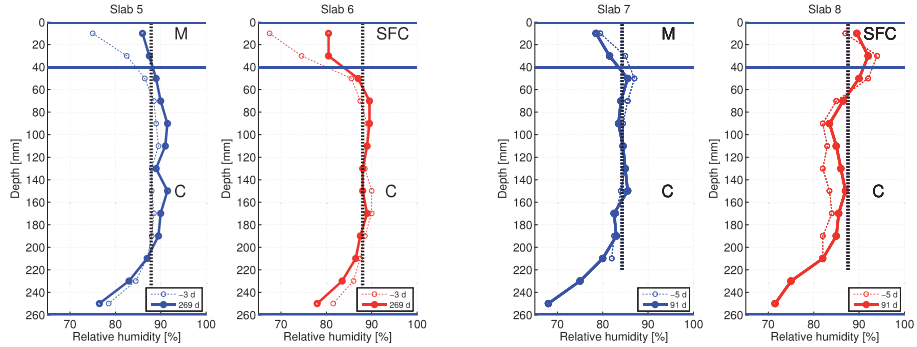

FIG. 3 A comparison of calculated RH_{∞} moisture distribution before and after flooring in four screeded slabs.

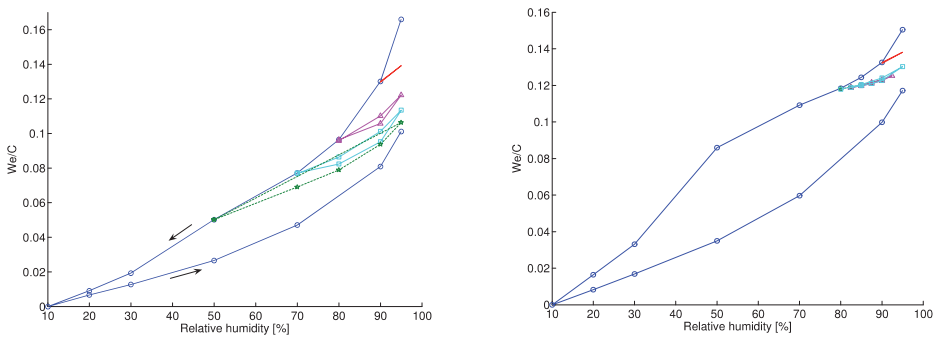

FIG. 4 Sorption isotherms of concrete C (left) and mortar M (right) including several scanning curves.

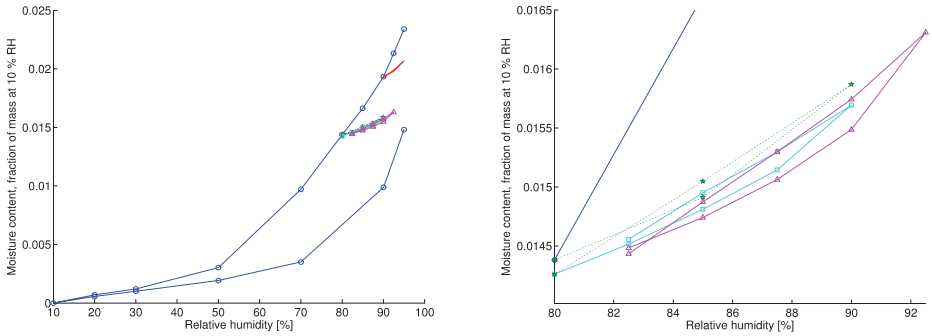

FIG. 5 Sorption isotherm of SFC, including scanning curves (left) and detail of SFC scanning curves (right)

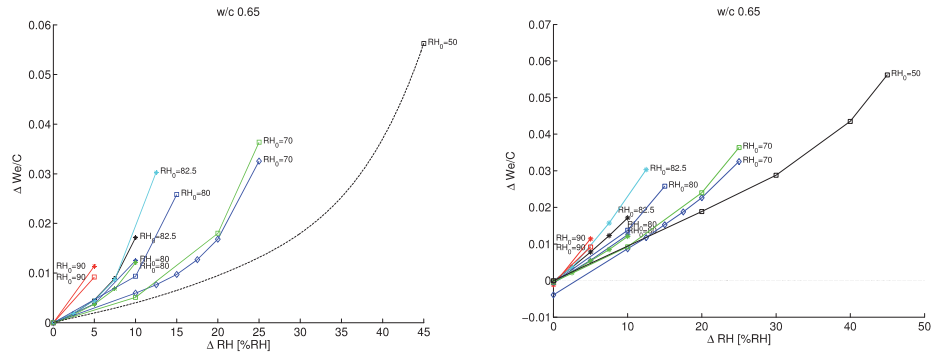

FIG. 6 Detail of ascending (left) and descending (right) scanning curves of concrete C.

5. Discussion

The vertical moisture distribution was determined before flooring and after a certain time of redistribution on four screeded concrete slabs, FIG. 3. The verifying experiments fit the qualitative moisture redistribution model fairly well. In addition, sorption isotherms, FIG. 4 and FIG. 5 including several scanning curves, FIG. 6, were determined on the applied materials. Results of the investigated parameters were applied in the quantitative moisture redistribution model, hence achieving a RH_∞ shown in FIG. 3 (vertical dashed lines).

Slab 5 and 6, FIG. 3 (right), were dried in 60 % RH and 20 °C for a long time (Åhs 2007) before flooring installation which explains the comparatively dry screed. However, the humidity increase after flooring is substantial exceeding 10 % RH in the surface layer (10 mm below the surface). Slab 7 and 8, FIG. 3 (left), were dried a short time (Åhs 2007) before flooring installation, hence explaining the comparatively humid screed. These two slabs, especially slab 8, bear the greatest resemblance to the qualitative model, showing a high humidity level in the screed. Further redistribution is to be expected in all slabs, since a uniform RH distribution is not yet attained, FIG. 3.

The determined moisture distribution after a certain time of redistribution corresponds to results achieved from the quantitative model, especially in slab 5-6. These two slabs represent a case when flooring is installed after a long time of drying. However, a humidity increase is expected in the screed surface, since redistribution is not yet completed. Given additional redistribution time the calculated RH_∞ may be achieved ultimately. Slab 7 and 8 represent a case where flooring is installed early after screeding, hence allowing limited drying of the screed.

Sorption isotherms for materials C, M, and SFC all demonstrate substantial hysteresis beginning from 10 % RH up to 95 % RH, FIG. 4 and FIG. 5. However, the hystesis for SFC is less significant below 50 % RH compared with material C and M. The ascending scanning curves retrieve the starting moisture content when returning to the desorption isotherm, indicating reversible characteristics. This feature is further demonstrated in FIG. 6 where the ascending (left) scanning curves' starting point is met by the descending (right) scanning curves.

Time aspects and possible chemical moisture fixation is not considered. The quantitative model is limited to determining the uniform moisture distribution, hence intermediate time steps is not achievable. Cement based materials are possibly still hydrating when flooring is applied and this may affect the redistribution process. Therefore, redistributed moisture may bind with unhydrated cement grains hence reducing the RH_{∞}.

The proposed quantitative moisture redistribution model requires input from the screeded slab's moisture distribution before flooring. Consequently its accuracy is dependent on the uncertainty of each input. It is therefore important to use material properties used and increase the precision of the determined moisture distribution. This may be achieved by a number of actions, i.e., determine humidity sensor uncertainty (Su and Wu 2004), evaluating measurement method, multiple moisture distribution determination and increasing the number of levels.

The current moisture distribution may be achieved from samples extracted from the floor slab or in-situ measurements. The uncertainty of such a measurement decreases with an increased sampling resolution and number of determined distributions. A higher resolution may demonstrate an unanticipated moisture distribution, hence improving data of each level's moisture history. Increasing the number of determined moisture distributions also exposes possible internal spread.

There are a few examples of sorption isotherms in literature (Powers and Brownyard 1947; Baroghel-Bouny and Chaussadent 1996; Johannesson and Janz 2002; Nilsson 2002; Anderberg and Wadsö 2004; Tada and Watanabe 2005; Espinosa and Franke 2006; Espinosa and Franke 2006; Baroghel-Bouny 2007; Åhs 2007). However, scanning curves for cement based materials are scarcely published (Ahlgren 1972; Baroghel-Bouny and Chaussadent 1994; Espinosa and Franke 2006; Espinosa and Franke 2006; Baroghel-Bouny 2007; Åhs 2007). Published cement based material properties are usually valid for old materials, in excess of 1 year old. Such data may be inappropriate to use on newly poured structures.

Besides material properties, temperature is decisive for moisture redistribution, as it affects the sorption isotherm in cement based materials and alters saturation vapour pressure. Ambient temperature conditions stabilise as the building envelope is finalized, hence diminishing the influence on moisture redistribution. However, a permanent temperature gradient is likely to occur since warm air is lighter than cold, thus heating the floor slab base. Such a temperature gradient may support a moisture transport towards the slab's upper surface hence increasing the humidity beneath flooring. In such a case, equation [2] must be rewritten in terms of vapour content v_{∞}, being constant after redistribution.

6. References

Ahlgren L. (1972). Fuktfixering i porösa byggnadsmaterial (in Swedish). Division of building technology. Lund, Lund University **Ph. D.:** 197.

Anderberg A. and L. Wadsö (2004). "Moisture in self-levelling flooring compounds. Part II. Sorption isotherms." *Nordic concrete research* 32(2): 16-30.

Baroghel-Bouny V. (2007). "Water vapour sorption experiments on hardened cementitious materials." *Cement and Concrete Research* 37(3): 414-437.

Baroghel-Bouny V. and T. Chaussadent (1994). Pore structure and moisture properties of cement-based systems from water sorption isotherms. Microstructure of Cement-based systems, Boston, Materials research society.

Baroghel-Bouny V. and T. Chaussadent (1996). Texture and moisture characterization of hardened cement pastes and concretes from water vapour sorption measurements. The modelling of microstructure and its potential for studying transport properties and durability, Kluwer Academic Publishers.

Baroghel-Bouny V.,M. Mainguy,T. Lassabatere and O. Coussy (1999). "Characterization and identification of equilibrium and transfer moisture properties for ordinary and high-performance cementitious materials." *Cement and concrete research* 29: 1225-1238.

Björk F.,C. A. Eriksson,S. Karlsson and F. Khabbaz (2003). "Degradation of components in flooring systems in humid and alkaline environments." *Construction and Building Materials* 17(3): 213-221.

Espinosa R. M. and L. Franke (2006). "Influence of the age and drying process on pore structure and sorption isotherms of hardened cement paste." *Cement and Concrete Research* 36(10): 1969-1984.

Espinosa R. M. and L. Franke (2006). "Inkbottle Pore-Method: Prediction of hygroscopic water content in hardened cement paste at variable climatic conditions." *Cement and Concrete Research* 36(10): 1954-1968.

Holm A. H. and H. M. Kuenzel (2002). "Practical application of an uncertainty approach for hygrothermal building simulations-drying of an AAC flat roof." *Building and Environment* 37(8-9): 883-889.

Johannesson B. and M. Janz (2002). "Test of four different experimental methods to determine sorption isotherms." *Journal of Materials in Civil Engineering* 14(6): 471-477.

Nilsson L.-O. (1980). Hygroscopic moisture in concrete - Drying, measurements & related material properties. Division of building materials. Lund, Lund University, Lund Institute of Technology. **Doctoral Dissertation:** 170.

Nilsson L.-O. (2002). "Long-term moisture transport in high performance concrete." *Materials and stuctures* 35: 641-649.

Pasanen A. L.,J. P. Kasanen,S. Rautiala,M. Ikaheimo,J. Rantamaki,H. Kaariainen and P. Kalliokoski (2000). "Fungal growth and survival in building materials under fluctuating moisture and temperature conditions." *International Biodeterioration and Biodegradation* 46(2): 117-127.

Powers T. C. and T. L. Brownyard (1947). "Studies of the physical properties of hardened portland cement paste, Bulletin 22." Res. Lab. of Portland Cement Association, Skokie, IL, U.S.A., reprinted from *Journal of the American Concerete Institute* (Proc.), vol. 43: 101-132, 249-336, 469-504, 549-602, 669-712, 845-880, 933-992.

Sjöberg A. (2001). Secondary emissons from concrete floors with bonded flooring materials - effects of alkaline hydrolysis and stored decomposition products. Department of building materials. Gothenburg, Chalmers University of Technology. **Ph. D-thesis**.

Sjöberg A. and C. Engström (2002). Measurements of stored decomposition products from flooring adhesives in a concrete floor, as a basis for choosing a new floor surface construction. Building Physics 2002 - 6th Nordic Symposium.

Su P. G. and R. J. Wu (2004). "Uncertainty of humidity sensors testing by means of divided-flow generator." *Measurement* 36(1): 21-27.

Tada S. and K. Watanabe (2005). "Dynamic determination of sorption isotherm of cement based materials." *Cement and concrete research* 35: 2271-2277.

West R. P. and N. Holmes (2005). "Predicting moisture movement during the drying of concrete floors using finite elements." *Construction and building materials* 19: 674-681.

Åhs M. (2005). Remote monitoring and logging of relative humidity in concrete. *Proceedings of the 7th symposium on building physics in the Nordic countries Reykjavik*, Iceland, The Icelandic building research institute.

Åhs M. (2007). Moisture Redistribution in Screeded Concrete Slabs. Div. of Building Materials Lund, Lund University, Lund Institute of Technology. **Licentiate in Engineering:** 54.

Åhs M. (2007). "Sorption scanning curves for hardened cementitious materials." *Construction and building materials* doi:10.1016/j.conbuildmat.2007.08.009.

VI

Influence of early drying of concrete on humidity under impermeable flooring

M. S. Åhs[a,1,*], L.-O. Nilsson[a,2,]

[a]*Division of Building Materials, Lund University, P.O. Box 118, 221 00 Lund, Sweden*

Abstract

Early drying of a concrete floor slab will limit cement hydration in the surface-near parts. After applying impermeable flooring redistribution will occur and the surface-near parts will be rewetted. This may cause further hydration and "delayed self-desiccation". An experimental series was set up to carefully quantify this effect. The quantification was performed by comparing the surface RH after complete redistribution in specimens subjected to early and late drying.

Keywords: Humidity (A), Drying (A), Curing (A), Concrete (E)

1. Introduction

Concrete floor slabs are usually dried a certain time before applying a moisture sensitive impermeable flooring, see Fig. 1a (left). After flooring, the residual moisture from the slab base redistributes, hence increasing the surface humidity see Fig. 1b (left). This increase continues until the humidity, in terms of RH, is uniformly distributed. There is a method to roughly quantify the expected uniform MD, in terms of RH, under an impermeable flooring in a concrete floor slab [1]. The method is based on results from a few computer simulations at isothermal conditions and a certain RH. A later study by Åhs [2], showed the importance of taking into account the moisture history dependence of the sorption isotherm when calculating the uniform MD in a concrete slab.

There are at least two previous studies where the uniform MD was found to be significantly lower than expected, when comparing with estimations according to the method described in [1]. The first of these studies was performed on vacuum-treated concrete, where moisture profiles were determined after over a year of redistribution under a sealed surface [3]. Recently a second study achieved similar results when investigating the drying of heated concrete floors [4]. Early drying yielded a humidity exposure to the flooring lower than expected, after the redistribution, in both cases. In neither of the studies it was possible to establish the reason behind this discrepancy.

One possible explanation to this significant humidity decrease may be a continued hydration of cement grains located near the surface. The dry climate has hindered cement hydration which becomes severely affected if the RH in the cement gel is below 80% RH [5]. This less hydrated cement may later react with redistributed moisture, hence providing internal drying. This drying may therefore reduce the anticipated humidity increase by the moisture redistribution. One possible theory behind such an assumption is that a part of the redistributed moisture becomes chemically bound to the unhydrated cement. Fig. 1c (left), shows an illustration of a possible explanation of the humidity decrease by additional hydration, chemical binding Fig. 1c (right). This effect could be called "delayed self-desiccation".

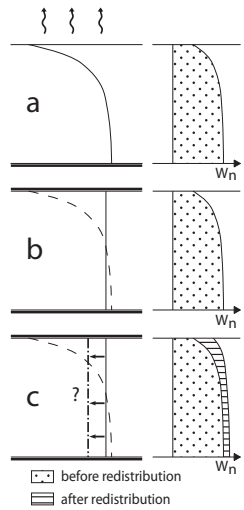

Figure 1: a) Single sided drying of a concrete floor slab b) Redistribution of moisture under an impermeable flooring c) Redistribution of moisture and chemical binding of redistributed moisture

*Corresponding author

Email addresses: magnus.ahs@byggtek.lth.se (M. S. Åhs), lars-olof.nilsson@byggtek.lth.se (L.-O. Nilsson)

[1]tel +46 46 222 49 20

[2]tel +46 46 222 74 08

2. Experimental approach

The effect of different drying conditions was investigated by curing w/c 0.65 concrete specimens using two different drying schemes. Batch 1 was cured in sealed conditions during one day while batch 2 was sealed during 56 days. These specimens were then exposed to 55% RH at a temperature of 20°C until achieving a uniform MD. The MD of the specimens were then determined after drying and after a certain time of redistribution.

Batch 1 was dried for 59 days and then the MD was determined before sealing batch 1. Batch 2 was allowed to dry for 32 days until the MD was found to match the MD in batch 1 before sealing, within ±1% RH. Immediately after establishing the equality between the MDs in batch 1 and batch 2, sealing was applied on the top surface of batch 2. This ensured that the humidity conditions in the two batches before redistribution were equivalent.

3. Material

Concrete with a w/c ratio of 0.65 was used for the experimental setup. The material was mixed and cast under laboratory conditions. The recipe is given in Table 1.

Table 1: Recipe of the used concrete

Material	C in kg/m^3
CEM I 52.5 R	250
Water	162.5
Dry sand 0-8 mm	976.4
Dry sand 8-12 mm	976.4

A relatively high w/c-ratio was used in order to limit self-desiccation. Self-desiccation decreases the humidity in concrete when moisture binds chemically to the cement particles, hydration, besides the physical binding in the pore structure, absorption.

4. Methods

Two sets of four concrete specimens, 100 mm high, batch 1 and batch 2, were cast in cylindrical polypropylene forms, with an inner diameter of 310 mm and a wall thickness of 20 mm. The form bottom consisted of two inner layers of 0.2 mm polyethylene foil in contact with the concrete and an outer layer of adhesive bitumen bearing aluminium foil on the outside. The polyethylene foils and aluminium foil were also used for sealing the top later. The eight specimens were cured for one day under a plastic foil.

In each form, eight tubes for Vaisala sensors were mounted at different heights to be able to determine the MD. The tubes, see Fig. 2, had an opening about 80 mm into the concrete specimen with the center 20-55 mm from the drying surface with an interval of 5 mm. Each opening was covered with surgical tape (3M Micropore) to prevent concrete from entering the tube at casting. Sealing paste was arranged around the tube inside the form, to prevent moisture leakage through the tube circumference, see Fig. 2. Rubber stoppers were used for sealing the tube openings when the RH probes were dismantled.

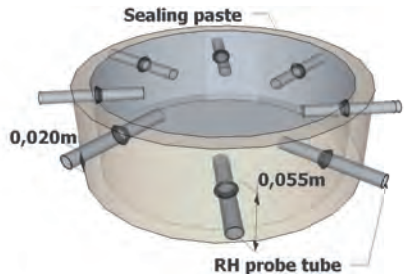

Figure 2: Polyethylene form with installed RH probe tubes

The MDs were determined with calibrated RH probes on several occasions; before drying, after a certain period of drying and redistribution. In addition, MD was also determined after drilling through the surgical tape and 20 mm into the concrete with a 16 mm diameter drill. All probes were read repeatedly from the time of installation until the final reading in order to ensure a moisture and temperature equilibrium.

The humidity below the sealing was determined after a certain time of redistribution by fixing a glass cup on top of the sealing after punching a 12 mm cylindrical hole, see Fig. 3. The glass cup was fixed by using butyl rubber tape in order to prevent leakage. Subsequently a RH probe was inserted into the glass cup by using three o-rings. The RH probe was installed 48 hours before the humidity was determined. The surface RH determination was performed several times to ensure that the major part of redistribution was complete.

Probe calibration was carried out using a humidity generator, Thunder 2500, at 50, 75, 85, 90, 95% RH at 20°C. The calibration was performed 7 days prior to installing the probes in batch 1 for determining the MD before redistribution. Calibrated RH is calculated by linear interpolation between the two closest calibration levels at an uncertainty estimated to less than ±0,5% RH, see Fig. 4.

Each level was assigned a unique probe to reduce the uncertainty that may arise if two probes show a different reading when exposed to a certain humidity. Since each probe was assigned a certain tube the systematic error of the measurement uncertainty was minimized in that sense. Each specimen's mass change was determined by using a balance with maximum capacity 34 kg and with a 0.1 gram resolution (Sartorius LE34001S).

Figure 3: Concrete specimen and glass cup attached on the top surface

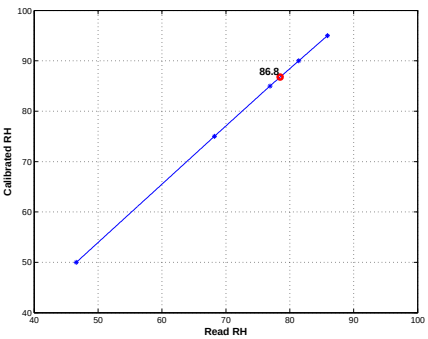

Figure 4: Calibration of RH probe, the result from the reading is 78.5 % RH and the calibrated result becomes 86.8 % RH

4.1. Hypothesis testing

The theory of how a curing technique may reduce the moisture exposure level of a flooring on a concrete floor may be expressed as a hypothesis, the null hypothesis:

The moisture exposure under a flooring after redistribution is independent of the applied curing technique before drying, if drying takes place at the same time as curing or if it takes place after a period of sealed conditions.

The hypothesis may be tested by using the student's two sample t-test and evaluate if the mean moisture exposure level under a flooring is affected by the curing technique. The variance of the two curing techniques are assumed equal. The standard deviation, S_{X_j}, of a single population in curing technique j is expressed in eq. (1):

$$S_{X_j} = \sqrt{\frac{\Sigma(X_i - \overline{X}_j)^2}{n-1}} \tag{1}$$

where, X_i, represents the RH under flooring in specimen i, $\overline{X}_j$, represents sample mean for curing technique j and, n, represents the population of that curing technique.

The grand standard deviation of both populations, $S_{X_1X_2}$, is evaluated in eq. (2):

$$S_{X_1X_2} = \sqrt{\frac{S_{X_1}^2 + S_{X_2}^2}{2}} \tag{2}$$

where, S_{X_j}, represents the standard deviation of curing technique j.

In this test the characteristic t statistic is calculated according to eq. (3):

$$t = \frac{\overline{X}_1 - \overline{X}_2}{S_{X_1X_2}\sqrt{\frac{2}{n}}} \tag{3}$$

where, $\overline{X}$ represents the mean of batch 1 and 2 respectively, and n, represents batch size. This t value is compared with a reference based on batch size and confidence level. The lower and upper confidence limits were calculated by using eq. (4)

$$\left[\overline{X}_1 - \overline{X}_2 \pm t_{\alpha/2}\,(n_1 - n_2 - 2)\,S_{X_1X_2}\sqrt{\frac{1}{n_1} + \frac{1}{n_2}}\right] \tag{4}$$

where $t_{\alpha/2}$ represents the t-distribution at a certain sample population.

5. Results

The MDs in batch 1 and batch 2, after drying and after a period of redistribution, are shown in Fig. 5a-d and Figures 7a-d. The MD in batch 2 before drying is shown in Fig. 6. The x-axis represents the relative humidity expressed in % RH. The y-axis represents the vertical position of the tube opening's center with reference to the drying surface. An RH measurement performed at a position 20 mm from the drying surface is therefore noted at -20 on the y-axis. The letter d, where stated, represents the number of days after sealing when measurements were performed.

In Fig. 5a the MDs including mean before sealing are shown for all specimens in batch 1. The achieved scatter is low and the maximum deviation from the mean MD at a certain level is 1.9% RH in specimen 3. The mean RH at level -20 mm is 79% RH and at -55 around 87.6% RH.

The MDs including the mean MD in batch 1 after a certain period of redistribution are shown in Fig. 5b. The achieved scatter with respect to the mean is low. The largest deviation is 1.0 % RH, this is found in specimen 2 at -20 mm. At level -20 mm the mean RH is 86.6% RH

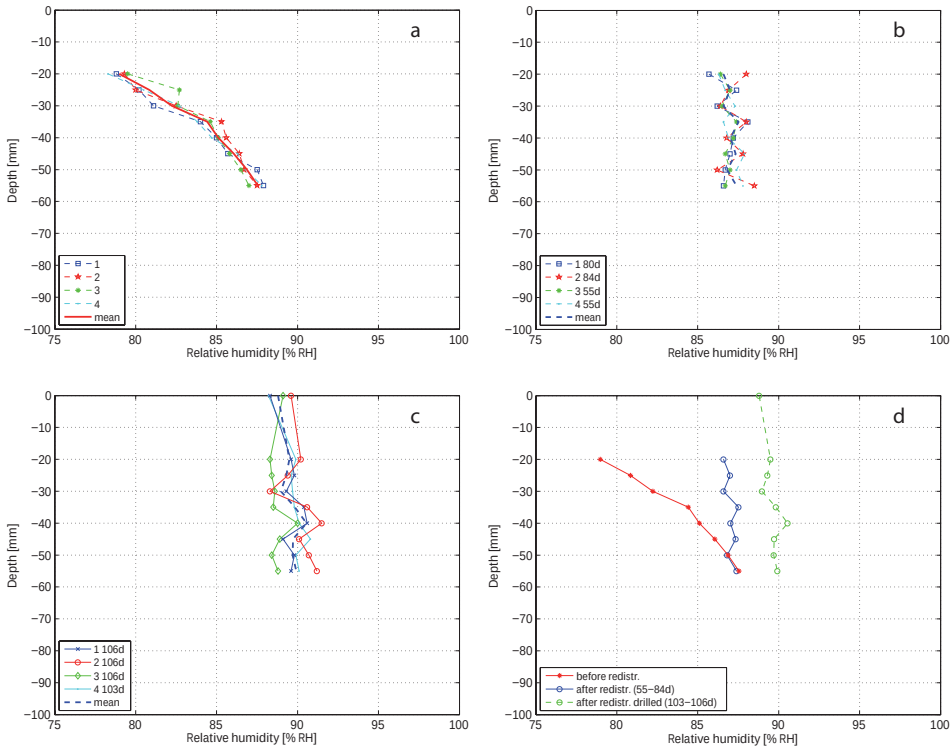

Figure 5: MD in batch 1 determined a) before redistribution, b) after redistribution, and c) after drilling. Diagram d) shows the mean of all specimens MD at an occasion specified in the legend

and at level -55 mm the mean RH is 87.4% RH. Batch 1's MD after more than 100 days of redistribution, is shown in Fig. 5c. The mean RH of the four specimens at level 0 mm is 88.8% RH, at level -20 mm 89.5% RH and at level -55 mm 89.9% RH. The largest deviation from the mean MD is -1.3% RH and was found in specimen 3 at level -50 mm. Fig. 5d shows the mean MD after drying, after 55-85 days and 103-106 days of redistribution. The mean RH is about 86.9% RH at that particular time. The largest deviation with respect to the mean MD, 1.3% RH, was obtained in specimen 3 at level -50 mm. The mean MD after drying and after 55-85 days of redistribution cross each other at level -50.5 mm.

The MD in batch 2 after 56 days of sealed curing is shown in Fig. 6. A particularly large deviation with respect to mean MD, 2.2% RH, was achieved for specimen 6 at level -40 mm. That deviation was investigated further. A drop of water was found in the tube opening facing the air. That water was probably a remainder from a water leakage through the surgical tape when casting and compacting the specimen. This water may not only increase the reading from the RH measurement it may also moisten the surgical tape and the concrete behind.

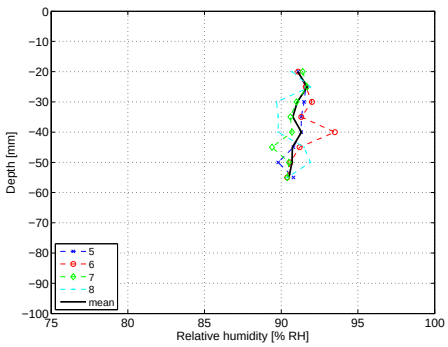

Figure 6: MD in batch 2 before drying

MDs in batch 2 show a low scatter before redistribution, see Fig. 7a. The mean MD in batch 2 is 79.3% RH at level -20 mm and at 87.1% RH level -55 mm. The largest deviation from the mean MD is found in specimen 8 at level -45 mm and is 1.3% RH.

After a redistribution period of 34-41 days the MDs in batch 2 show a low scatter with respect to the mean MD, see Fig. 7b. The mean MD of the four specimens is 86.7% RH at level -20 mm and 87.4% RH at level -55 mm. The largest deviation from the mean MD is 1.4% RH and is found in specimen 6 at level -40 mm. Fig. 7c shows the MD determined for all four specimens in batch 2, including mean MD, in drilled holes after 81-84 days of redistribution. The mean MD of the four specimens in batch 2 is 89.5% RH at level 0 mm, 88.7% RH at level -20 mm, and 89.3% RH at level -55 mm. The largest individual deviation with respect to mean MD, 1.2% RH, is found in specimen 6 at level -40 mm. Fig. 7d shows the mean MD in batch 2 before drying, before redistribution, after 31-41 days of redistribution, and after 81-84 days of redistribution determined after removing surgical tape. The MD after drying and after a certain time of redistribution cross each other at level -55 mm at a RH of 87.1% RH.

A minor mass change was noticed in the sealed specimens ranging from a loss of 0.8 g to a gain of 0.2 g. The mass gain is of an insignificant magnitude. By assuming that the moisture content is approximately 3.5 mass-% at 87% RH it is possible to calculate the moisture content in each specimen. This assumption results in a moisture content of approximately 560 g. This implies that a change of 0.3 grams of water per specimen entails a reduction of 0.002% of moisture content which may be considered as an insignificant reduction in RH, about 0.05% RH.

5.1. Hypothesis testing

The null hypothesis was tested according to the two sample t-test. The evaluation was accomplished at the surface level, which was exposed to RH levels below 80 % RH. The results for batch 1 were [88.3 89.6 89.1 88.2] % RH which gives a mean of 88.8 % RH and [89.0 89.4 88.5 90.3] % RH for batch 2 which gives a mean of 90.3 % RH.

The standard deviation of the RH in batch 1 and 2, are noted in Table 2 and Table 3 respectively.

Table 2: Evaluation of standard deviation of humidity under sealing of batch 1

% RH	$\overline{X}_{batch1}$	$X_i - \overline{X}_1$	$(X_i - \overline{X}_1)^2$	S_{X_1}
88.3		-0.5	0.25	
89.6	88.8	0.8	0.64	0.6683
89.1		0.3	0.09	
88.2		-0.6	0.36	
Σ			1.34	

Table 3: Evaluation of standard deviation of humidity under sealing of batch 2

% RH	$\overline{X}_{batch1}$	$X_i - \overline{X}_2$	$(X_i - \overline{X}_2)^2$	S_{X_2}
89.0		-0.3	0.09	
89.4	89.3	0.1	0.01	0.7616
88.5		-0.8	0.64	
90.3		1	1	
Σ			1.74	

The grand standard deviation of both populations, $S_{X_1X_2}$ equalled 0.7165, was calculated by using eq. 2. An 80 % confidence interval with a $t_{0.1}(4+4-2) = 0.906$ was formed. The lower and upper confidence limits, [-0.9590, -0.0410] in the confidence interval were calculated by using eq. 4. This means that 0 is excluded from the confidence interval, hence implying that the two curing techniques do

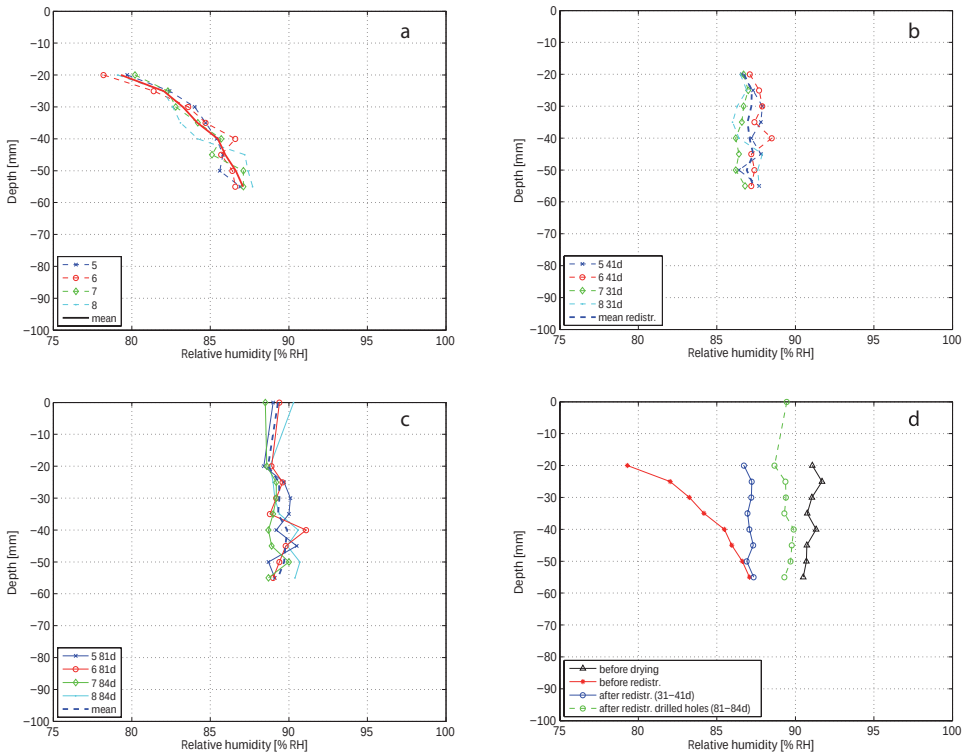

Figure 7: MD in batch 2 determined a) before redistribution, b) after redistribution, and c) after drilling (except at surface). Diagram d) shows the mean of all specimens MD at an occasion specified in the legend

show a difference in humidity exposure under an impermeable flooring at a probability of 80%.

6. Discussion

The assessment of a possible decrease of the humidity exposure under a flooring was performed by comparing two differently dried concrete batches using a statistical approach. The two batches were dried until achieving equal MDs before sealing and the obtained spread before redistribution was low. In addition, the determined MDs showed that at least 20 mm of the concrete top exhibited a humidity below 80% RH before sealing. Those measurements indicated that a substantial part of the material may have a potential to decrease the humidity under flooring by chemically binding the redistributed moisture.

The mean humidity after redistribution in batch 1 and batch 2 is 88.8% RH and 89.3% RH respectively. This suggests a decrease in humidity exposure of 0.5% RH if the concrete is cured in a 55% RH environment compared with curing under sealed conditions at 20°C. Hypothesis testing shows that the mean RH of the two batches at level 0 mm differ by a probability of 80%. According to the probability test, an independent two-sample t-test, the results may have occurred by coincidence. The probability should at least reach 95% in order to be considered as significant. However, hypothesis test performed on an significance level of 5% shows that the obtained difference is too small. Therefore, the difference is considered insignificant.

Determination of MD after redistribution showed that the main part of redistribution was completed within a period of 1.5 to 3 months, see Fig. 5b and Fig. 7b. The humidity at -20 mm was about 87% RH and the MD profile was almost vertical in batch 1, see Fig. 5b. The humidity at -20 mm and the MD in batch 2 show similar results, see Fig. 7b. The intersection of MD before and after redistribution in batch 1 occurs at a depth of 50.5 mm at a humidity of 87.0% RH, and in batch 2 it occurs at a depth of 55 mm at a humidity of 87.2% RH.

The results of the study also shows that the depth at which the humidity after drying is equal to the surface humidity after redistribution is found at 50% or even 55% of floor thickness, given an impermeable flooring attached without adhesive. In other words, it is possible to assess the moisture exposure on an adhesive after redistribution by determining the humidity at a depth of 50 mm to 55 mm in a 100 mm thick floor slab. This reasoning applies to single-sided drying of a comparably high w/c ratio, and to an impermeable sealing. This result agrees well with previous studies [6, 7] which showed that the intersection between the MD before and after a certain time of redistribution was found as deep as 53% of the slab thickness. However, West and Holmes [6] simplified the performed FE analysis to only consider the diffusion coefficient and neglected other important properties of the material, such as the sorption isotherm and the hysteresis phenomenon exhibited by concrete. Another more recent work performed by Rantala and Levio [8] also determined MD in a concrete ground floor slab and found that the previously suggested estimation of the intersection point by Nilsson [1] is located at a depth of 40% of the slab thickness. A method to estimate the humidity below a flooring after redistribution including the hysteresis phenomenon exhibited by cement based materials is shown in [2, 9].

There is a significant difference in the results from the humidity measurements performed before and after of the surgical tape. The arithmetic mean in RH of the MD of batch 1 was 2.6% RH-units higher when the surgical tape was removed by drilling. The moisture level in batch 2 showed results that was 2.3% RH-units higher. It is reasonable to assume that surgical tape has affected the flow of moisture between the concrete and the air, hence reducing the moisture exchange. Assuming that moisture flow from the concrete through the tape is low and that some leakage occurs through the rubber stopper, it is likely to obtain a reduced RH reading of the RH probe. Apart from a possible moisture leakage, sorption properties of the surgical tape may also disturb the measurements.

Moisture distribution in batch 2 determined *before* drying shows that the RH in the upper part of the specimen is higher than in the lower, the difference is about 1% RH, see Fig. 6. All specimens MD in batch 2 show this appearance. A possible explanation could be that the concrete is inhomogeneous as a result of pouring, a form of w/c segregation. A higher w/c ratio means that cement paste has a lower degree of self-desiccation. The higher humidity at the top may imply that w/c is slightly higher in that area. The self-desiccation means that RH is reduced down to 90.5% RH as a consequence of the hardening procedure. Since batch 1 was poured in the same way, it is not possible to exclude that a similar segregation occurred.

Mass change for each test specimen is low, between -0.8 and 0.2 g. The mass loss may be due to several factors, and there may be a leak in the sealing. Moisture may for instance diffuse out of the forms through the slit at the opening facing the air. Moisture may also escape when when the probe is attached and detached from the specimen since they were not in position throughout the experiment.

It is possible that the effect of early drying conditions would have been greater if drying would have been executed in a drier environment than 55 % RH. The cement used in this experimental configuration may reduce the effect of early drying conditions. The study may have shown a different result if the cement would have been an ordinary Portland cement instead of a rapid hardening cement, since the latter one has a larger surface area. This surface area increase the contact between mixing water and cement hence improving the rate of hydration.

The significant decrease in humidity under the flooring, shown in the two previous studies, may be explained by undetected leakage. It is likely to achieve great moisture

losses as a result from leakage in a heated floor construction, as the driving potential for moisture flow becomes large in such a set up. The experimental setup did not allow detection of mass losses during redistribution in the previous studies.

7. Conclusion

The study failed to reject the hypothesis that the moisture exposure on an adhesive under an impermeable flooring on a concrete floor is independent of the curing process. This result may be interpreted as a rejection of the suggested theory that incompletely hydrated cement has a potential to decrease the impact of redistributed moisture under a flooring. Thus early drying is shown to have a small impact on the redistribution of moisture in a concrete floor.

The study also shows that the intersection of the MDs after drying and after redistribution is found at 50-55% of the depth of a single-sided dried concrete slab. A measurement performed at 40 % of the slab thickness as suggested in earlier studies, will give a too low estimation of the maximum moisture exposure under the flooring.

If surgical tape is used between concrete and air it may cause a systematical error to the RH uncertainty. When the tape was removed RH increased consistently by about 2.5% RH units.

8. References

[1] L.-O. Nilsson, Moisture measurements Excess moisture in concrete slabs on grade. Drying and measurement methods. (in Swedish), Tech. Rep. TVBM-3008, Div Building Materials, Lund University, 1979.

[2] M. Åhs, Moisture Redistribution in Screeded Concrete Slabs, Licentiate thesis, Lund University, Lund Institute of Technology, 2007.

[3] L.-O. Nilsson, J. Aavik, Drying of residual moisture in vaccuum treated concrete floors on ground on thermal insulation. Part C: Drying of residual moisture - Validation in a laboratory. Part D: Drying of residual moisture - In situ measurements(in Swedish), Tech. Rep. P-93:13, 1993.

[4] A. Sjöberg, L.-O. Nilsson, Moisture measurements in heated concrete floors. Part II: Impervious floorings (in Swedish), Tech. Rep. TVBM-3140, Div of Building Materials, Lund University, 2008.

[5] T. Powers, A discussion of cement hydration in relation to the curing of concrete, in: Proceedings 27, Highway Research Board, Washington, D.C., 178–188, 1947.

[6] R. West, N. Holmes, Predicting moisture movement during the drying of concrete floors using finite elements, Construction and building materials 19 (2005) 674–681.

[7] N. Holmes, R. West, Moisture re-distribution in concrete under impermeable coverings, in: Role of Cement Science in Sustainable Development - International Symposium Celebrating Concrete: People and Practice, Thomas Telford Services Ltd, Dundee, United kingdom, 299–308, 2003.

[8] J. Rantala, V. Leivo, Drying of in situ cast concrete ground slabs and covering criteria, Building and Environment 44 (2) (2009) 331–337.

[9] M. Åhs, A quantitative model of moisture redistribution in dual layer concrete slabs with regards to hysteresis, in: C. Rode (Ed.), Proceedings of the 8th Symposium on Buliding Physics in the Nordic Countries, Dept. of Civil engineering, Technical University of Denmark, Copenhagen, 873–880, 2008.

VII

A method to determine the critical moisture level for unsaturated transport of ions

M. S. Åhs[a,1,*], L.-O. Nilsson[a,2], M. Ben Haha[b,3]

[a] *Division of Building Materials, Lund University, P.O. Box 118, 221 00 Lund, Sweden*
[b] *Empa, Swiss Federal Laboratories for Materials Testing and Research, 8600 Dübendorf, Switzerland*

Abstract

This study describes a method to obtain a certain humidity level by a certain drying treatment. This treatment was applied on cement based materials in order to identify the critical moisture level above which ion transport can occur. The drying is performed in two steps, first in one direction to reach a certain moisture level and then in the opposite direction to identify if ions can move at this lower level. This treatment gives an opportunity to determine ion transport at a well defined humidity, both in terms of moisture content and RH. Ion transport was indicated by analyzing the potassium distribution on slices of mortar by SEM-EDS.

Keywords: Humidity (A), Drying (A), Physical Properties (C), Transport Properties (C), Mortar (E)

1. Introduction

Ion transport in unsaturated concrete occurs in several applications. Concrete floor slabs usually have to be dried to reach a certain level of moisture before floor coverings may be applied. One reason for this is to avoid hydrolysis of adhesives. This hydrolysis occurs if the humidity is high at the same time as the pH is high. This hydrolysis may be sustained as the drying concrete causes alkali transport, especially when drying occurs from a high humidity level. The hydrolysis splits large molecules, i.e., polyacrylates, in the adhesive into smaller molecules, volatile organic compounds, VOCs. Commonly these compounds consists of various alcohols, such as 1-butanol and 2-ethyl-hexanol, which are considered to have an unpleasant odour. These alcohols are emitted through the flooring to the indoor environment, thus adding to the exposure of adverse chemical substances of its occupants. In addition to a disagreeable odour, these compounds are believed to have an adverse impact on people's health [1, 2]. Another problem with this type of degradation is that blisters may occur and that the adhesive deterioration will reduce the bond between the concrete and flooring material.

To be able to quantify the required drying, the critical limit for transport of alkali ions must be known. Alkali ions are only able to move in a solution, in this case the liquid pore water. In non-saturated mortar, water is present both as a thin adsorbate on large pores' surfaces and as capillary condensed water in narrow pores. The thin adsorbate provides a very limited water volume for ion transport in contrast to the capillary condensed water in narrow pores. The major part of the ion transport therefore occurs in the narrow pores and the larger pores actually become an obstacle to liquid phase transport in non-saturated mortar. A reduction of continuous liquid water paths is for this reason an important means to decrease the ion transport, and this reduction is obtained by drying. Ion transport in a partially dried concrete is, besides the liquid water present in the pores, limited by the pore structure tortuosity and its connectivity.

Transport of ions in a drying mortar mainly occurs due to capillary transport of moisture towards the drying surface. This capillary convective transport, carries the dissolved ions through the material in continuous paths of liquid moisture. The ions in the pore solution are therefore accumulated at some distance from the drying surface. As drying continues the quantity of continuous water paths decreases, especially near the surface where the humidity first decreases, there by limiting the opportunity for ion transport.

Another cause of ion transport is diffusion, where differences in pore solution concentration is the driving potential. This transport generates movement of ions from a high concentration towards a lower concentration. As the ions accumulate at the drying surface the driving potential for diffusion increases. The accumulated ions at the surface generate an ion transport in the opposite direction of the capillary convective transport introduced by drying. However, the transport caused by diffusion is limited, because of two reasons. The ion transport caused by diffusion is slower than the convective transport and the quantity of air filled capillaries that hinders the diffusion increases as drying continues.

*Corresponding author
Email addresses: magnus.ahs@byggtek.lth.se (M. S. Åhs), lars-olof.nilsson@byggtek.lth.se (L.-O. Nilsson), mohsen.ben-haha@EMPA.ch (M. Ben Haha)
[1]tel +46 46 222 49 20
[2]tel +46 46 222 74 08
[3]tel +41 44 823 49 47

Since the critical ion transport limit depends on liquid water content, it is reasonable to assume that it also depends on the moisture history. The moisture content obtained by drying is higher than obtained by wetting, if exposed to an equal relative humidity (RH). This implies that there may be a greater opportunity for ion transport in a mortar that has obtained a certain RH by drying rather than by re-moistening. It is therefore important to address the moisture history issue, besides the actual RH, when stating the critical moisture limit for ion transport.

Previous attempts to determine chloride ion transport in non-saturated concrete at various RH, were mainly focused on finding diffusion coefficients of chloride ions and often neglected the effect of the moisture history.

Nielsen and Geiker [3] performed studies on a partially saturated mortar at various RH levels. However, these humidity levels were obtained by increasing the humidity in an earlier dried material, hence introducing an unintended source of error. In addition, another error was introduced as the diffusion process was introduced by immersion in a saline solution, hence increasing the surface humidity to saturation.

Guimarães et al. [4] performed a moisture conditioning according to [5] and used ground solid NaCl that was put in contact with the concrete. Such a treatment may increase the degree of saturation reached by earlier conditioning, since saturated NaCl generates 75% RH which most likely is above the expected RH at a degree of saturation of 0.5 for the mortars used in that study.

Climent et al. [6] used a combustion gas from heated PVC to create a driving potential for ion diffusion into moisture conditioned concrete samples. However, this study also used a method to dry specimens quickly at elevated temperatures (50°C) and later redistribution hence generating a profile in moisture content by absorbtion/desorption processes.

Francy [7] also investigated ion transport in unsaturated cement based materials and results from this work showed that chloride ion transport could be identified at a saturation degree above 0.5.

All these studies use chloride ions as an indicator of ion transport. One major drawback with this approach is that these ions may react with the cement gel and become fixed to the material structure.

An attempt by Hedenblad and Nilsson [8] to determine alkali ion transport with respect to the humidity was not successful, since drying in different climates caused early alkali transport to the drying surface at all moisture levels.

2. Material

Two mortars with a w/c ratio of 0.4, L, and 0.65, H, were used for the experimental setup. The materials were mixed and cast under laboratory conditions. Mixture description is shown in table 1.

Two mortar mixtures were used in order to study the difference of ion transport at various moisture contents and also how it is influenced by the water cement ratio. In addition, these two mixtures allow testing the method on materials exhibiting different degrees of self-desiccation.

Table 1: Mixture description for the used materials. Quantities are presented in kg/m^3

Material	L	H
CEM I 52.5 R	702	333
Water	281	217
CEN-Standard sand EN 196-1 0-2 mm	1199	1602

Standard sand, 0-2 mm, naturally rounded sand which is rich in quartz, was used in order to achieve a homogenous material mixture.

3. Methods

3.1. Specimen preparation and moisture conditioning

Two batches of mortar cylinders (H and L), 200 mm long and 100 mm in diameter, were cast in steel forms. The H cylinders were sealed by adhesive bitumen aluminium foil after one day of sealed curing. The L cylinders were cured immersed in water for 56 days before sealing with adhesive bitumen aluminium foil.

Immediately after curing, each cylinder was cut into 30 mm thick specimens by using a water cooled saw. The surplus water was removed by using a moistened cloth. Subsequently, each specimen was sealed on one side by using two layers of 0.2 mm plastic foil fixed by aluminium tape. The plastic foils were fixed on three overlapping stripes of adhesive aluminium tape, 50 mm wide, forming an aluminium sheet 130-140 mm in diameter. The aluminium sheet was carefully folded and taped onto the circumference of the specimen by using a rigid plastic tube to smoothen down creases. The other side was kept open to allow drying in a 55% RH and 20°C climate.

Each specimen of material H was treated according to a conditioning sequence consisting of three stages labelled A, B and C, see Fig. 1. Stage A represents the 1^{st} one dimensional drying of a specimen and stage B represents the sealed specimen achieving a uniform moisture distribution (MD) in terms of RH as a result of the redistribution of moisture. Stage C represents the 2^{nd} one dimensional drying after removing the sealing at the opposite side, hence reversing the moisture flow. Two of the specimens of material L, which exhibit a substantial self-desiccation, were only subjected to a 2^{nd} drying, and the control specimen was completely sealed and never subjected to any external drying.

An illustration of the obtained distributions of moisture and ions is shown in Fig. 1. The MD in terms of RH is represented by thin solid lines, the dashed line represents the *uniform* MD achieved after sealing and redistribution, the dash dotted line represents the MD after opening the second side of the specimen, and the expected (Potassium, K) ion distribution is represented by a dotted line. The

thick solid line represents an imagined critical humidity below which alkali transport is hindered. Additionally, the sealing is represented by a thick solid line.

Stage A, see Fig. 1A, represents the drying of a specimen. RH_1 represents the MD in a specimen that has dried a shorter time compared with another specimen represented by RH_2. At Stage B, the specimens were completely sealed after drying by using the plastic foil aluminium disc to achieve a uniform MD, see Fig. 1B. After sealing each specimen was weighed to detect any leakage. The other sealing is removed and a 2^{nd} drying is applied in stage C, see Fig.1C. This stage is divided into two parts, in which the RH level is above an assumed critical moisture level C_1. In this case alkalis have redistributed and the concentration has increased on the right side of the specimen, see Fig. $1C_1$. In Fig. $1C_2$, the RH level is below the critical moisture level. This is shown by the non-increasing ion concentration to the right of the specimen.

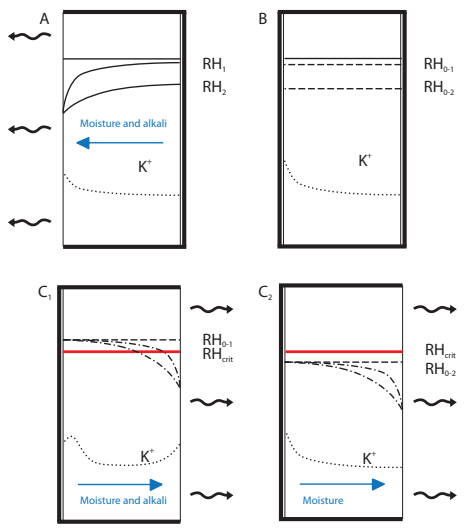

Figure 1: The stages of the conditioning sequence and anticipated changes of RH and ion distribution. C_1 (left) represents a specimen conditioned to a RH level above and C_2 (right) below the critical humidity level, respectively.

The moisture content in mortar is dependent on earlier humidity exposure, as the sorption isotherm exhibits hysteresis, cf. Fig. 2. This has to be accounted for when conditioning the specimen for later analysis of ion transport. As the specimen dries, the humidity decreases in all parts of the specimen because of the moisture flow generated by the dry environment. The moisture content decrease in each part of the specimen may be deduced from the desorption isotherm. However, as the specimen becomes sealed, moisture will continue to flow to the previously open side until a uniform RH distribution is achieved. This will increase the humidity in the dry surface mortar. The gain in humidity will follow an absorption scanning curve, thus leaving the desorption isotherm. The moisture content will therefore become lower at the newly sealed side than in the hitherto not opened side. This redistribution will generate a non-uniform MD in terms of moisture content in contrast to the uniform MD in terms of RH. About half of the specimen from the newly sealed side will be exposed to this humidity increase and exhibit a lower moisture content. The other half of the specimen will instead exhibit a uniform moisture content as well as a uniform relative humidity.

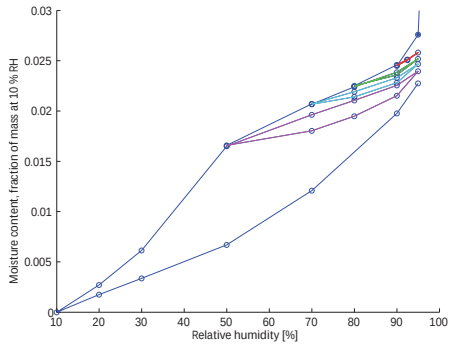

Figure 2: Sorption isotherm and scanning curves of a w/c 0.65 mortar.

The RH on each side of the specimen was determined after a certain time of moisture redistribution, in order to verify that a uniform RH was obtained. This was accomplished by determining the surface RH after replacing the sealing with a specially designed glass cup with an attached glass test tube and an inserted RH probe, see Fig. 3. The glass cup was made of a shortened ordinary glass beaker, with a diameter of 100 mm, and a glass tube joined to the beaker by melted glass to a circular hole at the centre of the beaker base. The glass cup covered the flat surface of the specimen and was fixed to the circumference by using adhesive aluminium tape. The RH probe was inserted through the glass tube until reaching the mortar surface. Sealing between the RH probe and the glass tube was obtained by using three o-rings. It was verified by gravimetric measurements, on a Sartorius balance LE1003S, before and after RH determination. The balance was continuously validated with a reference mass, 200.002 g, in order to monitor possible drift.

Subsequently, the never opened side was uncovered by removing the glass cup, to obtain moisture flow in the opposite direction at the desired uniform humidity level, see Fig. 1C. The glass cup on the other side was replaced with

sealing when the RH reading had decreased with >5 % RH. This verified that the humidity throughout the specimen were lower than the humidity obtained by redistribution.

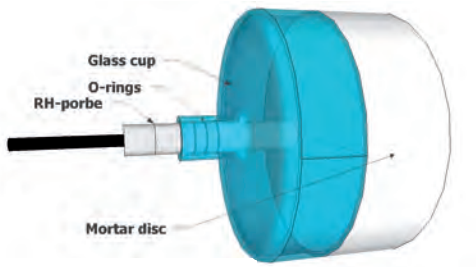

Figure 3: A mortar specimen shown with a glass cup and a RH probe attached to determine the RH at the mortar surface, to verify that stage B is completed.

RH readings were performed not earlier than 72 hours after installation to avoid a non equilibrium state in terms of moisture and temperature between sensor, air and material surface. This arrangement made it possible to validate the presence of a uniform internal RH distribution.

Wet sawing may affect the moisture conditions inside the mortar specimen. In order to minimize such disturbances the H specimens were cut one day after curing when the major part of the pore system still was saturated. The L specimens were considered to be less affected by wet sawing because of the dense material and the short exposure of liquid water. Edge effects were minimized by discarding material less than 10 mm from the top and base surfaces of the cylinder.

3.2. Analysis of ion concentration distribution

Slices of mortar with a thickness of 3 mm were cut using a dry saw on the transversal side of the sample, in line with moisture flow. They were subsequently dried at 40°C for 24 hours. This suggests that the alkali in the pores of the hydrates in the analyzed region has precipitated (as alkali hydroxides or as a carbonates phase, depending on the CO_2 contained in the environment and in the material when the samples were dried prior to analysis).

The outer layer of the slice was removed using sand paper. The prism was then impregnated with low viscosity epoxy resin in a vacuum chamber, at a pressure of 100-200 Pa. After impregnation, the prism was enclosed with epoxy resin, forming a cylinder. This epoxy cylinder was then polished by using a successively finer grinding discs, down to a fineness of 0.1 μm, to remove the epoxy from the mortar surface. An abrasive polymer suspension, a suspension with a diamonds of 0.1 μm, was used at the final stage. This fine surface roughness is needed to obtain consistent results from the EDS analysis. Then the polished surface was coated with carbon (a few nm) and examined using a Philips ESEM FEG XL 30 scanning electron microscopy (SEM).

Backscattered electron images (BSE) coupled to energy dispersive X-ray spectroscopy (EDS) were applied to determine the element compositions of the matrix. They were later analyzed quantitatively to determine the atomic as well as the weight percentage of the alkali in the analyzed zones by monitoring the changes of the composition using either the wt.-% or the atomic ratios over the sample. The analyses were carried out using an accelerating voltage of 15kV to ensure a good compromise between spatial resolution and adequate excitation of the FeKα peak.

To cover the profile of a specimen ($\sim$27 mm), around sixty images were taken per specimen at a magnification of 1000 separated by a distance of 0.4-0.7 mm. To capture the ion concentration distribution through the mortar specimen the analysed images were randomly arranged in relation to the x-axis, in contrast to the even distribution in relation to the y-axis. The location of the image was manually selected to locate areas with a low aggregate content. This made it possible to distinguish the chemical composition of the cement gel, hence revealing expected changes in content of various ion species. No other criteria except the presented were involved when choosing the image location.

Around (80$\sim$100) EDS points, arranged in a eight by ten or ten by ten grid, were taken per image in order to have statistically representative samples. Each image covered an area of around 0.15×0.15 mm^2. Different filters were applied [9, 10] to exclude the portlandite as well as the aggregates from the analysis. A "chemical filter" based on the element ratios was also applied to include mainly C-S-H, AFt and AFm susceptible to present a high nanoporosity volume and thus representing the best locations for precipitation of alkalis. The applied chemical filter included points with a Ca/Si atomic mass ratio between 0.5 and 2.7. Roughly around 50 points were used from each image for the analysis which leads to around 3000 points to describe the profile of the alkalis in the specimens.

Each image were treated separately to calculate the mean wt.-% of the selected ion species and the mean distance from the secondly dried surface. The distance of 0 mm represents the surface, hence negative figures represent an increasing distance from the surface. Redistribution of alkali was analysed by first calculating the mean wt.-% potassium of half of the specimen subjected to the second drying, using iteration. This was done by finding the level of wt.-% at which the area covered by a trapezoid integration above and below this level were equal, within a difference of <0.001 (wt.-%·mm), see Fig. 4.

Alkali redistribution was assessed by quantifying the area above the mean wt.-% at the surface. This area span from the surface to the first point where the alkali distribution intersected the mean wt.-%. Then the mean area of the three specimens was calculated, except for mean area of the L specimen which included areas from two specimens. Alkali redistribution was considered to have

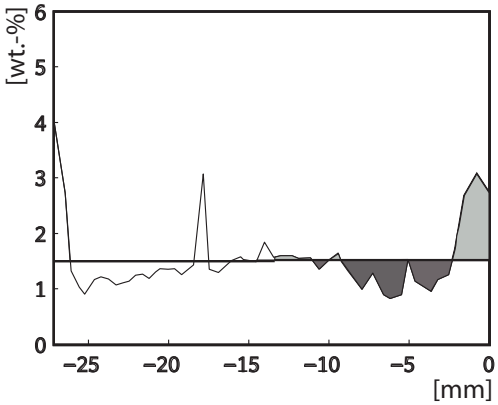

Figure 4: Calculation of mean concentration of alkali. Pale grey shaded area above mean is equal to the darker shaded area, below mean.

occurred when obtaining an area above the mean wt.-%.

One specimen per each humidity level were subjected to drying in one direction only. These were regarded as a control specimens, showing the redistribution of alkali as a result of the primary drying. The results from these specimens were also subjected to the described data analysis to quantify the mean wt.-% and the area above it at the surface.

4. Results

4.1. Moisture conditioning

The time of the 1^{st} drying, surface humidity and difference between the two humidities are specified in Table 2(H) and Table 3(L). The first column shows the specimen set label, the second column shows the drying time. The humidity determined for the surface subjected to both drying and re-wetting, is shown in the third column RH_{left}, and the surface subjected to drying only, is shown in the fourth column RH_{right}. The difference between the two sides, shown in the fifth column, is less than 1.1 % RH in material H and less than 0.2 % RH in material L. Note that the L specimens were not subjected to the 1^{st} drying since the self-desiccation dries the material significantly without exposure of a low RH.

4.2. Potassium distribution at various RH

Potassium content distributions in mortar H are shown in Figs 5-8. These figures are divided into four diagrams showing the distribution in each specimen. The top left diagram in each figure represents a specimen subjected to drying from one side only and the other diagrams show

Table 2: Obtained surface humidity of mortar H at each side of specimen at stage B in the moisture conditioning sequence. Quantities are presented in number of days and % RH

Specimen set	1^{st} drying [days]	RH_{left} [%]	RH_{right} [%]	abs(ΔRH) [%]
A	2	91.8	92.1	0.3
		92	92	0.0
		92.8	92.8	0.0
B	43	85.1	85.2	0.1
		83.8	84.3	0.5
		85.7	84.6	1.1
		84.9	84.9	0.0
		84.6	84.2	0.4
C	58	83	83	0.0
		82.4	82.8	0.4
		83.4	82.9	0.5
		83.6	83.3	0.3
		83.6	83.6	0.0
D	146	79	77.9	1.1
		77.9	77.4	0.5
		76.7	77.7	1.0
		78	78	0.0
		77.8	77.4	0.4

Table 3: Obtained surface humidity of mortar L at one side of specimen at stage B in the moisture conditioning sequence. Quantities are presented in days and % RH

Specimen set	1^{st} drying [days]	RH_{left} [%]	RH_{right} [%]	abs(ΔRH) [%]
E	-	-	-	-
	-	90.6	90.6	0.0
	-	90.2	90.4	0.2

the results after a complete drying treatment. The distribution of potassium content for three specimens of mortar L is shown in Fig. 10. This figure is divided into three diagrams showing the distribution in each specimen, the top left representing a completely sealed L specimen which was never subjected to external drying. The other two specimens were subjected to 2^{nd} only from the level shown.

The potassium content is shown on the y-axis and the x-axis represents the average position of the SEM-EDS analysis image, in mm, with reference to the right surface (the right hand side in each diagram). The average potassium content in each image is represented by the thin solid curve and is quantified as the wt.-%. The average content through half of the specimen, right and left, is shown as a solid horizontal line. The midpoint is at around -14 mm, depending on the specimen thickness.

The distributions of potassium content are significantly non-uniform, see Figs 5-8. All but one of the distributions, show a low scatter, see Fig. 5(top left diagram). The content of potassium in each set have accumulated at the left, except for two specimens in set A see Fig. 5. There is also a significant decrease in potassium content about 3-5 mm

from the left surface. Furthermore, a clear accumulation of potassium ions is found at the right of each specimen, in all specimens subjected to the complete drying treatment. There is also a clear decrease in potassium content, some 3-5 mm from the right surface. The decrease at 3-5 mm from the right surface is less clear at 78 % RH, because of the obtained scatter, see Fig. 8.

The scatter of ion content distribution in mortar L is low except for one specimen (top right). Despite this scatter there is a clear peak of alkali at the right surface in the two specimens subjected to drying. The decrease in potassium content is located about 3-5 mm from the drying surface.

In Fig. 9, the average area above the average potassium content at the right is shown (the control specimen is not included), the whiskers represent the minimum and the maximum area obtained in each set. It is clear that the area increases with an increasing humidity level.

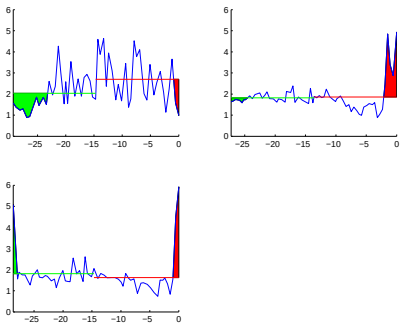

Figure 5: Distribution of potassium in H specimens after the 1^{st} (left top) and 2^{nd} drying at 93 % RH.

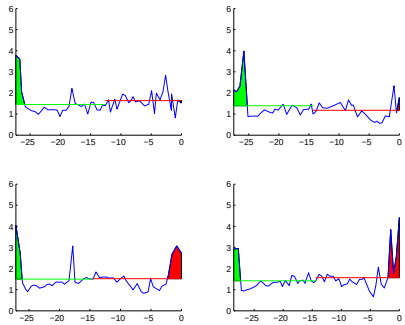

Figure 6: Distribution of potassium in H specimens after the 1^{st} (left top) and 2^{nd} drying85 % RH.

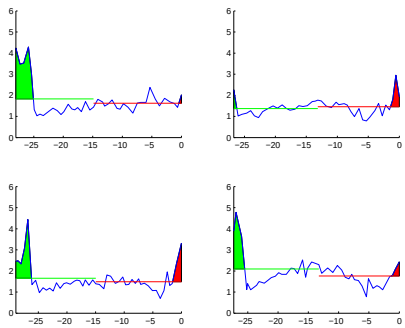

Figure 7: Distribution of potassium in H specimens after the 1^{st} (left top) and 2^{nd} drying at 83 % RH.

5. Discussion

A study of transport of ions present in the pore solution of concrete was performed by Hedenblad and Nilsson [8]. However, the drying method gave rise to ion movement in all drying climates, most likely because of a high initial alkali transport to the drying surface.

A novel drying treatment was applied on mortar discs to achieve a uniform distribution in terms of relative humidity and moisture content. First, drying was applied on the plane surface of the otherwise sealed mortar disc at 55% RH and 20 °C. Secondly, this surface was sealed to obtain moisture redistribution. Thirdly, the opposite surface was subjected to drying at 55% RH and 20 °C, after completion of the moisture redistribution.

The presented treatment was shown to provide specimens conditioned to humidities of 78%, 83%, 85% and 93% RH suitable for determining ion redistribution in unsaturated concrete. This approach was shown to provide uniform and consistent initial conditions in moisture content and RH.

Furthermore, the ion distribution was found to remain uniform after the 1^{st} drying and later redistribution, cf. Fig. 7. This is important as a non uniform distribution may give rise to driving potential counter to the moisture flow governed by drying. In such a case, ion distribution may reduce the effects of capillary convective transport mainly at high humidity levels. Additionally, it is important to be able to show that redistribution of ion really occurs at the humidity level of interest.

An advantage of using the described treatment compared to the method presented by Nielsen and Geiker [3],

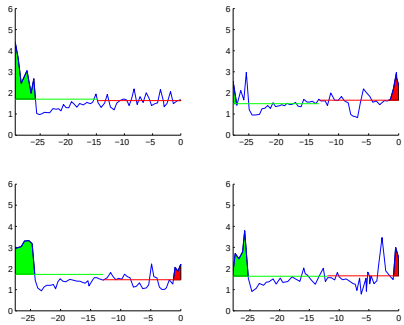

Figure 8: Distribution of potassium in H specimens after the 1^{st} (left top) and 2^{nd} drying at 78 % RH.

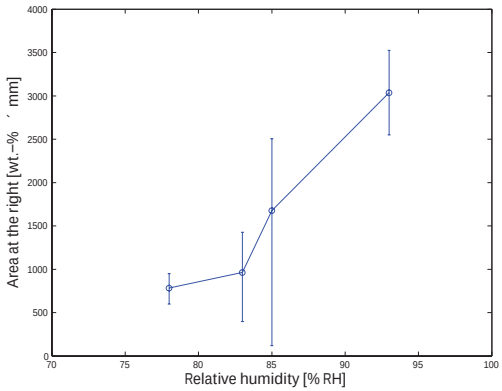

Figure 9: Average area above average potassium content with respect to RH.

Climent et al. [6], Guimarães et al. [4], is that the moisture history is consistent in the region of interest. In addition, the presented treatment does not introduce an alien ion species, e.g. Cl^-, into the concrete. Introducing such a ion species affects the properties of the liquid moisture in the pore system.

Alkali distribution was determined by using an SEM-EDS instrument. The preparation of the specimen does not seem to affect the ion redistribution, see figures 5-8. The sample preparation procedure applied to enable the SEM-EDS analysis, does not seem to introduce moisture redistribution. This inference is drawn based on the uniform ion distribution in the majority of the specimens not subjected to the 2^{nd} drying.

The sample preparation fixes the potassium content

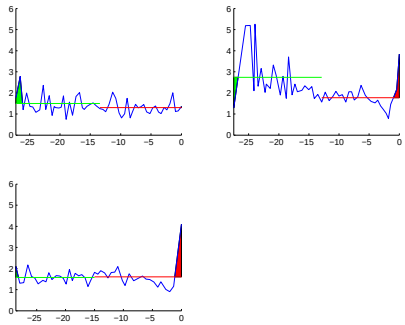

Figure 10: Distribution of potassium in L specimens after self-desiccation (top left) and after the 2^{nd} drying at 91% RH.

at impregnation. Therefore it is possible to re-run the SEM-EDS analysis in case of doubtful results or achieving a large scatter. Re-runs were not performed in this study. Before applying the presented SEM-EDS method, two samples from the same mortar specimen was subjected to two SEM-EDS runs, to show that the technique gave consistent results. The results from this measurement are not included in this study.

Redistribution of alkalis were distinguished by determining the area above the average potassium content at the top surface. The average content was assessed on the top half of the specimen thickness. This quantification was established based on the fact that the moisture content and RH distribution in this part of the specimen is regarded as uniform at the start of 2^{nd} drying. The moisture content in the opposite part is in general lower, especially at the base surface. Therefore, the major part of ion transport takes place in the top. Additionally, the results showed that the the reduction in alkali content at the opposite side was insignificant. This suggests that mainly ions closest to the drying surface participated in the redistribution.

Determination of alkali content through the specimen clearly showed that the 2^{nd} moisture flow generated a significant ion redistribution, regardless of initial humidity. The quantity of ion distribution decreased with a decreasing humidity level. The alkali content at the side subjected to the 2^{nd} drying increased substantially even at a humidity of 78% RH.

6. Conclusion

The drying treatment was found to generate specimens with a uniform distribution of moisture content, RH and ion. Furthermore, the applied SEM-EDS analysis and the method to filter data out showed consistent results. The

procedure of validation of detecting ion redistribution was also. The method is therefore suitable to apply in investigations of the critical moisture for unsaturated transport of ions.

The critical limit of ion transport was found to be less than 78 % RH, when the humidity is reached from pure desorption, in the tested H specimens. Even though a on going self-desiccation during external drying, transport of ions was registered in the L specimens at 91 % RH. This indicates that the critical limit is less than 91 % RH in the tested L specimens.

7. references

[1] K. Andersson, V. Bakke, O. Bjorseth, C. G. Bornehag, G. Clausen, J. K. Hongslo, M. Kjellman, S. Kjaergaard, F. Levy, L. Molhave, S. Skerfving, J. Sundell, TVOC and Health in Non-Industrial Indoor Environments, Indoor Air 7 (2) (1996) 78–91.

[2] A. L. Sunesson, I. Rosén, B. Stenberg, M. Sjöström, Multivariate evaluation of VOCs in buildings where people with non-specific building-related symptoms perceive health problems and in buildings where they do not, Indoor Air 16 (5) (2006) 383–391, 09056947.

[3] E. Nielsen, M. Geiker, Chloride diffusion in partially saturated cementitious material, Cement and concrete research 33 (1) (2003) 133–138, ISSN 0008-8846.

[4] A. Guimarães, M. Climent, G. de Vera, F. Vicente, F. Rodrigues, C. Andrade, Determination of chloride diffusivity through partially saturated Portland cement concrete by a simplified procedure, Construction and building materials 25 (2) (2011) 785 – 790, ISSN 0950-0618, doi:DOI: 10.1016/j.conbuildmat.2010.07.005.

[5] L. Parrot, Moisture conditioning and transport properties of concrete test specimens, Materials and structures 27 (172) (1994) 460–468, ISSN 0025-5432.

[6] M. Climent, G. de Vera, J. Lopez, C. Garcia, C. Andrade, Transport of chlorides through non-saturated concrete after an initial limited chloride supply, in: Andrade, C and Kropp, J (Ed.), 2^{nd} International RILEM Workshop on testing and modelling the chloride ingress into concrete, vol. 19 of *RILEM Proceedings*, ISBN 2-912143-22-5, 173–187, 2000.

[7] O. Francy, Modélisation de la pénétration des ions clorures dans les mortier partiellement saturés en eau, Ph.D. thesis, Université Paul Abatier, 1998.

[8] G. Hedenblad, L.-O. Nilsson, Critical moisture levels of some building materials - Preliminary study (in Swedish), Tech. Rep. TVBM-3028, Div of Building Materials, Lund University, 1987.

[9] M. Ben-Haha, K. De Weerdt, B. Lothenbach, Quantification of the degree of reaction of fly ash, Cement and concrete research 40 (11) (2010) 1620–1629.

[10] M. Ben-Haha, E. Gallucci, A. Guidoum, K. L. Scrivener, Relation of expansion due to alkali silica reaction to the degree of reaction measured by SEM image analysis, Cement and concrete research 37 (8) (2007) 1206–1214, ISSN 0008-8846, doi: 10.1016/j.cemconres.2007.04.016.

LUND UNIVERSITY